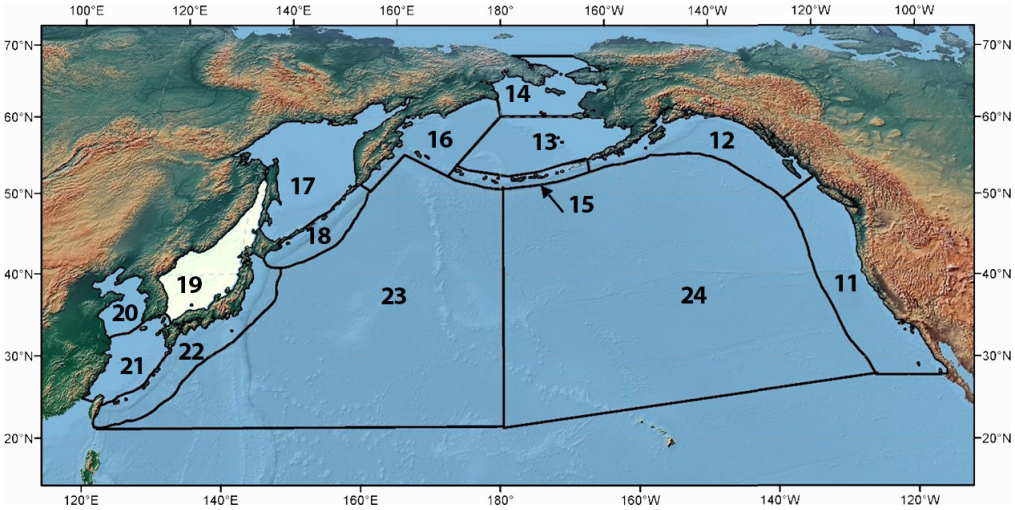

PICES

Regional Report for PICES Region: 19

PICES SPECIAL PUBLICATION 7

Marine Ecosystems of the North Pacific Ocean 2009–2016

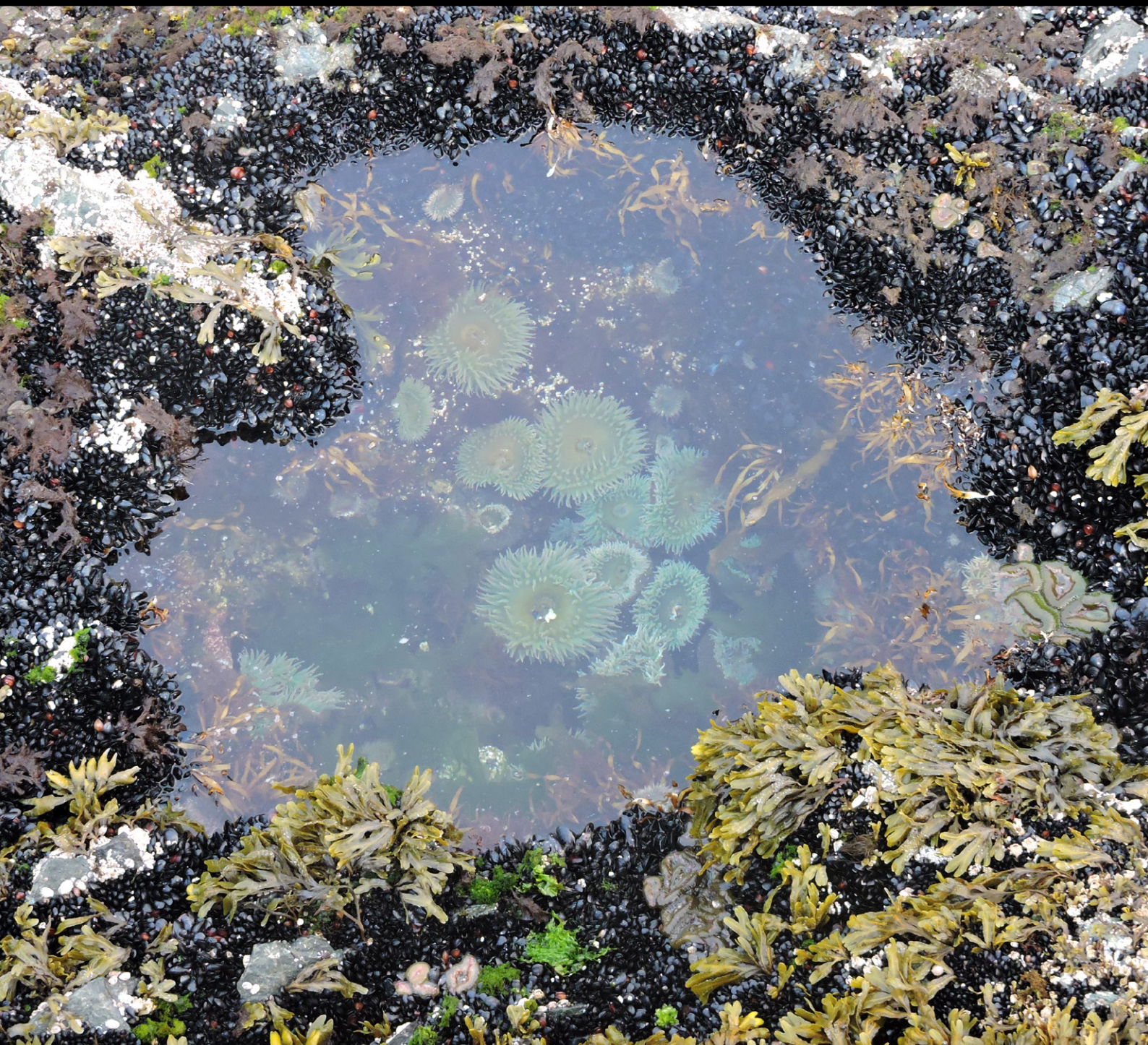

PICES North Pacific Ecosystem Status Report, Region 19

Vyacheslav B. Lobanov

V.I.Il'ichev Pacific Oceanological Institute,

Far Eastern Branch of Russian Academy of Sciences

Vladivostok, Russia

Contributors: K. Kim (Seoul National University, Korea), S. Glebova (Pacific Branch of All-Russian Fisheries Research Institute, TINRO, Russia), L. Mezentseva (Far Eastern Regional Hydrometeorological Research Institute, Russia), S.H. Nam (Seoul National University, Korea), H. Na (Seoul National University, Korea), K.-A. Park (Seoul National University, Korea), Y.-K. Cho (Seoul National University, Korea), O. Trusenkova (V.I. Il'ichev Pacific Oceanological Institute, Russia), E. Ustinova (Pacific Branch of All-Russian Fisheries Research Institute, TINRO, Russia), A. Lazaryuk (V.I. Il'ichev Pacific Oceanological Institute, Russia), G. Kim (Seoul National University, Korea), J. Hwang (Seoul National University, Korea), T-H. Kim (Seoul National University, Korea), J. Ishizaka (Nagoya University, Japan), Y.-W. Lee (Korea Maritime Environment Management Corporation, Korea), W. Kim (Pusan National University, Korea), P. Chandler (Institute of Ocean Sciences, Canada), H.-C. Choi (National Institute of Fisheries Science, Korea), N. Dolganova (Pacific Branch of All-Russian Fisheries Research Institute, TINRO, Russia), N. Iguchi (Fisheries Resources Institute, Japan), Y. Zuenko (Pacific Branch of All-Russian Fisheries Research Institute, TINRO, Russia), H. Kubota (Fisheries Resources Institute, Japan), K. Fujiwara (Fisheries Resources Institute, Japan), S. Kang (National Institute of Fisheries Science, Korea), C. I. Lee (National Institute of Fisheries Science, Korea), M. Kim (Seabirds Lab. of Korea, Korea), D. Ochi (Fisheries Resources Institute, Japan), A. Trukhin (V.I. Il'ichev Pacific Oceanological Institute, Russia), H. W. Kim (Cetacean Research Institute, NIFS, Korea), Y.-R. An (National Marine Biodiversity Institute, Korea), K. Hattori (Fisheries Resources Institute, Japan), S. Minamikawa (Fisheries Resources Institute, Japan), S.W. Hong (Korea Marine Litter Institute, OSEAN, Korea), W. J. Shim (Korea Institute of Ocean Science and Technology, Korea), M. Choi (National Institute of Fisheries Science, Korea), B.-S. Yoon (Korea Maritime Environment Management Corporation, Korea), H.B. Moon (Hanyang University, Korea), D.-W. Hwang (National Institute of Fisheries Science, Korea), H. Maki (National Institute for Environmental Studies, Japan), A. Sevastianov (Far Eastern Regional Hydrometeorological Research Institute, Russia), T. Lishavskaya (Far Eastern Regional Hydrometeorological Research Institute, Russia), T. Belan (Far Eastern Regional Hydrometeorological Research Institute, Russia), K. Aksentov (V.I. Il'ichev Pacific Oceanological Institute, Russia), V. Kulik (Pacific Branch of All-Russian Fisheries Research Institute, TINRO, Russia)

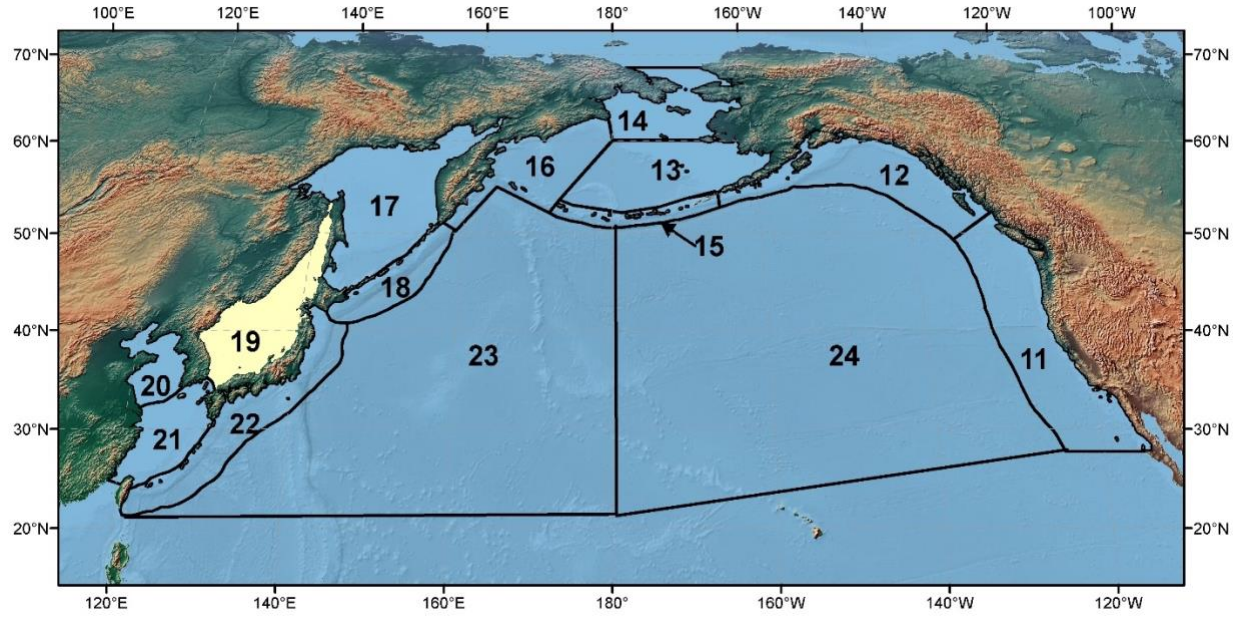

Figure R19-1. The PICES biogeographical regions and naming convention for the North Pacific Ocean with the area discussed in this report highlighted.

1. Highlights

- **Atmospheric processes** over Region 19 in winter are mostly controlled by the Aleutian depression which center was slightly moving to the east since the middle of the 2010s. This leads to a weakening of winter monsoon (northern winds) and decrease in cold air outbreaks and an increasing number of atmospheric cyclones over the sea. The intensity of both Hawaiian High and Far Eastern Low controlling the summer processes was also increasing. This resulted in a decrease in summer cyclones over the sea and the domination of monsoon-type southern winds. All these processes supported a long-term warming trend in air temperature which reached its maximum of the 30-years period.
- **SST** was steadily growing with a centennial increase trend of +1.72 for the central, +1.31 for the southern and around zero for the northern parts of Region 19. However, this trend has significantly slowed down during the last decade.
- **Sea level** in Region 19 had a positive trend over a major part of the sea during 2008-2014. It was however slightly weaker than in 1995-2000, with the median growth rate of 7.1 mm/year.
- **Vertical structure of water masses and ventilation processes** are very important issues for this quasi-isolated deep basin. Trends of warming and decreasing of the dissolved oxygen content of deep and bottom waters, which were associated with global warming and slowing down of winter convection processes, became slightly inconspicuous in the 2010s in comparison to the 1990s. Prominent changes of vertical structure with lower oxygen supply into intermediate and deep waters (500-1500 m) were also observed.
- **Changes in coastal upwelling** intensity associated with interannual changes in wind pattern were observed in the southwestern (off Korea) and northern (off Russia) parts of

Region 19. In particular, a long-term decreasing trend of the upwelling index during the summer seasons of 1948-2018 was reported for the Korean coast and considered to be caused by the changes in the summer monsoon. However, strong interannual variations were noted with a significantly high and low upwelling index in July 2013 and July 2018, respectively.

- **Sea ice** in Region 19 is formed in the northwestern (Peter the Great Bay) and the northern (Tatar Strait) parts of the sea. A slow long-term decreasing trend of 8.8% of the ice cover in the Tatar Strait observed over 1882-2018 has been continuing over the last decades. However, there were high differences between periods of low (2008-2011 and 2014-2015) and high (2012-2013 and 2016-2018) ice cover of around 10-15% of the total ice-covered area of the strait.
- **Significant wave height** was observed to become higher in the 2010s, especially in the eastern part of Region 19 which provides an implication for ecosystem changes through vertical mixing enhancement in the upper portion of the sea.
- **Concentrations of nitrate and phosphate** were almost constantly depleted in summer at the surface layer (0–25 m) with N:P ratios lower than 10. However, in winter, the concentration of phosphate has been decreased from 0.44 to 0.30 μM, although the concentration of nitrate was almost constant. Consequently, N:P ratio increased from 11 to 16, getting closer to the Redfield ratio (16) over the last 40 years. The decrease of phosphate seems to be associated with the intensification of water stratification owing to warming. However, a decrease of N was not observed and that was considered due to the anthropogenic N inputs from the atmosphere.
- **Rapid acidification** in Region 19 was reported based on the estimation of pH from long-term measurements of dissolved oxygen concentration from 1965 to 2015 and showed that pH in the interior of Region 19 decreased. A slowdown of deep water ventilation and accumulation of CO_2 supplied from organic matter decomposition was suggested as the cause of the rapid acidification. In addition, global acidification also contributes to this process. Further acidification in the future is proposed as the deep water ventilation slows down, which needs to be monitored further.
- The time series of **chlorophyll-a concentrations** observed by MODIS shows no clear trend over the studied period, while some prominent interannual variability was found. This corresponds well with the in situ observations of seasonal chlorophyll-a concentrations in the eastern coastal areas of Korea where its high concentrations were observed in August of 2013 and 2014. These two peaks could be explained by higher nutrient input during the rainy season.
- Annual mean biomass density of **meso- and macro-zooplankton** in the southwestern part of Region 19, off Korea, tended to increase from 2010 to 2019 with annual and bimonthly fluctuations, and also with one marked shift in 2017. During the same period, the numerical density of the dominant four taxa (copepods, chaetognaths, amphipods and euphausiids) generally increased with a notable shift in 2017 except for euphausiids. No clear spatial or temporal trends in the total abundance of zooplankton were observed in the southern area of Region 19 (off Japan). In the northern area, the dominant cold-water species abundance has recently been decreasing which coincides with and, supposedly, was caused by the warming of the sea and its productivity decline. In contrast, an abundance of southern migrants became larger.
- **Giant Jellyfishes invasion** which occurred in the southern part of Region 19 in the middle of the 2000s and caused serious harm to the fisheries and tourism has not been observed during the 2010s. However, some insignificant cases may be occurring as it was reported in the coastal waters of Korea in August of 2018 near Pohang City.
- Climate change is considered as the main reason for the simultaneous decline of most of commercial **fish stocks** over the recent decades except for yellow tail; excessive

fishery in the southwestern area is considered as an additional possible reason of the stock exhaustion.

- There are not enough data to assess an interannual variability of **marine birds and mammals in Region 19 except the data on the** spotted seals counted in Peter the Great Bay in the northwestern part of the sea (Russia) which shows steady growth by 4 times over the period 2002-2017.
- **Marine pollution** in Region 19 shows no serious warning. There are no drastic changes over the last decade. It seems that management policies taken by the countries reduced the risk of pollution. In particular, the volume of marine debris and concentration of antifouling biocides off Korea has decreased. In contrast, the concentration of mercury in coastal sediments off northern Korea has been steadily growing.
- **Marine trophic level** has shown a decreasing trend in Russian waters over the recent decade.

2. Introduction

K.Kim, V.Lobanov

Region 19 is a marginal sea bounded by the Asian mainland on the west and north and the archipelago of Sakhalin and Japanese islands on the east and south. It spans the latitudinal range from 35°N to 52°N and is bordered by the Russian Federation, the Democratic People's Republic of Korea, the Republic of Korea, and Japan (Figure R19-1).

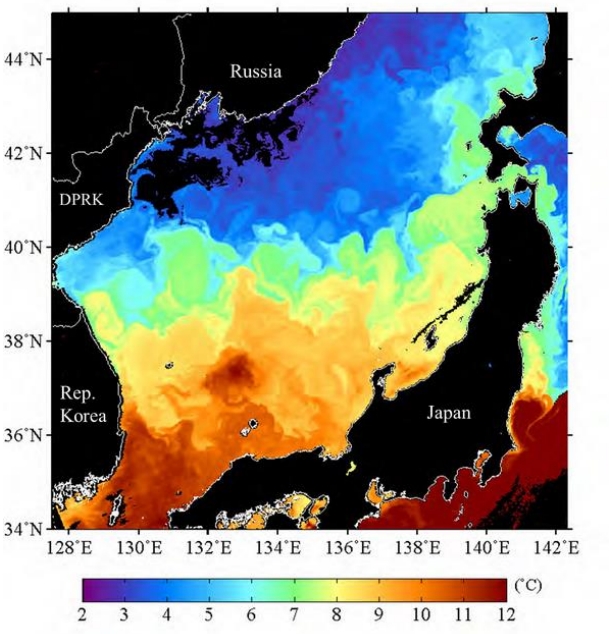

Region 19 contains several deep basins and is connected with the North Pacific Ocean by shallow and narrow straits. It is strongly influenced by the inflow of warm salty water entering from the south through the Korea Strait meeting cool fresher water in the north. The two formations create an interface called the Polar Front (or sub-polar, sub-arctic front), at about 40°N (Figure R19-2).

Figure R19-2 (left). Distribution of sea surface temperatures in Region 19 (from NOAA/AVHRR data, April 5, 2011).

Surface currents circulate in a counter-clockwise direction transporting warmer and more saline water to the north, with some water flowing out to the North Pacific through the Tsugaru Strait between the islands of Hokkaido and Honshu and to the Sea of Okhotsk through La Perouse (Soya) and Tatar (Mamiya) straits farther north. The returning currents bring fresh and cold water along the Asian coast to the south (Figure R19-3).

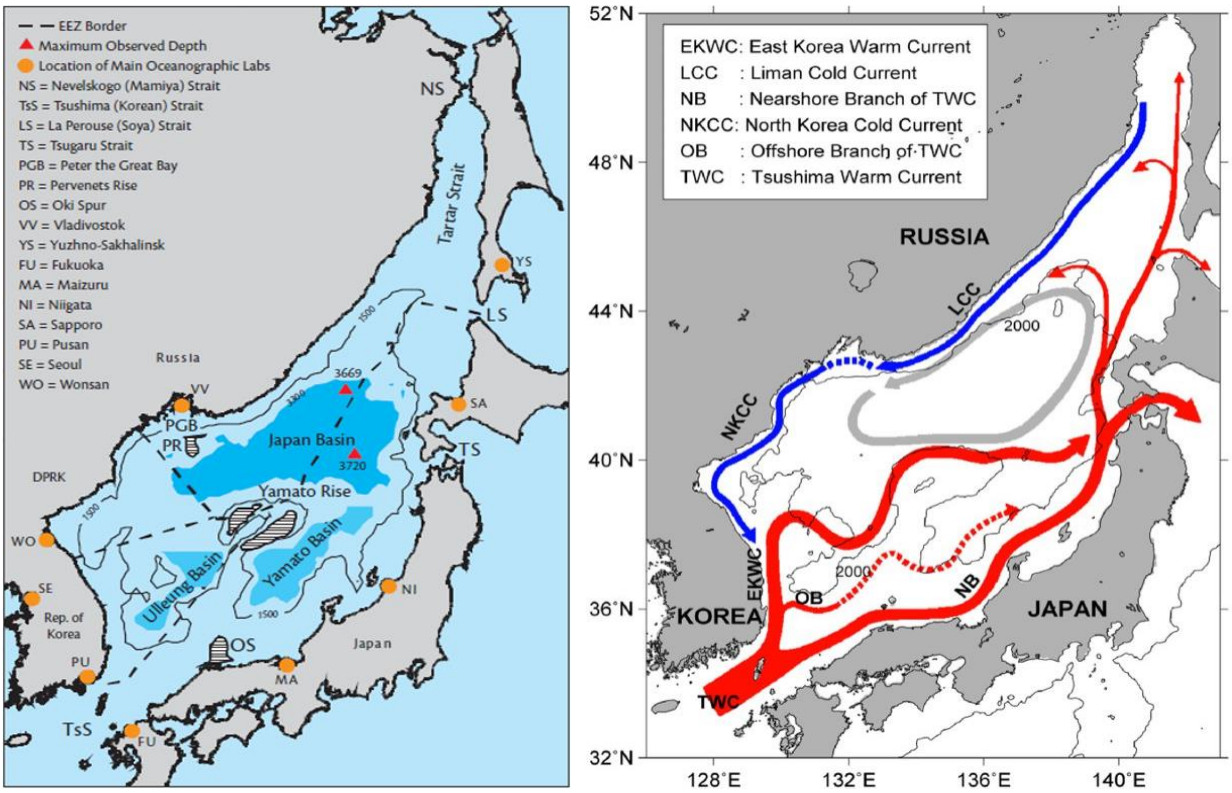

Figure R19-3. Main geographic features of Region 19 (left) (from Danchenkov et al., 2006) and schematic representation of surface currents (from Park et al. 2013).

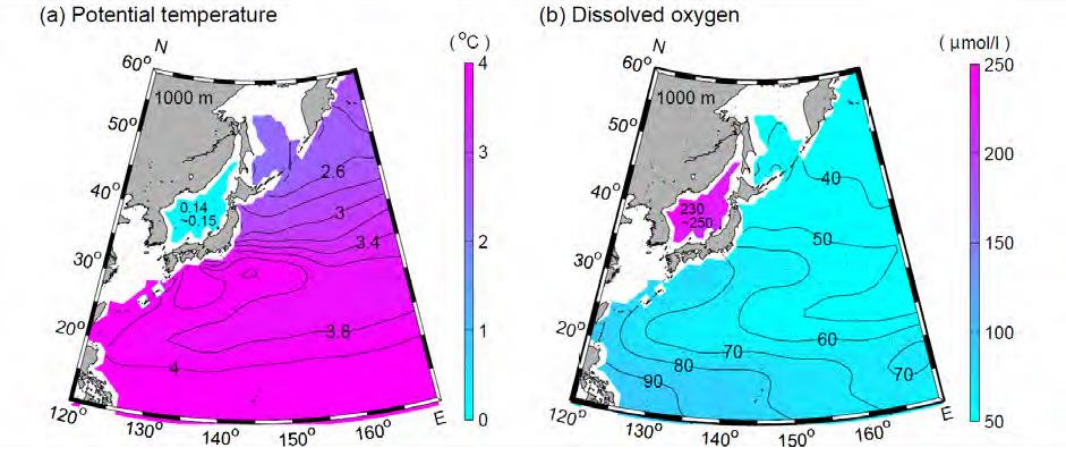

Figure R19-4. (a) Horizontal distributions of temperature and (b) dissolved oxygen at 1000 meter depth in Region 19 and the surrounding Pacific Ocean (Locarnini et al. 2010; Antonov et al. 2010; Garcia et al. 2010).

The deep waters are very cold and rich in dissolved oxygen because of severe winters that form dense cold water, which sinks and ventilates deep-sea layers (Fig. R19-4). The physical, chemical and biological characteristics of Region 19 are highly variable and sensible to climate changes as, for example, the drastic decrease in dissolved oxygen concentration in deep waters in association with recent global warming and weakening of vertical ventilation, (e.g. Gamo et al.

1986; Kim et al. 2001; Yoon at al., 2018). Variability of vertical mixing, water inflow, and growing anthropogenic impact led to changes in the carbonate cycles and ecosystem of Region 19. Because of Region 19's complex nature, it is often referred to as the World Ocean in miniature.

3. Atmosphere

S.Glebova, L. Mezentseva

The climate of Region 19 is strongly controlled by seasonal atmospheric action centers – Aleutian Low (AL) and Siberian High (SH) in winter (Fig. R19-5A) and Far Eastern Depression (FD) and Hawaiian High (HH) in summer (Fig. R19-5B, C) – which intensity and location have been changing over last decade. Since the middle of the 2010s, SH has been increasing while its center was moving slowly to the south and west getting far from the coast. AL has been moving to the northwest and its intensity has also increased (Fig. R19-6). The western location of AL shows the strongest impact on the winter atmospheric processes over Region 19. A number of cases of V type (Glebova et al., 2009) cold weather patterns including cold air outbreaks over Region 19 were much higher in the late 1990s and early 2010s when the AL had a maximum western location (Fig. R19-6). At the same time, the number of atmospheric cyclones over the region was less as their trajectories were shifted southward and located over the ocean to the south of Japan. This supported more frequent cold air outbreaks over the sea from the north (meridional transport index) thus decreasing air temperature and increasing ice content.

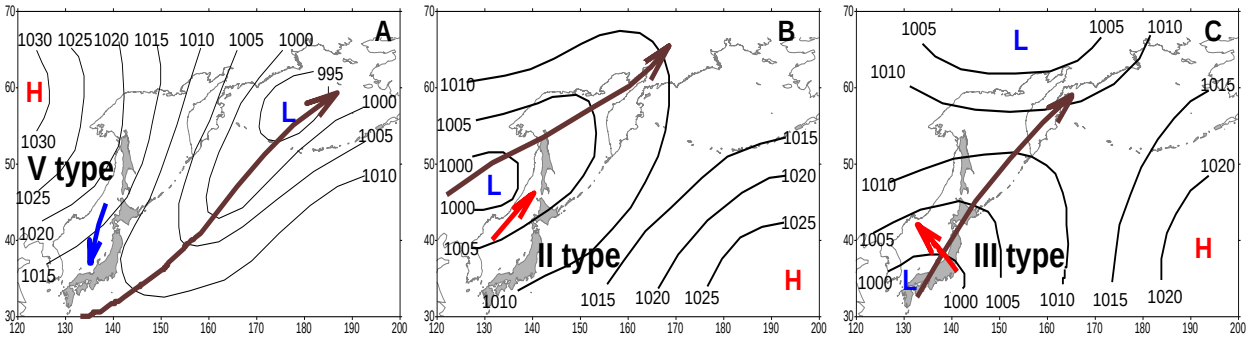

Figure R19-5. Dominant synoptic situations over the northwestern Pacific and marginal seas typical for (A) winter and (B, C) summer. Black arrows show dominant tracks of atmospheric cyclones while red and blue arrows show wind direction over region 19. Weather pattern types (II, III and V) are explained in the text.

However, since 2013 the AL moved back to the east resulting in a weakening of winter meridional monsoon transport and an increase in the number of cyclones passing over Region 19. This caused the increase of air temperature over the region which reached by the end of 2010s its maximum of 30 years (Fig. R19-6).

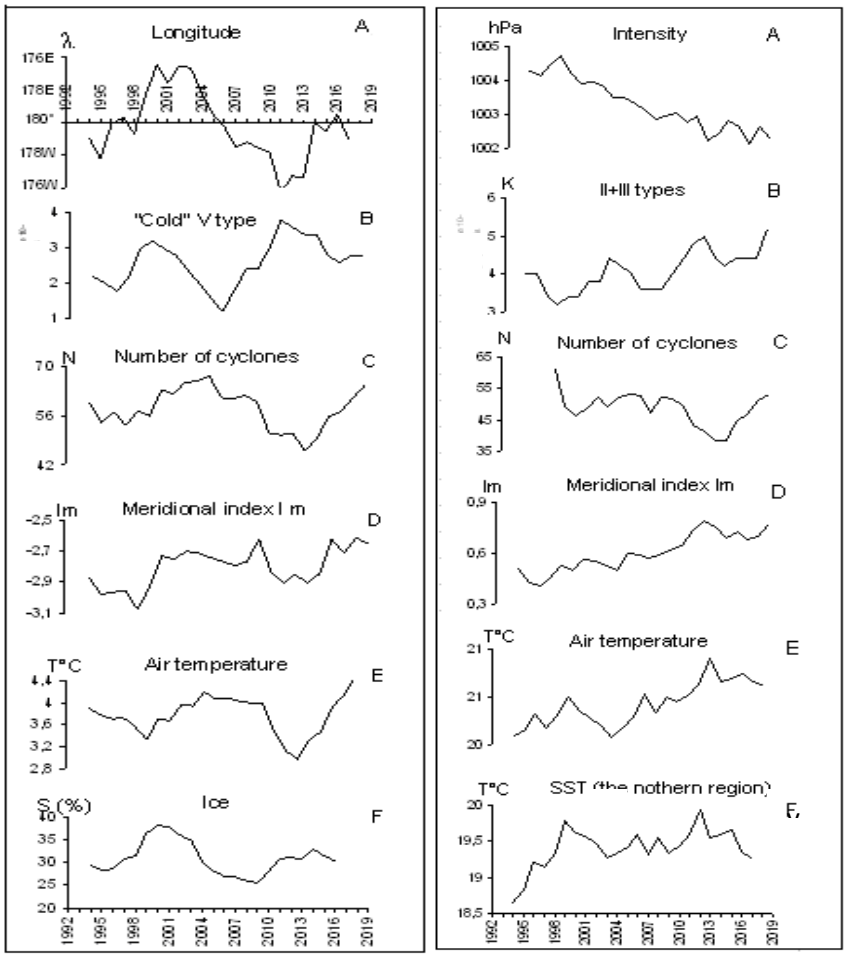

Figure R19-6. Interannual variability of winter (Left) and summer (Right) processes over Region 19. (Left) - variability of the longitude of Aleutian depression center (A), frequency of “cold type” atmospheric processes (B), number of cyclones (C), index of meridional circulation Im (D), air temperature (E) and ice cover in the Tatar Strait (F). Negative Im values correspond to northern winds. (Right) - variability of intensity of the Far Eastern Depression (A), frequency of monsoon type atmospheric processes (B), number of cyclones (C), index of meridional circulation Im (D), air temperature (E) and SST in the northern part of Region 19 (F) (40-45°N, 130-140° E).

The location and intensity of summer atmospheric action centers, Far Eastern Depression (FD) and Hawaiian High (HH), have been also changing over the last decade. Over the 2010s they have been moving in opposite directions. The FD – to the west and south while the HH – to the north and east. Their intensity has been increasing. As a result, monsoon types of weather patterns when the main cyclonic activity occurred over the coastal area of the continent (II type) or over southern Japan (III type) (Glebova et al., 2009) determined by entering subtropical cyclones or typhoons were dominant (Fig. R19-5 B, C). Then the number of cyclones passing over Region 19 has been decreased having a minimum in 2013-2014 (Fig. R19-6 Right C). Stable southern monsoon winds caused an increase in air and seawater temperature in the region, especially in its northern area.

Along with the increasing number of atmospheric cyclones since 2013, there is an increase of stormy weather cases with winds over 17 m/s over the northern part of the region (Fig. R19-7) (Mezentseva, 2019). This is caused by tropical cyclones entering the region at the end of the summer-fall season.

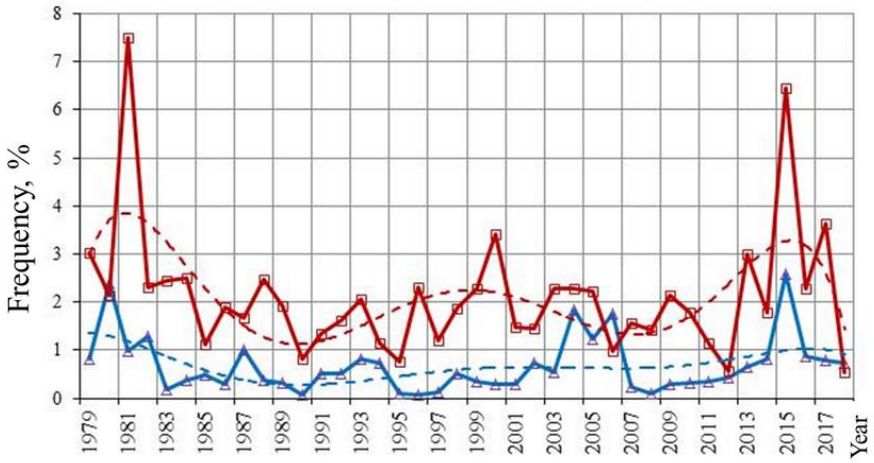

Figure R19-7. Interannual variability of strong winds (>17 m/s) over the Regions 19 (blue line) and 17 (red line) in the July-October period. Dashed line – polynomial approximation (Mezentseva et al., 2019 with additions by the authors).

4. Physical Ocean

S.H. Nam, H. Na, K.-A. Park, Y.-K. Cho, V. Lobanov, O. Trusenkova, E. Ustinova

4.1 SST trends

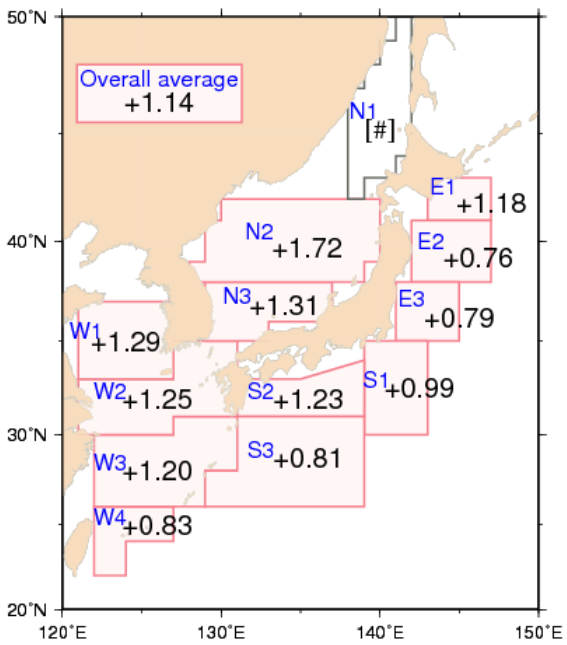

Sea surface temperature (SST) in Region 19 shows a steadily growing trend over a long-term period (1900 to 2019) with a centennial increase trend of +1.72 ºC for the central, +1.31 ºC for the southern and around zero for the northern parts of Region 19 (JMA, 2020) (Fig. R19-8). Based on NCEP/NCAR reanalysis data a long-term decadal trend estimated over 1982-2018 was even higher +0.24 ºC with a maximum increase in summer (+0.34 ºC) and minimum in winter (+0.21 ºC) (Rostov et al., 2020). However, this trend has significantly slowed down during the last decade.

Figure R19-8 (left). Increase rates of area-averaged annual mean Sea Surface Temperature around Japan from 1900 to 2019 (°C per century). The statistically significant trend at the confidence levels of 99 % (JMA, 2020).

Long-term increasing trends estimated by using 37-year-long satellite data from 1982 to 2018 were significantly slowed down during the last two decades (Lee and Park, 2019). Time series of linear SST trend map over a moving 20-year-long period and the percentage of the number of the grids and regional averaged warming and cooling trends support this reduction in the surface warming rates. Further analysis revealed continuous SST increasing in the summer but frequent extreme SST cooling in the winter during the recent decades. More frequent events of extremely low SST were found during the recent decades, which were suggested to link to the Arctic Oscillation (Lee and Park, 2019).

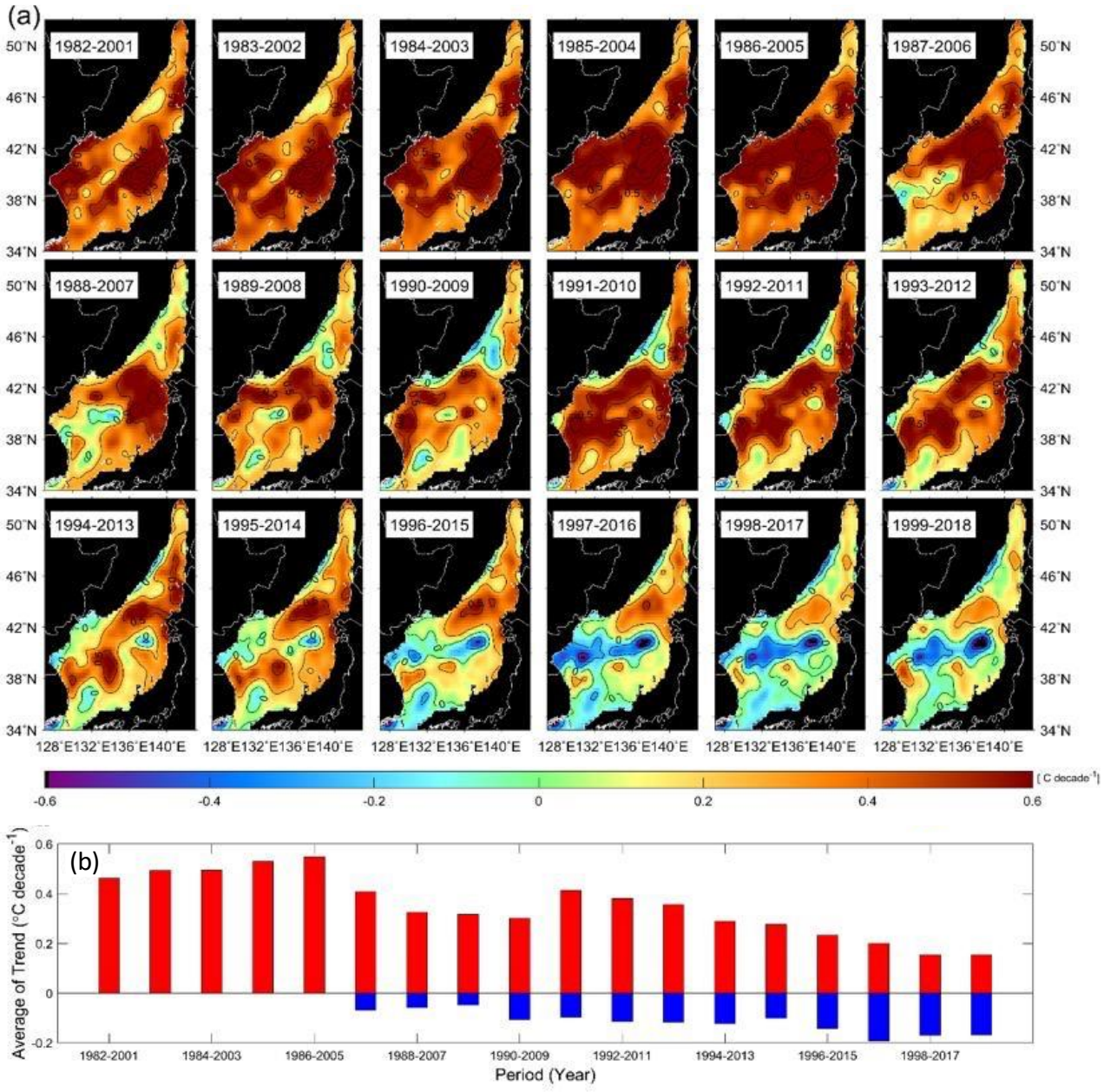

Figure R19-9. (a) Spatial and temporal variation of Sea Surface Temperature for the observation period of 20 years and (b) average warming and cooling trend of the grids with positive (red bar) and negative (blue bar) trends, respectively (modified from Lee and Park, 2019).

4.2 Decadal and interannual variations of upper hydrography

Decadal variability of upper (depth shallower than 500 m) ocean heat content and east-west contrast of its variations south of the subpolar front over the past 30 years, particularly since 1995, were reported by Yoon et al., 2016 and Na et al., 2012. The high amplitude ocean heat content variations after 1995 are mainly attributed to heaving effects, associated with winter wind stress curl in the northern part, due to major branches of warm current in the southwestern part (Yoon et al., 2016). Interannual variations of upper ocean heat content in the western part affecting sea surface wind patterns in winter are also linked to winter precipitation in the mountainous cities along the Korean east coast (Park and Nam, 2017). Physical properties of intermediate water in the southwestern part vary over decades in close connection to the Arctic Oscillation as the same water properties (e.g., same spiciness) were observed at the deeper layer under the positive phase of the Arctic Oscillation, e.g., 1994, 1999, 2006, 2007, and 2008 (orange shaded in Fig. R19-10). Interannual variations of the intermediate water properties are well beyond the relationship with the Arctic Oscillation showing significantly lower spiciness (fresher and colder) in the spring of 2010 than 2001 under nearly the same Arctic Oscillation phase (Nam et al., 2016).

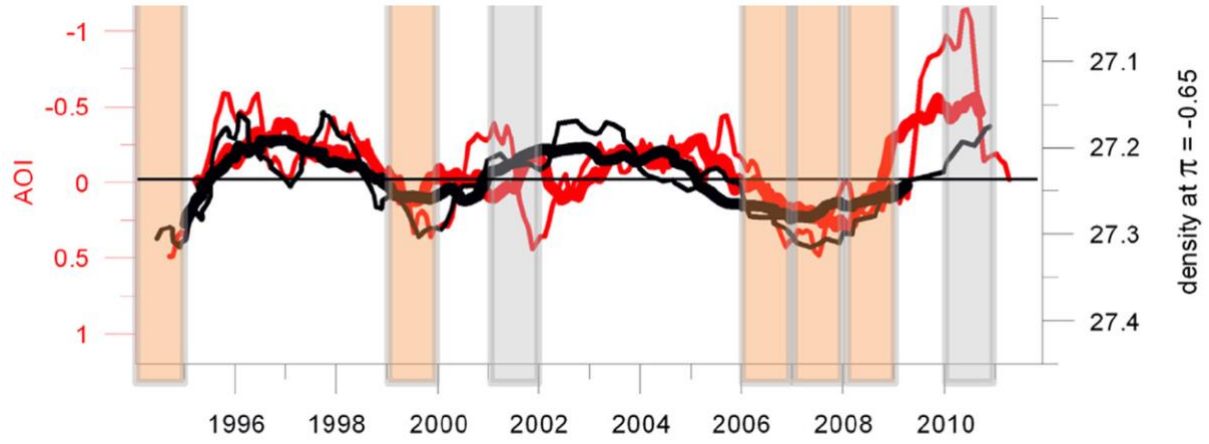

Figure R19-10. 15-month-moving-averaged (thin black) and 3-year low-passed (thick black) time series of iso-spiciness density compared with those of Arctic Oscillation index (AOI, thin and thick red lines). Here, the y-axes for the AOI and density are upside down for convenience. Two years of high AOI 2001 and 2010, and 5 years of low AOI 1994, 1999, 2006, 2007, and 2008, are remarked with grey and orange shades, respectively (Nam et al., 2016).

4.3 Re-initiation of bottom water formation and the recent slowdown of decreasing bottom water dissolved oxygen

Ship-based hydrographic data collected via 19 research cruises between 1993 and 2016 show spatio-temporal variability of water properties from surface to bottom. Time series data collected in the central Japan Basin (deepest part) for the recent decades indicate slightly (but significantly) increasing trends of temperature or deepening isotherms accompanying notable decadal oscillations at depths below 500 m (Fig. R19-11).

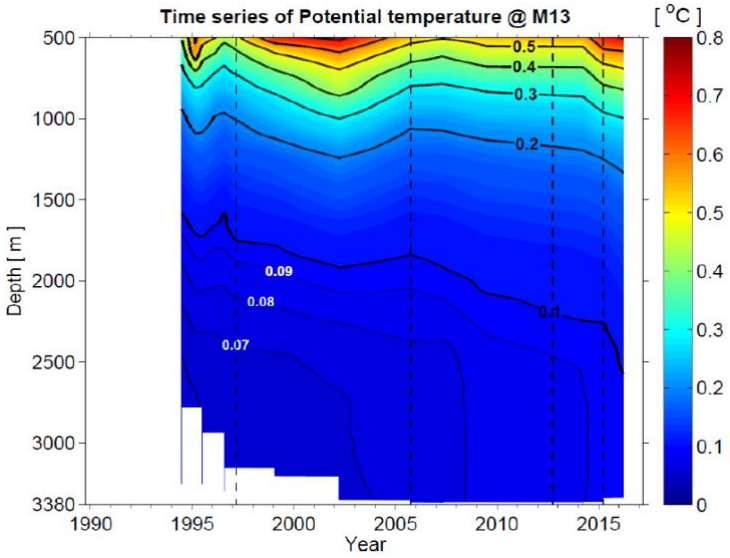

Figure R19-11. Time-depth contour of potential temperature observed in the central Japan Basin from 19 CREAMS and EAST-I cruises between 1993 and 2016. From submitted ETSO by S-H Nam.

One of the main reasons why Region 19 is widely recognized as a “miniature ocean” (Kim et al. 2002; Talley et al., 2003) and “natural laboratory” (Kim et al. 2001) for studying global oceanic processes and interactions between the physical, biogeochemical and climatic processes, stems from its anomalously high dissolved oxygen, e.g., higher than anywhere else in the Pacific, even the South Pacific (Kim et al., 2004; Talley et al., 2006). Vigorous changes and significant ventilation to the bottom depths yield such a high level of dissolved oxygen and a short time-scale of overturning (decades) compared to that of the global ocean (thousands) in this semi-enclosed deep basin. One such example is decadal changes of ventilation and re-initiation of bottom water formation found from an analysis of hydrographic data collected in the central Japan Basin over the recent decades under the CREAMS program. Long-term deepening in deep water boundaries has been recognized over decades, yet a slowdown of the long-term trend in the 2000s was found only recently (Yoon et al., 2018). The slowdown of the long-term deepening in deep water boundaries (between Central Water and Deep Water and between Deep Water and Bottom Water) and bottom water dissolved oxygen is supported by structural changes observed in the deep water masses and results of the 1-dimensional model and allows the formation of a three-layered deep structure expected to remain until at least 2040 (Fig. R19-12).

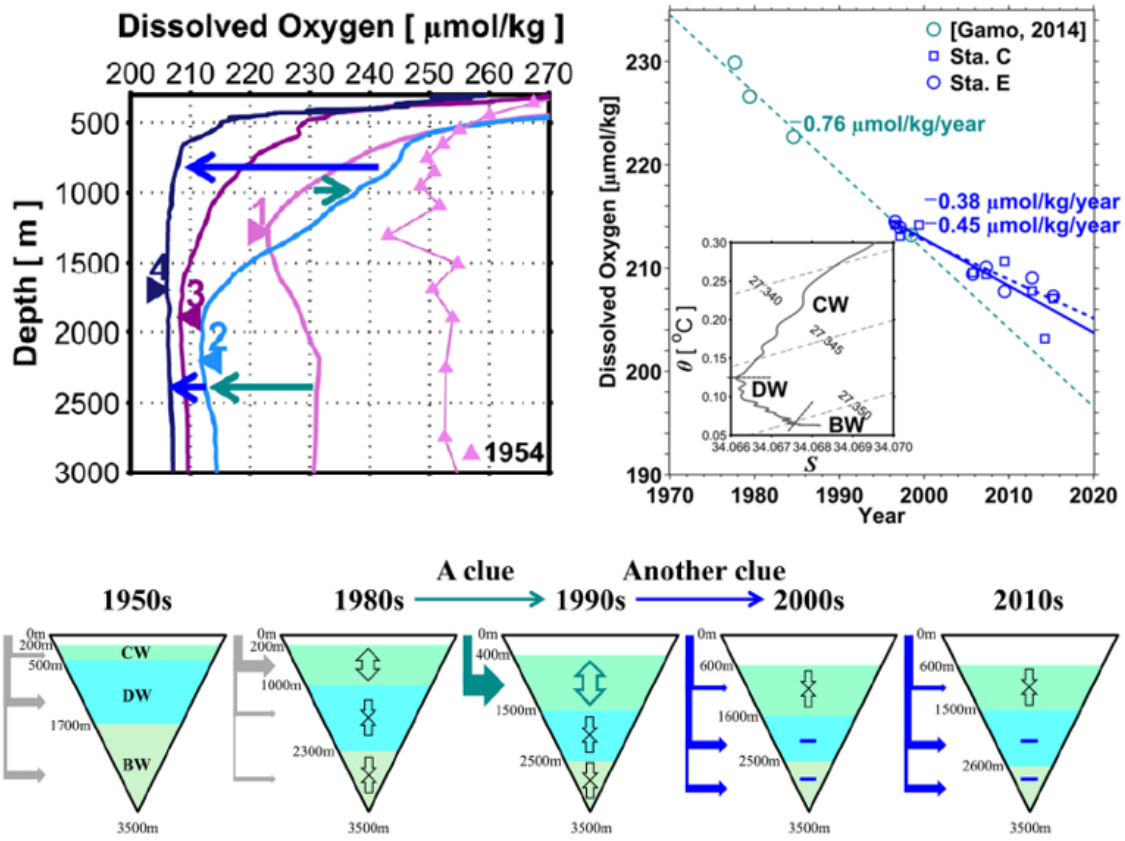

Figure R19-12. Time series of Bottom Water dissolved oxygen observed from 1977 to 2015 in eastern Japan Basin (green open circles reported by Gamo et al. (2014) and blue open circles by Yoon et al. (2018)), and central Japan Basin (blue squares reported by Yoon et al. (2018)). Green and blue dashed lines indicate linear trends of dissolved oxygen declining before and after the late 1990s, respectively. A potential temperature-salinity diagram for data collected in the central Japan Basin in June 1999 is shown in the bottom-left inset. CW – central water, DW – deep water, BW – bottom water. Structural changes of the three-layer water mass structure resulting from the 1-dimensional model are shown in the lower panel (Yoon et al., 2018).

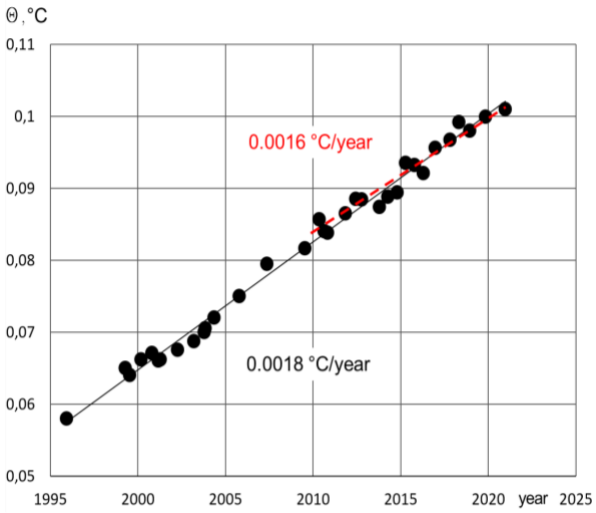

A continuing warming trend of bottom water (2900-3500 m) of the central basin of Region 19 was estimated as 0.0018 °C/year based on CREAMS program observations of 1995-2020 (Fig. R19-13). A slowing down of the trend to 0.0016 °C/year was observed over the recent decade.

Figure R19-13. An interannual increasing trend of potential temperature of the central deep basin during 1995-2020 of 0.0018°C/year. A decrease of the warming rate was observed since 2010 with a trend of 0.0016°C/year (modified from Lobanov et al., 2014).

4.4 Variation of sea level

Sea level trends were estimated using the Copernicus Marine Service (CMEMS) daily gridded sea level anomalies (SLA) from January 1, 1993, through June 3, 2020 (https://marine.copernicus.eu). They are positive in the entire sea and the mean trend is equal to 3.6 mm/yr, which is slightly higher than the global ocean mean trend of 3.42 mm/yr. The spatial trend pattern is rather homogeneous in the entire sea; however, the trends are stronger in the southern area, up to 7 mm/yr in the south-western part and up to 6 mm/yr in the south-eastern part (Fig. R19-14a). To study other kinds of long-term variability, the SLA was analysed using empirical orthogonal functions (EOFs), with fluctuations on the timescales shorter than 1.5 yr preliminarily removed (hereafter the low-frequency SLA). EOF 1 accounts for 56.4% of the total variance; the spatial pattern is everywhere positive and resembles the trend pattern (Fig. R19-14a, b). Therefore, EOF 1 captures sea level fluctuations which are simultaneous in the entire sea. The temporal variability, i.e. the principal component, closely follows the low-frequency SLA averaged in the entire sea, with a correlation of 0.988. Quasi-biennial fluctuations are evident in the temporal variability (Fig. R19-15), as was previously found for the southern (Hirose and Ostrovskii, 2000) and entire (Trusenkova and Kaplunenko, 2013) sea.

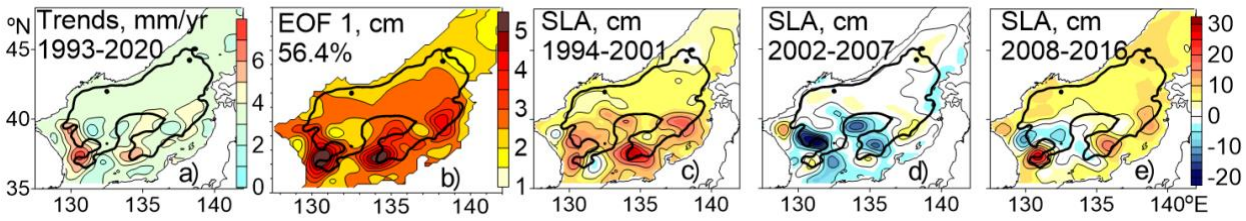

Figure R19-14. (a) Sea level trends (mm/yr) for 1993–2020; (b) EOF 1 (cm) for the low-frequency SLA; the sea level change (cm) for (c) 1994–2001, (d) 2002–2007 and (e) 2008-2016. 1500 m isobath is shown by a thick black line.

With the interannual fluctuations removed by smoothing the mean SLA by using the 6-year window, the decadal variability was identified, with the sea level rise in 1994–2001 and 2008–2016 (positive phases) and the slight decline in 2002–2007 (negative phase) (Fig. R19-15). The sea level rise was the strongest in the first positive phase (1994–2001), in line with the earlier findings (Kang et al., 2005; Trusenkova, 2018). During that time, the sea level increased by 5–10 cm in most of Region 19 and by 15–20 cm in the Tsushima and Yamato Basins (Fig. R19-14c). The second positive phase was weaker, although northward of 40°N the sea level increase was close to its state in 1994–2001, there was a belt of the decreasing sea level in the southwestern area (38°–39.5°N and westward of 133°–135°E; Fig. R19-14e). In the negative phase of 2002–2007, there was a sea level decline southward of 40°N, mostly between -2.5 and -5 cm and as strong as -20 cm in the Tsushima Basin (Fig. R19-14d). These results are close to those derived with the use of the shorter record (1993–2015; Trusenkova, 2018).

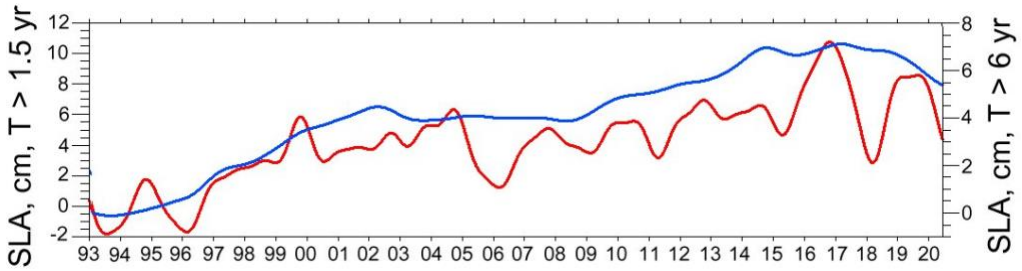

Figure R19-15. Sea level anomalies (SLA) averaged over the entire sea (cm), with variability on the timescales shorter than 1.5 yr removed (red line, left-hand side y-axis), and the same time series smoothed with the 6 yr running window (blue line, right-hand side y-axis).

4.5 Long-term trend of surface wave height

Significant wave height (SWH), derived from data collected from August 1991 to July 2015 using nine satellite altimeters along with validation from in-situ buoy measurements, is significantly higher in the eastern part than in the western part of the sea, and shows characteristic seasonality with high (> 2.5 m) wave height in winter and low (< 1.0 m) in summer (Woo and Park, 2017). The trends of the normal and extreme (99th percentile) wave height in the sea are +0.0056 m/year and +0.0125 m/y, respectively (Fig. R19-16). The higher wave height is getting more extreme with time during the recent decades, which provides an implication for the ecosystem through vertical mixing enhancement in the upper layer of the sea. This is supported by the close relation between interannual trends of SWH and Chl-a as shown in Fig. R19-16.

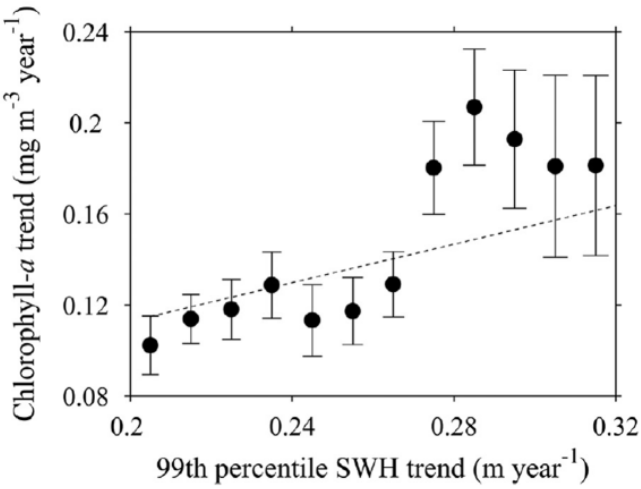

Figure R19-16. Time series of chlorophyll-a concentration trends as a function of the trends of 99th percentile significant wave heights (SWH) in Region 19 in April during the past decade from 2003 to 2014, where the dotted line is a linearly least-squared line (Woo and Park, 2017).

4.6 Interannual variation of summer mean alongshore current off the southwestern coastal boundary

Long (~16 years) time series measurements of the vertical profile of current off Region 19's south-western coastal boundary were used to analyse interannual variation in the summer mean surface circulation in the alongshore direction off the Korean east coast (Park and Nam, 2018). More northward (southward) currents were observed during 2001, 2009, 2010, and 2014 (2002, 2006, and 2012) in association with two dynamic factors: 1) southward propagating coastal-trapped waves, forced primarily by remote winds off the Russian coast in the north, and

2) strength and cross-shore movement of the northward flowing offshore current, East Korea Warm Current (Fig. R19-17).

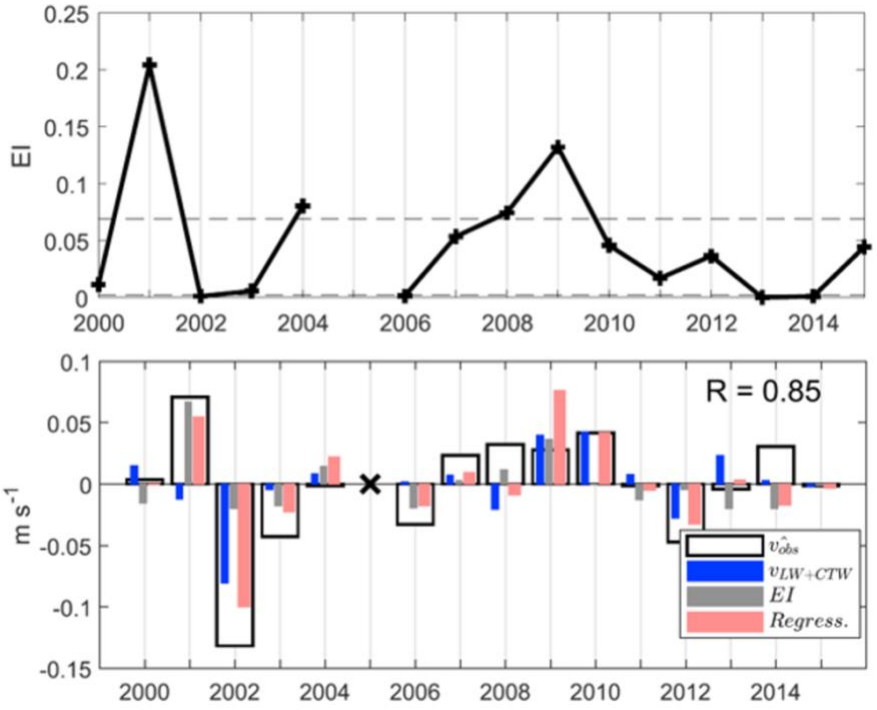

Figure R19-17. (Upper) Time-series of the East Korea Warm Current index (EI) with the 25th and 75th percentiles in dashed lines. (lower) Time-series of multi-regressed, remote and local wind-induced current velocity anomaly (blue bar) and EI (gray bar) on the observed current are shown with the pink bar to compare with the observed current (black open box) (modified from Park and Nam, 2018).

4.7 Changes in coastal upwelling off southwestern boundary

Changes in coastal upwelling intensity associated with the interannual changes in wind pattern were observed in the southwestern (off Korea) and northern (off Russia) parts of Region 19. In particular, a long-term decreasing trend of the upwelling index (UI) during summer seasons was reported for the Korean coast using the NCEP/NCAR reanalysis data from January 1948 to September 2018 (Shin, 2019). The long-term decreasing trend of wind-driven UI was statistically significant in June and July, and the sum of UI in May, June, and July (Fig. R19-18), and weakening sea surface wind (particularly upwelling favourable wind) off the coast linked to summer monsoon was suggested as a main cause for this change. Over the recent 7 years from 2012 to 2018, the UI was significantly high (low) in July 2013 (July 2018) resulting from enhanced (reduced) difference in sea level pressure in the south-western part of Region 19 (Shin, 2019).

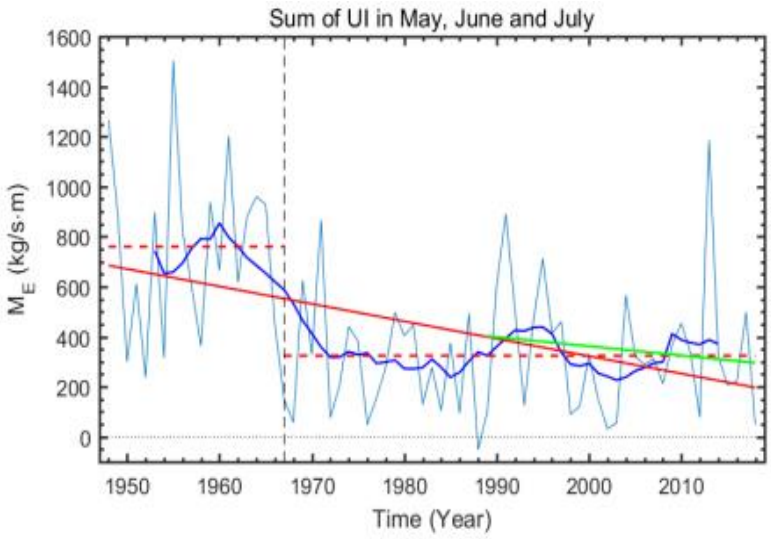

Figure R19-18. Time series of the sum of wind-driven, coastal upwelling indices, UI (M_E) of May, June and July (light blue) and its 10 year moving average (blue). Linear regression lines for the whole period (red line) and a recent 30-year period (green line) were added. The mean values of upwelling indices from 1948 to 1966 and from 1967 to 2018 were represented by the red dashed lines (Shin, 2019).

4.8 Sea ice

Sea ice in Region 19 forms in the northwestern (Peter the Great Bay) and the northern (Tatar Strait) areas. A few recent publications (Ustinova and Sorokin, 2013; Tsypysheva et al., 2016; Pishchalnik et al., 2019) show similar results on a constant decreasing tendency of the ice-covered area (ice cover) after the severe winter of 2000–2001 and strong year-to-year variability observing over recent decade (Fig. R19-19). The longest time series reconstruction of ice cover data in the Tatar Strait over 1882-2018 shows that a slow decreasing long-term trend of 8.8% has been continuing over the last decades (Fig. R19-20). However, there were prominent differences between periods of low (2008-2011 and 2014-2015) and high (2012-2013 and 2016-2018) ice cover of around 10-15% of the total ice-covered area. Such large year-to-year differences are especially noticeable at the end of the winter season, in March (Fig. R19-21). It is also noted that interannual ice-cover variations in the Tatar Strait do not coincide well with its variability in the Okhotsk Sea located nearby and a decreasing ice-cover trend over recent 137 years in the Tatar Strait is two times lower than one in the Okhotsk Sea (Pishchalnik et al., 2019).

In Peter the Great Bay located in the northwestern part of Region 19, there was also a decreasing ice cover trend reported over 2010-2020 (Fig. R19-22). The figure shows the variability of ice thickness in the most isolated parts of Peter the Great Bay - Amurskiy Bay and Novik Bay. Relatively warm winter with higher air temperatures in 2006-2009 corresponds to years of positive phase of the Arctic Oscillation and deeper intermediate water in the western part of Region 19. However, air temperatures of the cold period and ice formation period do not match the negative phase of the Arctic Oscillation, raising the relative importance of local processes and other modes of climate variability.

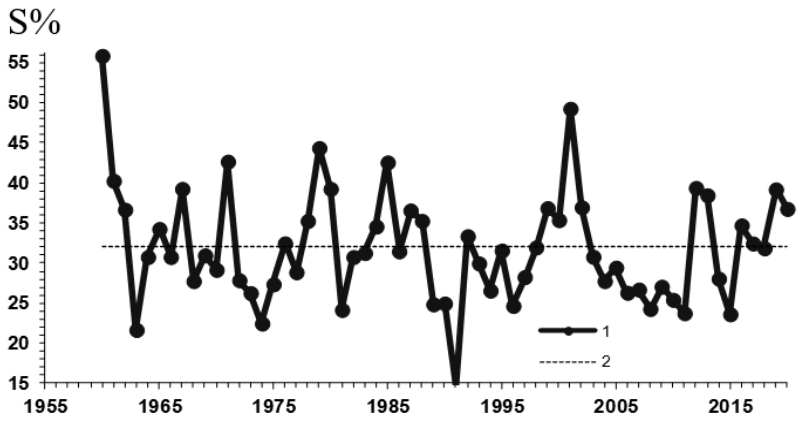

Figure R19-19. Variations of mean winter ice cover (S, %) in the Tatar Strait during the period of 1960-2020. 1 – mean annual values; 2 - average long-term value (Ustinova and Sorokin, 2013, with additions by the authors).

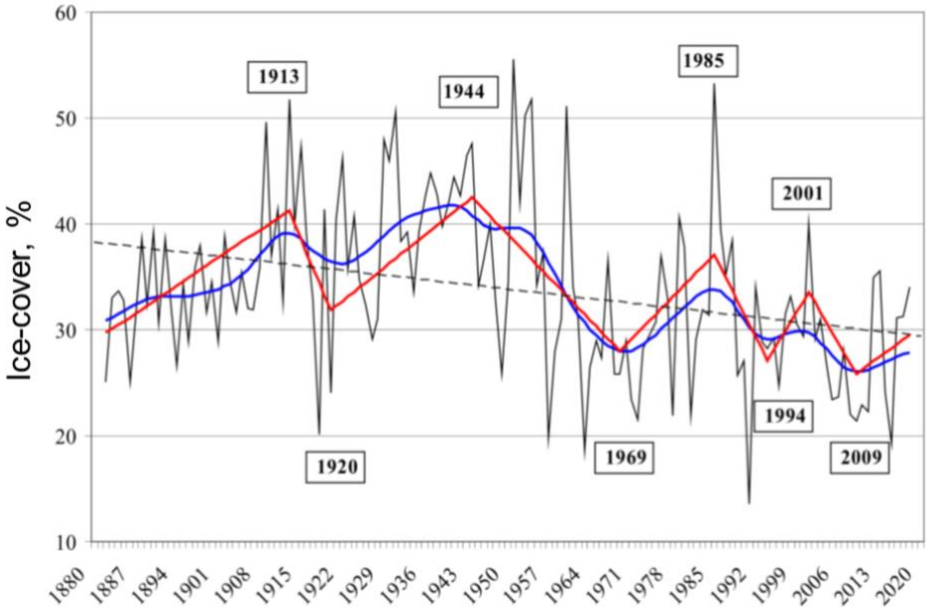

Figure R19-20. - Long-term variations of the ice cover in the Tatar Strait from 1882 to 2018. The linear trend is shown by a dashed line, smoothed by Kaiser-Bessel by a blue line, and piecewise linear trend by a red line (Pishchalnik et al., 2019).

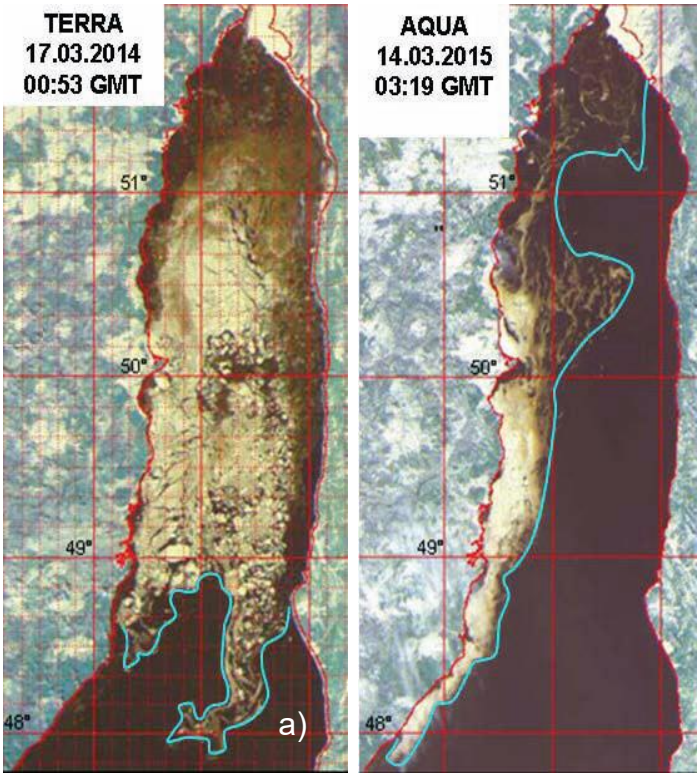

Figure R19-21. Drastic year-to-year variations of ice cover in the Tatar Strait in the end of winter. Satellite images of (a) MODIS/Terra of March 17, 2014, and (b) MODIS/Aqua of March 14, 2015. Blue line is a border of the sea ice covered area (Tsypysheva et al., 2016).

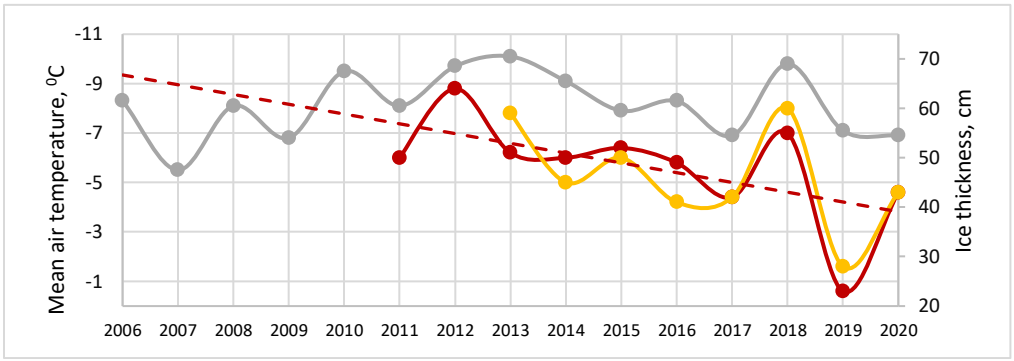

Figure R19-22. Interannual variability of ice thickness in Amurskiy Bay (red) and Novik Bay (yellow) and mean air temperature of the cold period in the Peter the Great Bay area in 2006-2020 (grey). The linear trend is shown by a dashed line (from submitted ETSO by A.Lazaryuk).

5. Chemical Ocean

G. Kim, J. Hwang, T-H. Kim

5.1 Nutrients

The concentrations of nitrate (~25.7 uM) and phosphate (~2.02 uM) in the deep layer (>1000 m) of the sea in region 19 were constant over the last decade (Figure R19-23). The data for Fig. R19-23 is from the website of the Japan Meteorological Agency (JMA, http:// www.data.jma.go.jp), Korea National Fisheries Research and Development Institute (NFRDI, at http://kodc.nfrdi.re.kr), and EAST and CREAMS programs. However, there were slight decreases of nitrate and phosphate between 200–700 m over the last decade, which may be associated with more active surface-water ventilation into the intermediate layer (Fig. R19-23). The ratios of N:P were almost constant (~13) between 200 and 3500 m, but they decreased significantly below 9 at the surface 0-100 m.

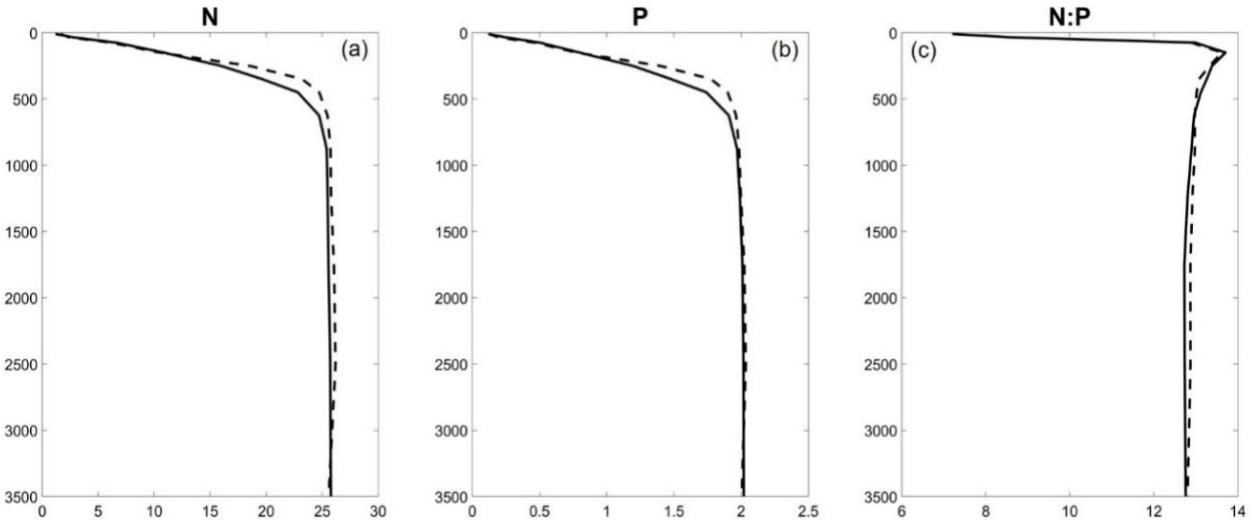

Figure R19-23. The vertical profiles of (a) nitrate and (b) phosphate concentrations, and (c) N:P ratios in Region 19. The dotted and solid lines represent the average value for 2000–2005 and 2015–2017, respectively.

In the surface layer (0–25 m) of Region 19, the concentrations of nitrate and phosphate were almost constantly depleted in summer, with N:P ratios lower than 10 (Fig. R19-24). However, in winter, the concentration of phosphate has been decreased from 0.44 to 0.30 μM, although the concentration of nitrate was almost constant (Fig. R19-24). Consequently, N:P ratio increased from 11 to 16, close to the Redfield ratio (16), over the last 40 years (Fig. R19-24). This decrease of phosphate seems to be associated with water stratification owing to warming, while the associated decrease of N was not observed owing to anthropogenic N inputs from the atmosphere.

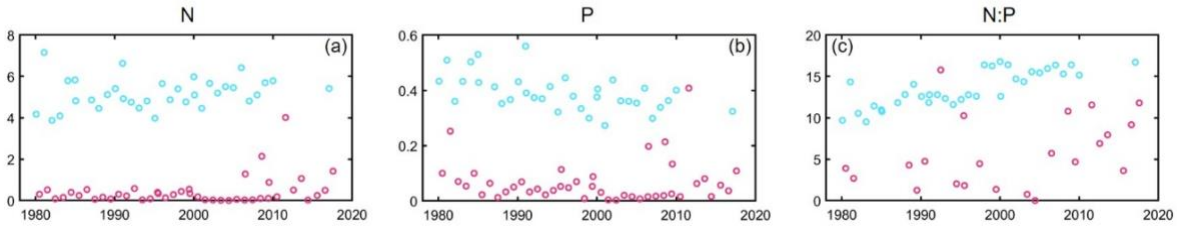

Figure R19-24. The trends for (a) nitrate and (b) phosphate concentrations, and (c) N:P ratios in the 0-25 m depth layer during winter (blue dot) and summer (red dot).

5.2 Dissolved organic carbon (DOC)

The distribution of DOC in Region 19 was reported by Kim and Kim (2010) and Kim et al. (2015). The average DOC concentrations over the entire area of Region 19 were 68 ± 6 μM in the surface layer (0–200 m) and 58 ± 4 μM in the deep (>200 m) layer (Figure R19-25a). In general, the DOC concentrations in the surface layer were comparable to those in the major world oceans (60–80 μM) (Carlson and Ducklow, 1995; Hansell and Carlson, 1998a; Doval and Hansell, 2000). The DOC concentrations in the deep layer of the sea were remarkably constant and significantly higher than those in the major oceans (34–43 μM) (Bauer et al., 1992; Sharp et al., 1995; Thomas et al., 1995; Hansell and Carlson, 1998b) and the Mediterranean Sea (avg.: 40 μM) (Santinelli et al., 2010). The DOC/apparent oxygen utilization (AOU) ratio (C/O_2 = -0.09) in the deep sea was much smaller than the Redfield ratio (C/O_2 = -0.77) (Kim and Kim, 2010; Kim et al., 2015). This DOC/AOU ratio indicates that the oxidation of DOC contributes insignificantly to deep ocean oxygen utilization (Kim et al., 2015). In addition, the source of DOC in the deep sea was found to be of marine origin on the basis of δ^{13}C-DOC signatures (Kim et al., 2015). These high concentrations of DOC in the entire deep water column seem to be due to low temperature (<1°C) and rapid turnover time of this marginal sea (~100 years).

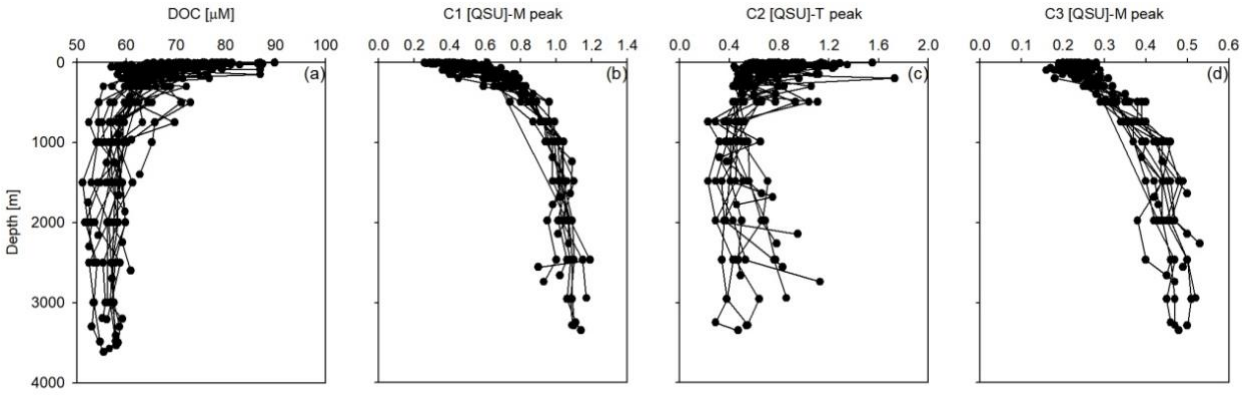

Figure R19-25. Vertical profiles of dissolved organic carbon (DOC; a) and three components of fluorescent dissolved organic matter (FDOM; b,c,d) in the sea of region 19 (DOC data from Kim et al., 2015 and FDOM data from Kim and Kim, 2016).

5.3 Fluorescent dissolved organic matter (FDOM)

The distribution of fluorescent dissolved organic matter (FDOM) in Region 19 was reported by Tanaka et al. (2014), Kim and Kim (2015), and Kim and Kim (2016). The fluorescent intensity of the protein-like component generally decreased with depth although some higher intensities were found in deep water (Figure R19-25c). The higher intensities in the surface water are likely to be linked to primary production and freshly produced organic substances.

The fluorescent intensity of the humic-like component was negatively correlated with salinity in the surface water of the sea and the continental shelves (Kim and Kim, 2015). This trend suggests that the Changjiang River water may be the primary source of humic-like FDOM occurring in the surface layer of Region 19. In contrast to the protein-like component, the humic-like component increased with depth, as typically described by previous studies (Yamashita and Tanoue, 2008) (Figure R19-25b,d). It seems to be associated with photobleaching at the surface-water layer and *in situ* microbial production in the deep-water column based on the positive relationship with AOU. In this region, the excess of the humic-like FDOM relative to that expected from the observed AOU was found below 1000 m depth (Tanaka et al., 2014; Kim and Kim, 2016). Kim and Kim (2016) showed that this excess FDOM originates from anaerobic FDOM production in the bottom sediment with exceptionally high sedimentary organic matter contents (1–5% wt).

5.4 Particulate organic matter

Flux of sinking particulate organic carbon (POC) has been measured by several studies using sediment traps. POC flux in the western and eastern Japan Basin, and in the Yamato Basin was reported for 2001 and 2002 (Otosaka et al., 2008). In addition to these, results in the Ulleung Basin were obtained in 2011-2012 (Kim et al., 2017). In the Ulleung Basin, monthly POC flux followed the temporal variation of net primary production (Figure R19-26). About 3 % of net primary production reached 1000 m. Annual average POC flux at 1000 m was 9.1 gC $m^{-2}yr^{-1}$. Biogenic opal accounted for 36 % of sinking particles on average and was the dominant component of the biogenic particles (~62 % of the biogenic particles). Spring and fall bloom peaks were mostly driven by biogenic opal flux implying the dominant role of diatoms. Biogenic $CaCO_3$ accounted for 14 % on average (Kim et al., 2017). Sinking particles in Region 19 contain a large fraction of lithogenic material derived from sediment resuspension and aeolian dust deposition. Aluminium content of the sinking particles was 2-3 % (Table R19-1). The Radiocarbon content of sinking POC was significantly lower than the values of dissolved inorganic carbon in the surface water at all sites showing significant contributions of aged organic carbon likely from sediment resuspension to sinking particles (Otosaka et al., 2008; Kim et al., 2017).

Table R19-1. Primary production (gC $m^{-2}yr^{-1}$) in the surface water, sinking POC flux (gC $m^{-2}yr^{-1}$), $\Delta^{14}C$ (‰), Al (%), and Al flux (g $m^{-2}yr^{-1}$) of sinking particles at ~1000 m in the major basins of Region 19. The data of the Japan Basin and the Yamato Basin are from Otosaka et al. (2008) and the data of the Ulleung Basin are from Kim et al., (2017). This table was modified from Kim et al. (2017).

		Ulleung Basin	W-Japan Basin	E-Japan Basin	Yamato Basin
Primary production	Satellite obs.	266	212	233	256
	in situ meas.	273			
Sinking POC flux (~1000 m)		9.1	11.2	4.4	8.7
$\Delta^{14}C$ (‰)		11±15	−13±18	−21±20	−3±28
Al %, (Al flux)		2.6 (3.1)	2.8 (4.3)	2.0 (1.0)	2.7 (2.5)

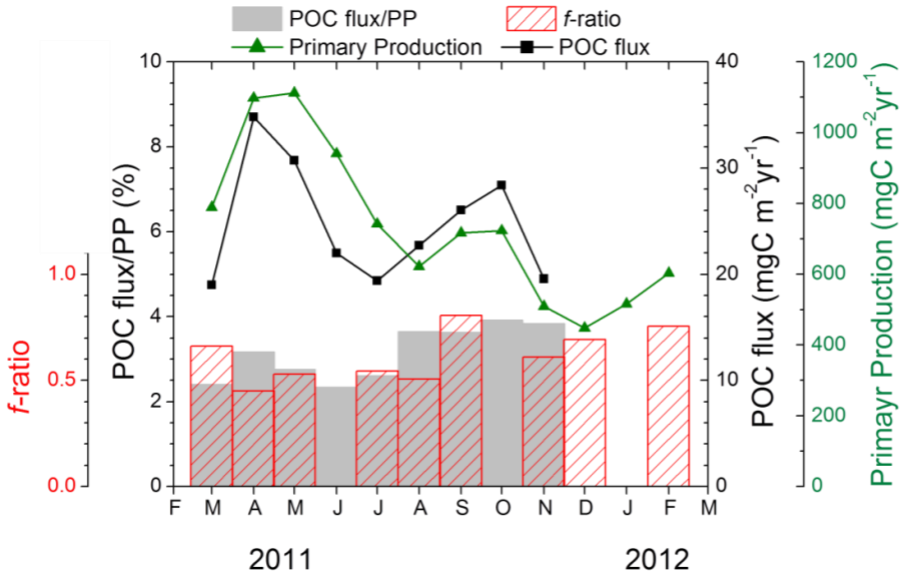

Figure R19-26. Monthly POC flux at 1000 m, primary productivity in the surface water (Joo et al., 2014), POC flux/Primary production ratio, and *f*-ratio (Kwak et al., 2013a, b) in the Ulleung Basin (Kim et al., 2017).

5.5 Carbonate system and acidification

Since the first systematic survey of CO_2 parameters in 1992 (Chen et al., 1995), several studies examined the carbonate system of Region 19. A large uptake of anthropogenic CO_2 from 1992 and 1999 was proposed by Park et al. (2006). However, the same authors showed that the CO_2 absorption rate decreased considerably from 1999 to 2007 from 0.6 ± 0.4 mol C $m^{-2}yr^{-1}$ to 0.3 ± 0.4 mol C $m^{-2}yr^{-1}$ (Park et al., 2008). This change in CO_2 absorption may be related to the change in deep water formation (Yoon et al., 2018) and needs to be further studied.
When the carbonate system of Region 19 is compared with the major ocean sites, values of dissolved inorganic carbon normalized to salinity of 35 (nDIC) were similar to the South Atlantic

(Figure R19-27; Na et al., in prep.). However, values of total alkalinity normalized to salinity of 35 (nTA) were lower than the South Atlantic. High primary productivity and relatively low export of $CaCO_3$ are presumably responsible for these characteristics (Na et al., in prep.). High DIC supply compared to low TA supply to the interior of Region 19 by biological pump makes the carbonate system vulnerable to acidification (Na et al., in prep.). This aspect should be further considered in the future study to project the future acidification of the sea.

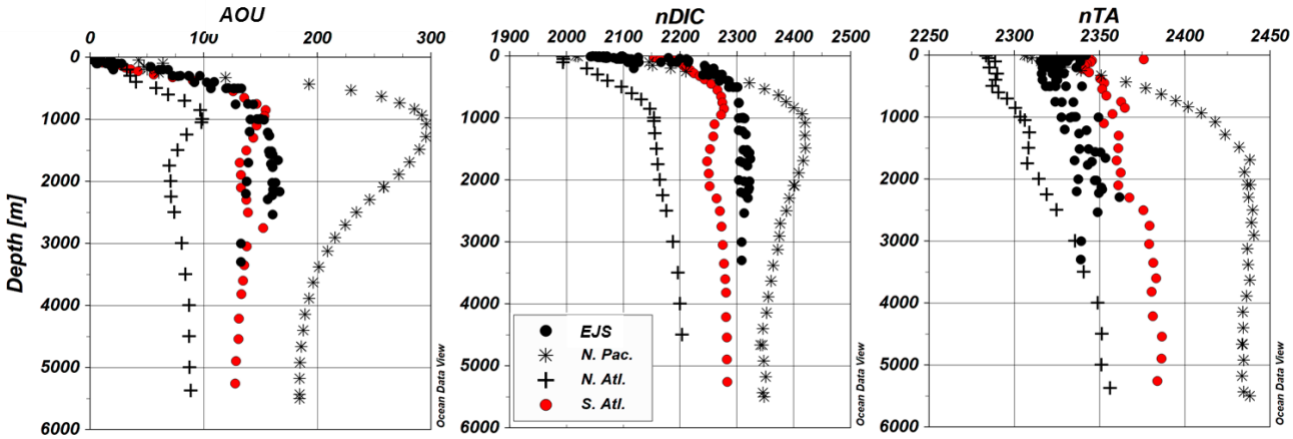

Figure R19-27. Apparent oxygen utilization (AOU), normalized dissolved inorganic carbon (DIC), normalized total alkalinity (TA) in Region 19 (EJS) are compared to those in the North Pacific (N.Pac.), North Atlantic (N.Atl.) and South Atlantic (S.Atl.) oceans (Na et al., in prep.).

In the surface water, rapid acidification indicated by fugacity of CO_2 (fCO_2) between 1995 and 2009 was reported for the Ulleung Basin (Figure R19-28; Kim et al., 2014). fCO_2 in the surface water was explained mostly by temperature variability. Non-thermal effect in fCO_2 was observed as decrease in summer and increase in winter. fCO_2 in the surface water increased during the study period at a rate of 2.7 ± 1.1 μatm yr^{-1}, which was higher than that in the atmosphere (1.8 ± 0.4 μatm yr^{-1}). Accordingly, estimated pH from total alkalinity and fCO_2 decreased at a rate of −0.03 ± 0.02 pH unit per decade. This rate was higher than observations at most ocean time-series stations (Kim et al., 2014).

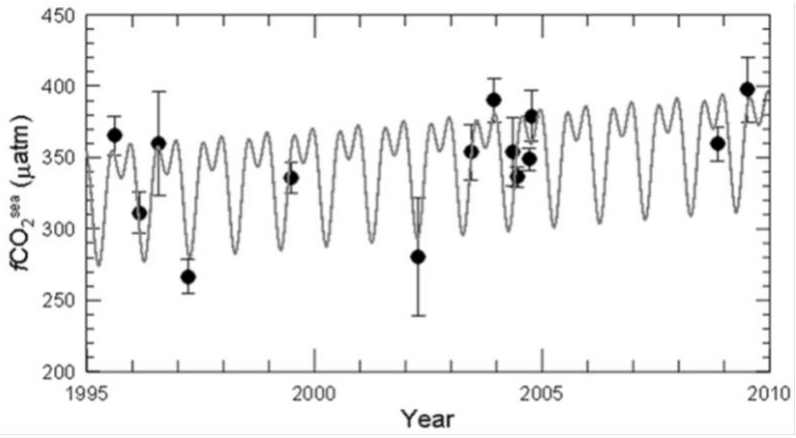

Figure R19-28. Temporal variation of fCO_2 (symbols) in the Ulleung Basin from 1995 to 2009. The gray curve represents fCO_2 fitted from a harmonic function analysis (Kim et al., 2014).

In the interior of Region 19, rapid acidification was reported by Chen et al. (2017). The authors estimated pH from long-term measurement data of dissolved oxygen (DO) concentration from 1965 to 2015 and showed that pH in the interior of the sea decreased (Figure R19-29; Chen et al., 2017). Slowdown of deep water ventilation and accumulation of CO_2 supplied from organic matter decomposition was suggested as the cause of the rapid acidification. Further acidification in the future is proposed as the deep water ventilation slows down (Chen et al., 2017), which needs to be monitored further.

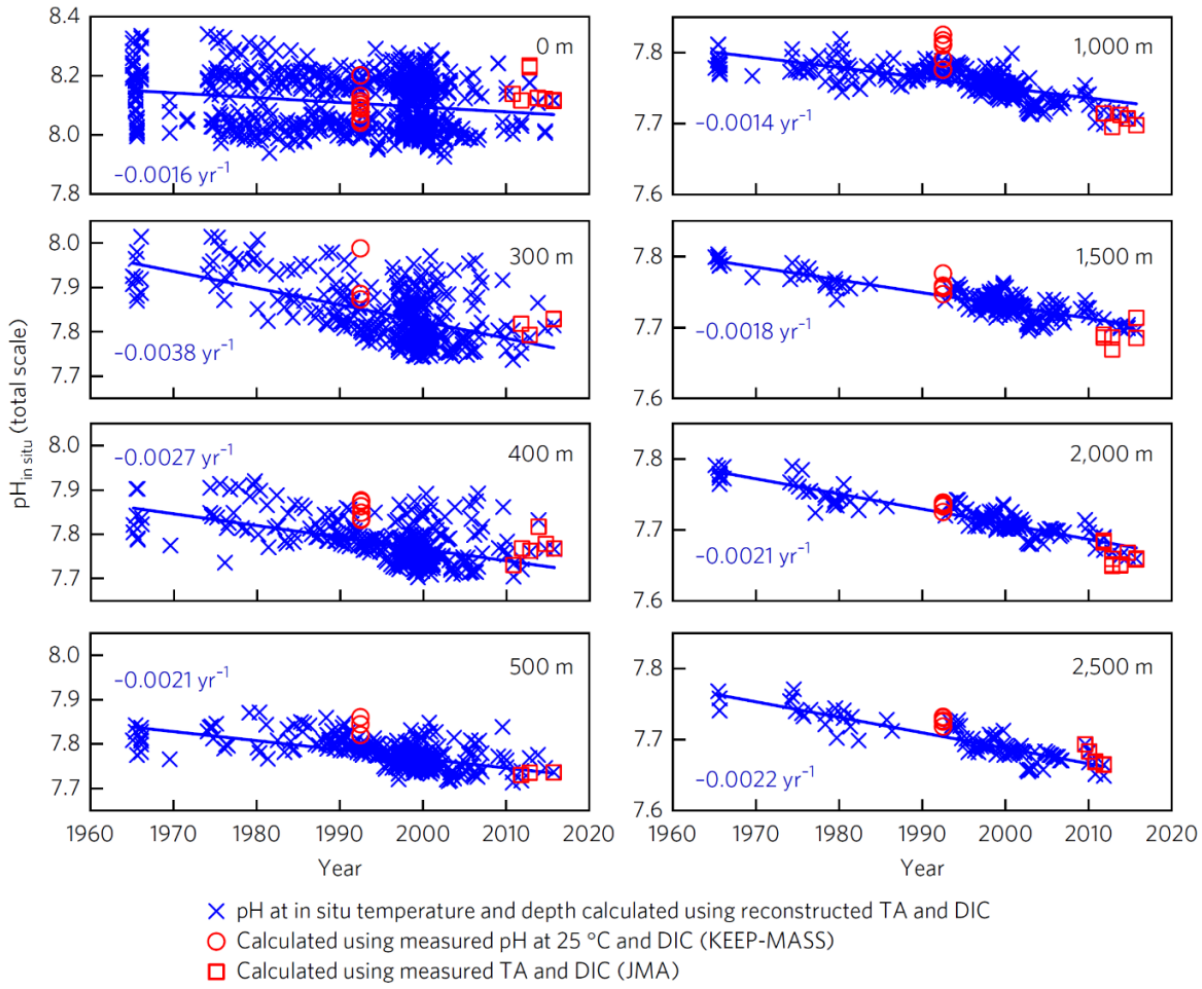

Figure R19-29 - Secular trend of pH at various depths between 1965 and 2015 (Chen et al., 2017).

6. Phytoplankton

J. Ishizaka, W. Kim, Y.-W. Lee, P. Chandler

6.1 Time Series of in situ chlorophyll-a off Korea

Time-series data of seasonal chlorophyll-a concentration in the eastern coastal areas of Korea were obtained from 2011 to 2015 (MOF, 2011, 2012, 2013, 2014, 2015). These data were measured at 87 stations along the Korean coast, from Geojin to Gijang (35.16°-38.44°N, 128.46°-129.59°E). The average concentrations of chlorophyll-a were in the ranges 0.74-7.22 mg m^{-3} (mean: 2.46 ± 1.70 mg m^{-3}) (Fig. R19-30). In general, chlorophyll-a concentration in surface seawater were high in August. It appears that chlorophyll-a concentration in surface seawater is related to nutrient input during the rainy season.

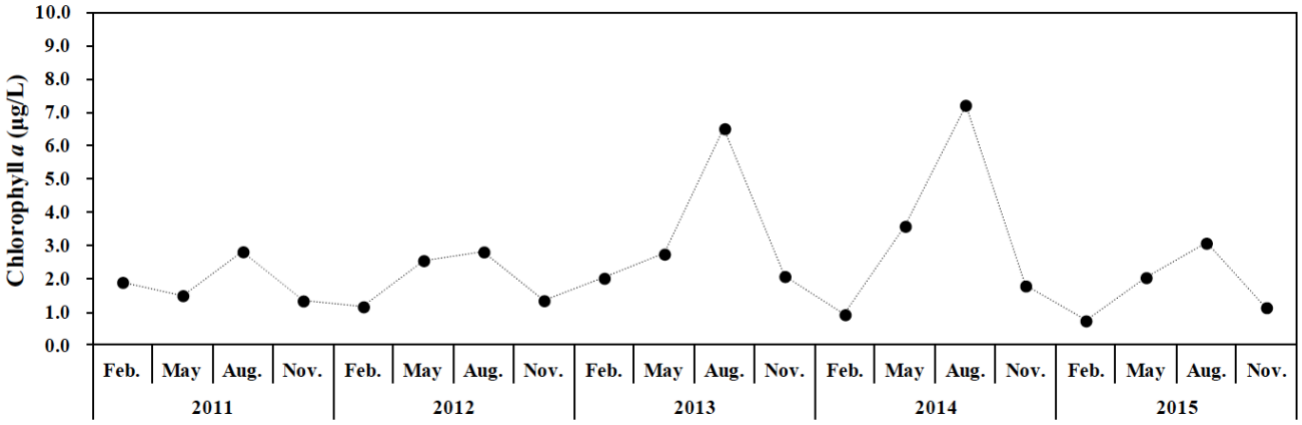

Figure R19-30. Temporal variations of monthly-mean chlorophyll-a averaged over all the 87 stations along the eastern coast of Korea from 2011 to 2015 (from submitted ETSO, Y.-W.Lee).

6.2 Time Series of satellite chlorophyll-a (GOCI) off Korea

Chlorophyll-a pigment concentration data have been produced over the sea areas around Korea from Geostationary Ocean Color Imager (GOCI) using the atmospheric correction and the OC3 chlorophyll-a algorithm (Ahn et al., 2015, 2016; Kim et al., 2016). Three-year time-series of weekly medians (2013-2015) were extracted from the GOCI data for the Ulleung Basin (southwestern part of Region 19 off Korea south of Ulleung Island). Fig. R19-31 represents for the 1st and the 3rd quantiles of all GOCI data in the weekly period acquired for the designated area. A strict quality control process has been applied to the GOCI data selection, where data samples with poor quality (e.g. near-cloud pixels) were discarded from the time series analysis.

Seasonal average plots of chlorophyll-a show clear variability with high concentrations observed in spring and fall seasons (Fig. R19-31). The time series exhibit the bi-modal seasonal pattern that corresponds to the two bloom seasons (spring and fall) and two minimum concentration seasons (summer and winter) (Fig. R19-32). The values of chlorophyll-a concentration are around 0.5 mg m^{-3} or lower except spring and fall.

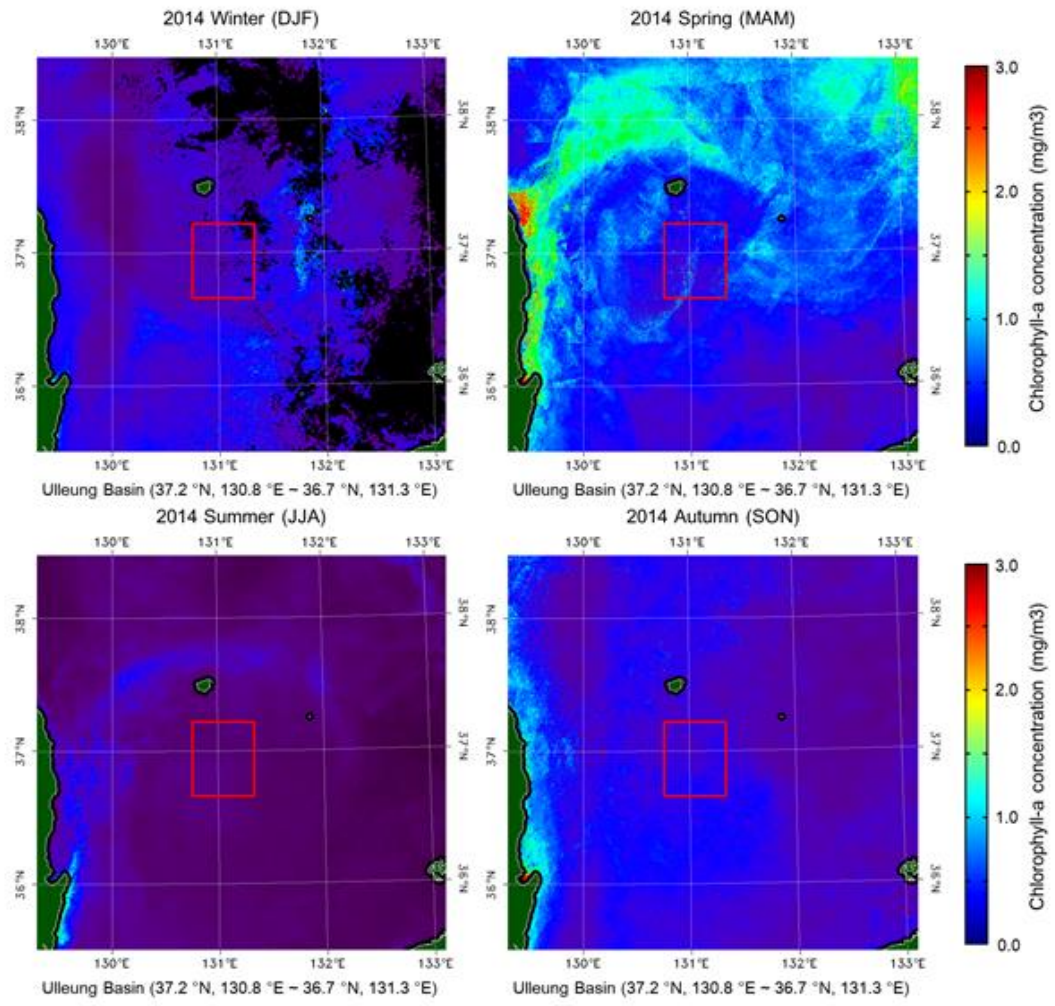

Figure R19-31. Seasonal distribution of 2014 GOCI chlorophyll-a in the Ulleung Basin area. Red square indicates the area of the time series shown in Fig. R19-32.

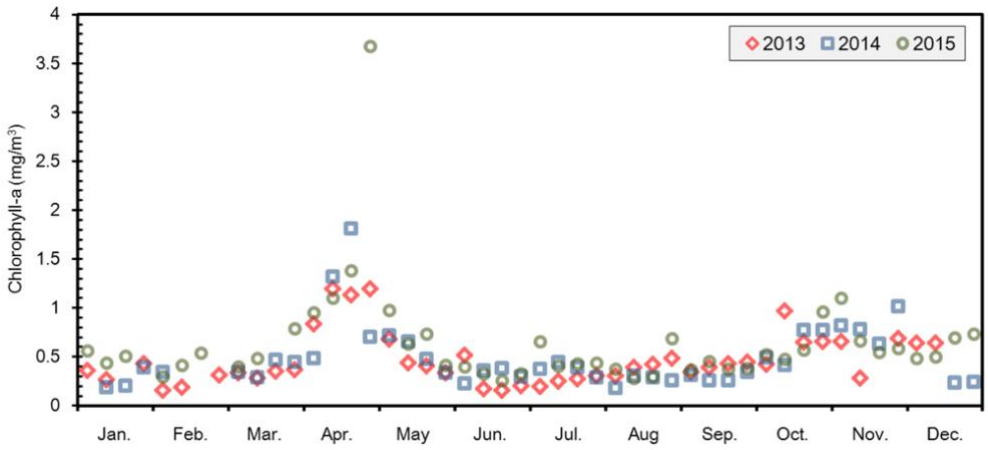

Figure R19-32. Time series of chlorophyll-a from Ulleung Basin area shown in Fig. R19.31 (from submitted ETSO, W. Kim).

6.3 15-year time series of satellite chlorophyll-a in three regions

Time series of chlorophyll-a concentration from July 2002 till December 2016 at three locations representing northeastern, central and southwestern parts of Region 19 averaged over an area of 1º latitude by 1º longitude, obtained from MODIS satellite data (NASA, 2018) are presented at Fig. R19-33. Two seasonal peaks (spring and fall) are noticeable at all three time series. Spring peak is slightly higher than the fall's one which is consistent with the observations presented in previous section. Seasonal peaks are slightly higher in the southern area (Fig. R19-33c) in compare with the central and northern areas (Fig. R19-33 a,b). This 15-years time series shows inter-annual variability with highest chlorophyll-a concentration during the spring bloom in 2015 in the northern area and 2008 in the central and southern areas. The 2008 spring peak was extremely high the south exceeding average value around 10 times.

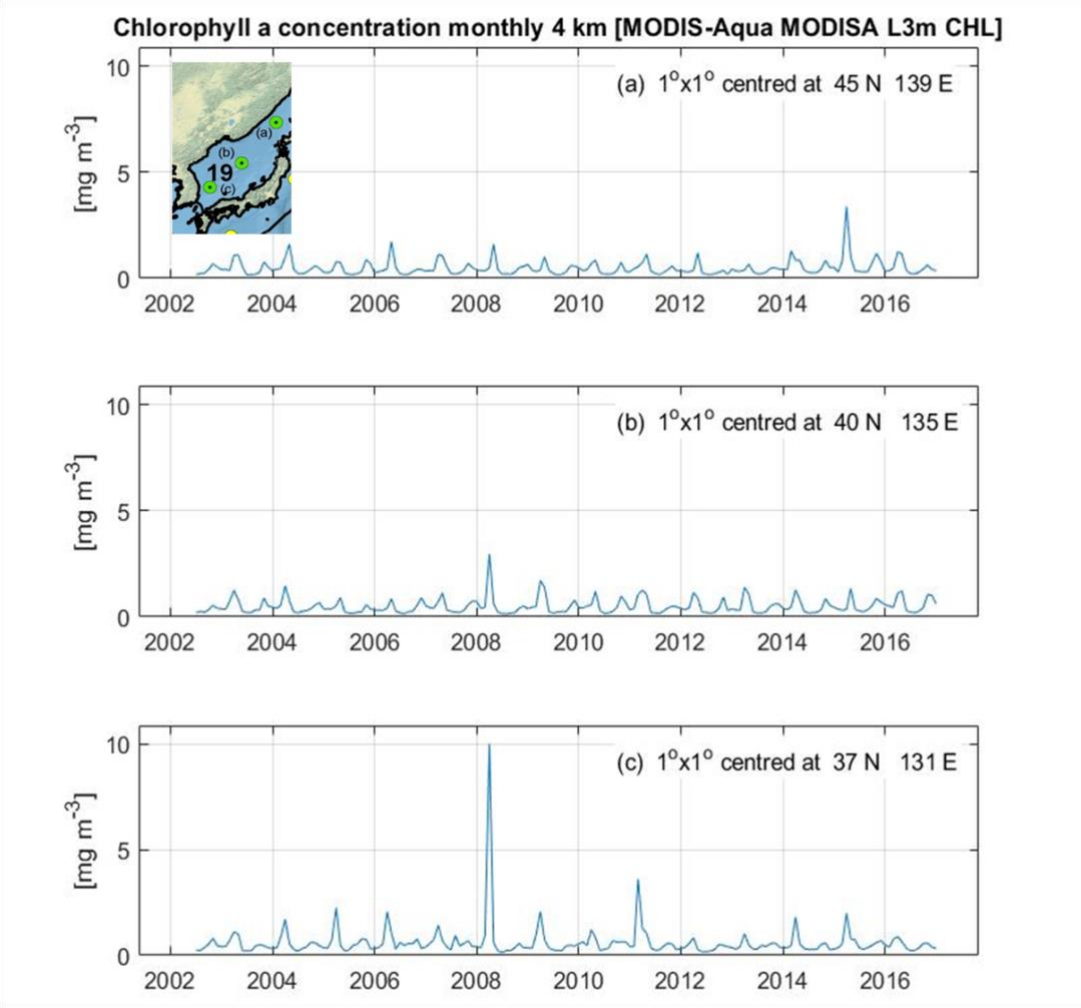

Figure R19-33. Time series of chlorophyll-a concentrations at three locations of Region 19 obtained from MODIS satellite data (green dots in map) (from submitted ETSO, P. Chandler).

6.4 22-year time series of satellite chlorophyll-a in four regions

Four points of Region 19, Primorye coast (46.5°N, 139°E), mid-Japan Basin (41°N, 136°E), southeast (38°N, 136°E) and southwest (38°N, 131°E) shown at Fig. R19-34, which were used by Yamada et al. (2004). Monthly and annual data, was extracted from the merged SeaWiFS and MODIS chlorophyll-a data from 1998-2019 from Environmental Watch System of NOWPAP/CEARAC (Terauchi et al., 2018).

Chlorophyll-a concentration was highest in the southwestern area (2-3 mg m^{-3}), followed by Primorye coast (1-1.5 mg m^{-3}), and northeast and mid-Japan Basin (0.4-0.5 mg m^{-3}) (Fig. R19-35). The seasonal pattern of chlorophyll-a concentration in these areas was generally consistent with the Ulleung Basin data shown in previous section. There are spring and fall blooms for all four areas, but variation was large in the southwestern area. The spring blooms are very conspicuous in some years in all four regions. The monthly and yearly variations seems to be large and trends were not very clear; however Sen's slope test indicates chlorophyll-a showed increasing trend in Primorye coast and mid-Japan Basin, and no trend in southwestern and southeastern areas. The reason or the regional difference in chlorophyll-a trend is not known and necessary to understand.

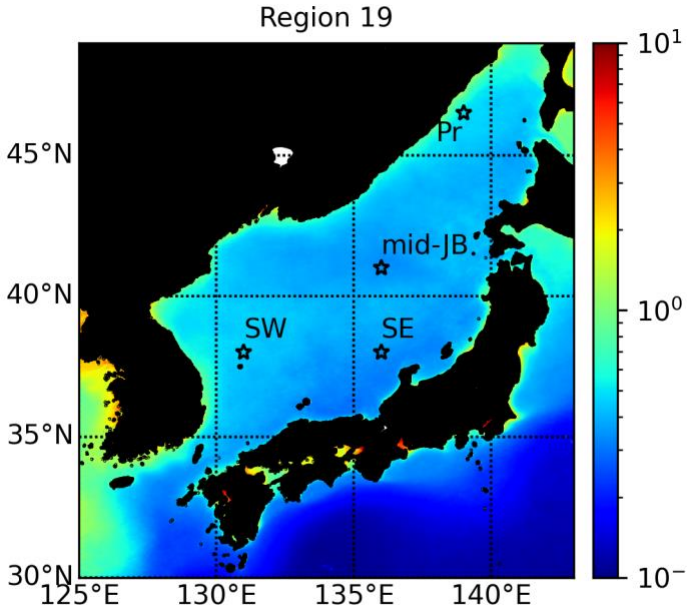

Figure R19-34. Chlorophyll-a averaged from 1998-2019 and locations of 4 stations for the time series. Pr, mid-JB, SE, and SW indicated Primorye coast (46.5°N, 139°E), mid-Japan Basin (41°N, 136°E), southeast (38°N, 136°E) and southwest (38°N, 131°E), respectively.

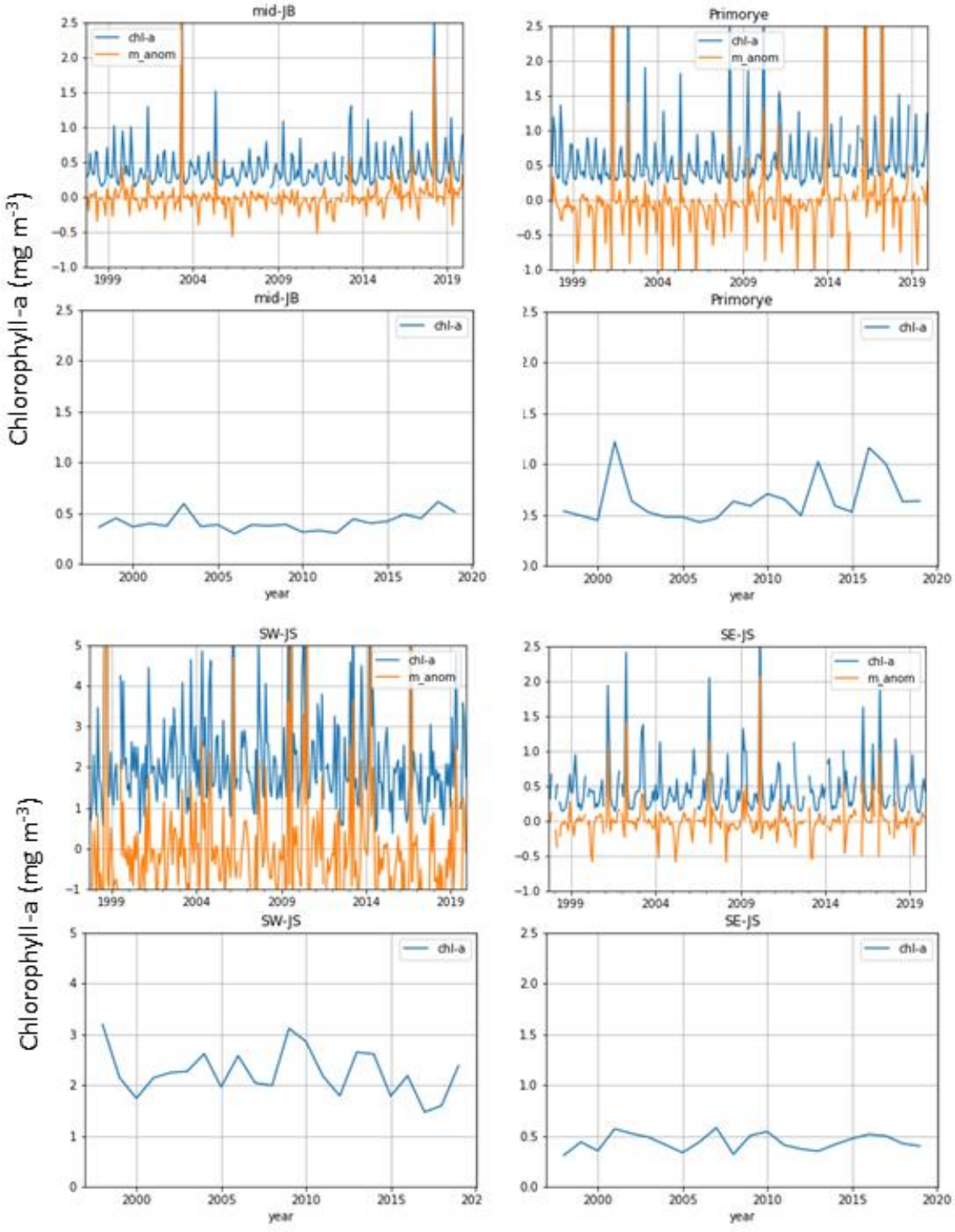

Figure R19-35. Satellite chlorophyll-a time series of 1998-2019 from four stations shown in Fig. R19-34. Top panel indicates monthly data of chlorophyll-a and monthly anomaly (m_anom). Bottom panel indicates yearly chlorophyll-a average calculated from the monthly data.

7. Zooplankton

H.-C. Choi, N. Dolganova, N. Iguchi, Y. Zuenko

In the southwestern part of Region 19, the total biomass density of zooplankton and abundance of its four main taxa (copepods, chaetognaths, amphipods, and euphausiids) are monitored by National Institute of Fisheries Science (Rep. Korea). The survey is conducted bimonthly (6 times/year, in February, April, June, August, October, and December) at 8 lines with 69 stations (Fig. R19-36). Spatially averaged biomass of total zooplankton was usually higher in spring (April) and fall (October) than those of other months, with the lowest value in summer (August) and winter (December) (Fig. R19-37).

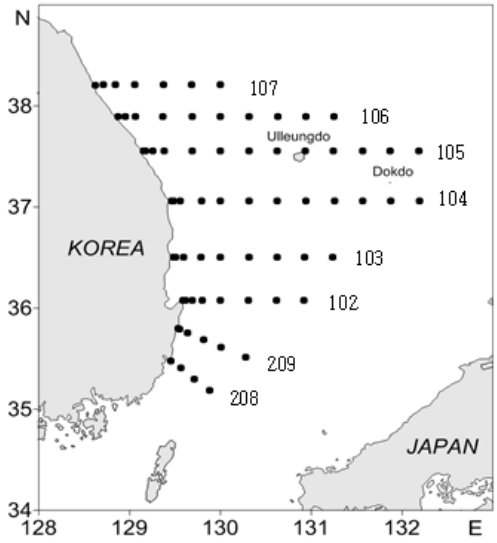

Figure R19-36. Sampling lines and stations of plankton survey in the southwestern part of Region 19.

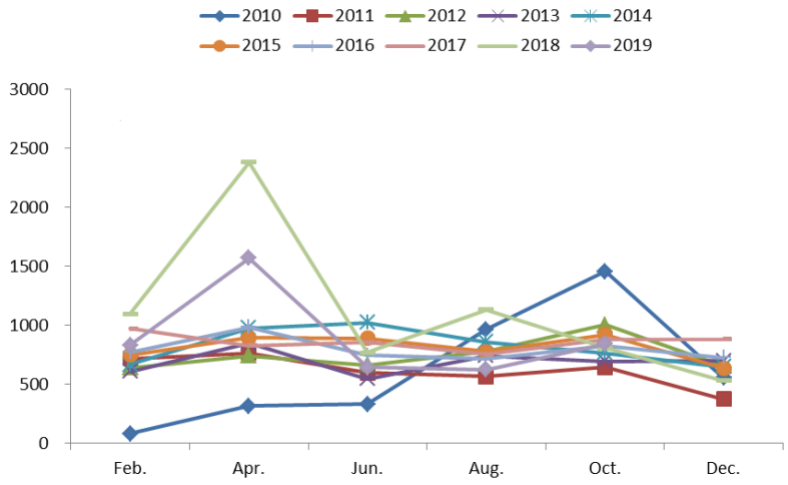

Figure R19-37. Seasonal fluctuations of total zooplankton biomass, by years (mg m^{-3}, wet weight). Data for December 2019 are absent.

In the last decade (2010-2019), the annual mean biomass of meso- and macro-zooplankton in this area tends to increase, with some fluctuations (Fig. R19-38). Annual mean anomalies of the total zooplankton biomass shifted from negative to positive values in the middle of decade (Fig. R19-39).

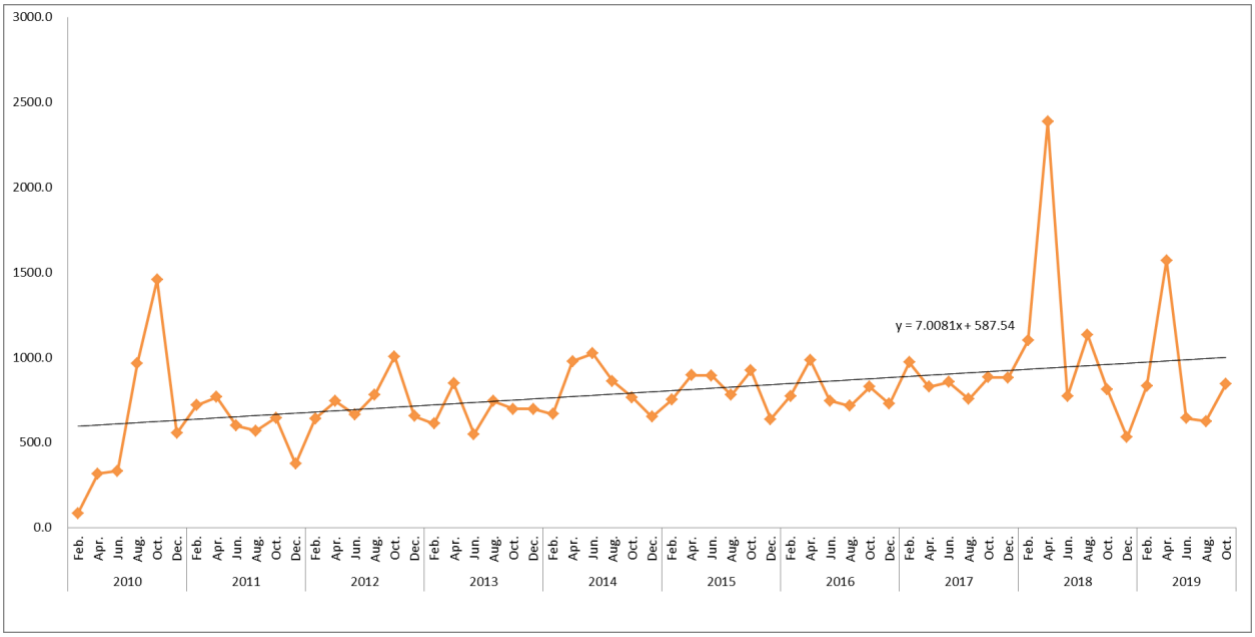

Figure R19-38. Dynamics of total biomass of meso- and macro-zooplankton, mg m^{-3}, wet weight. Linear trend for 2010-2019 is shown.

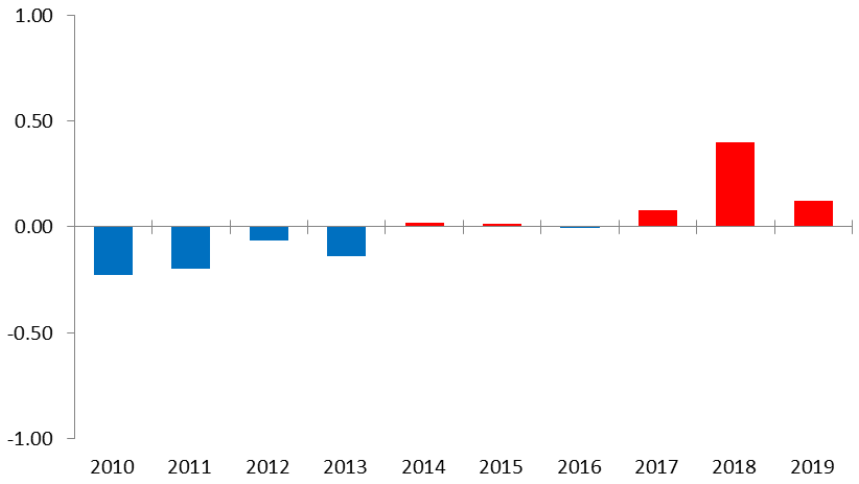

Figure R19-39. Interannual variability of the annual anomaly of total zooplankton biomass.

Abundance of the main taxonomic groups had a similar decadal trend and variability, except that of euphausiids. The abundance of copepods, chaetognaths, and amphipods increased abruptly after 2016 (Fig. R19-40). Copepods and chaetognaths showed the highest values in

2019, but the highest value of amphipods was recorded in 2018, and slightly decreased in 2019. On the other hand, changes of euphausiids abundance tended to be the opposite of the other three taxa, although they increased merely after 2018, as well. Seasonal variations of these groups are also different - copepods are the most abundant in April, euphausiids – in April-June, amphipods – in June, but chaetognaths – in October.

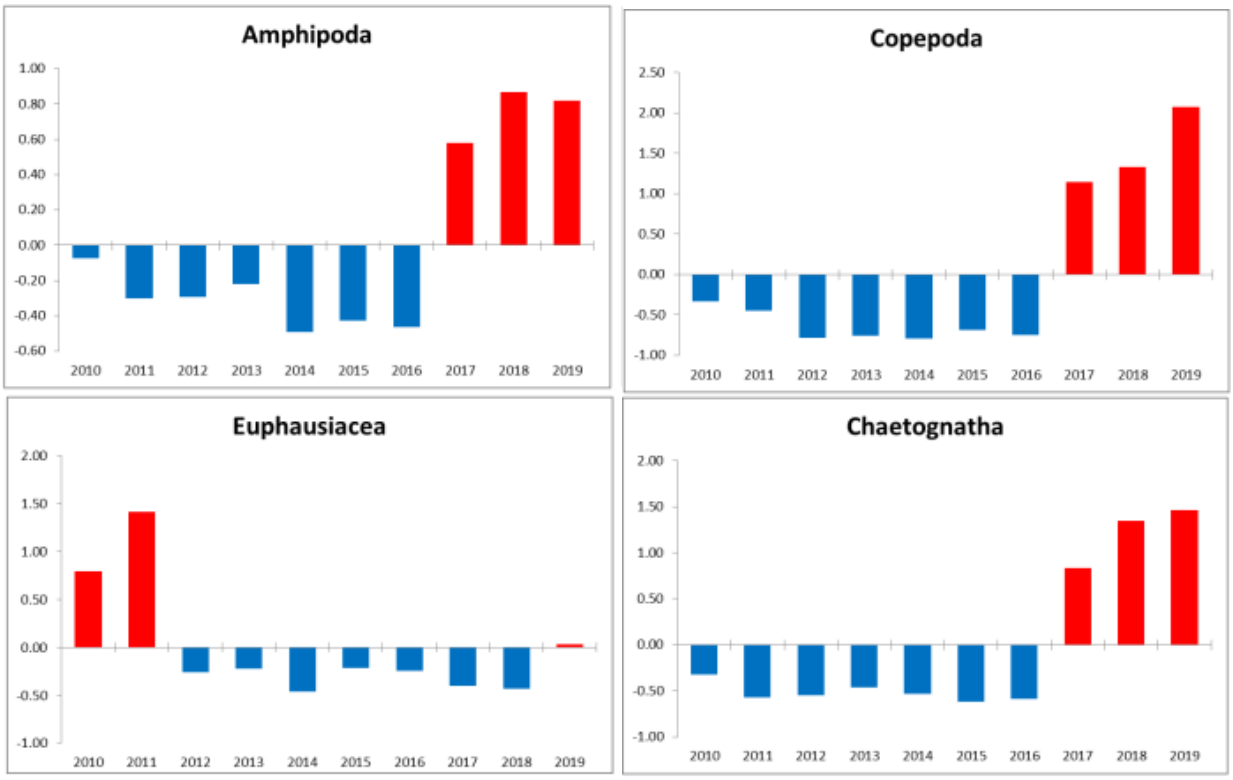

Figure R19-40. Standardized annual anomalies for abundance of four taxonomic groups of zooplankton.

In the southern and southeastern parts of Region 19 occupied by the coastal branch of Tsushima Warm Current, zooplankton community was monitored by the Fisheries Research Institute (Japan) in May from 1999 to 2013 at 26 stations located at the coastal area between Wakasa Bay and Toyama Bay (Kodama et al., 2018b). The samples were collected with vertical hauls of a NORPAC net (0.335 mm mesh, 0.45 m mouth diameter) from the layer of 150 m depth to the sea surface. In total, 78 species were identified, with 7 copepods species (*Psudocalanus newmani, Oithona plumifefra, Paracalanus parvus, Calanus vanus, C. sinicus, O. atlantica, calanus affinis),* 1 appendicularia (*Oikopleura longicauda*), 1 euphausiacea (*Euphausia pacifica*), and 1 cladocera (*Evadne nordmanni*) among the top 10 dominant species (Fig. R19-41). Multivariable analysis shows no clear spatial or temporal tendency in the total abundance of zooplankton. Warm-water species dominated in the whole monitored area, except Toyama Bay, where cold-water species were numerous because of the offshore position of the warm current. The species richness (number of species per station) was higher in 2000-2002, 2009 and 2011-2013 than in other years.

Appendicularians are one of the major zooplankton groups in Region 19. Compared with production data of predominant zooplankton species in the southern part of Region 19, despite their smaller biomass, appendicularians are an important secondary producer (Tomita et al. 1999). Monitoring of the appendicularians in the southern area was conducted in July from 2011 to 2015 at 49 stations (Kodama et al 2018b). At every station, zooplankton were collected with vertical hauls of NORPAC net (0.100 mm mesh, 0.45 mouth diameter) up to the surface from a depth of 200m. Ten appendicularian species were identified and *Oikopleura longicauda* was the most dominant species. The abundance was positively related to habitat temperature although salinity and Chl a concentration were not significantly related to abundance. *O. longicauda* and other appendicularians were high in 2013 but the reason for yearly variation is not clear (Fig. R19-42).

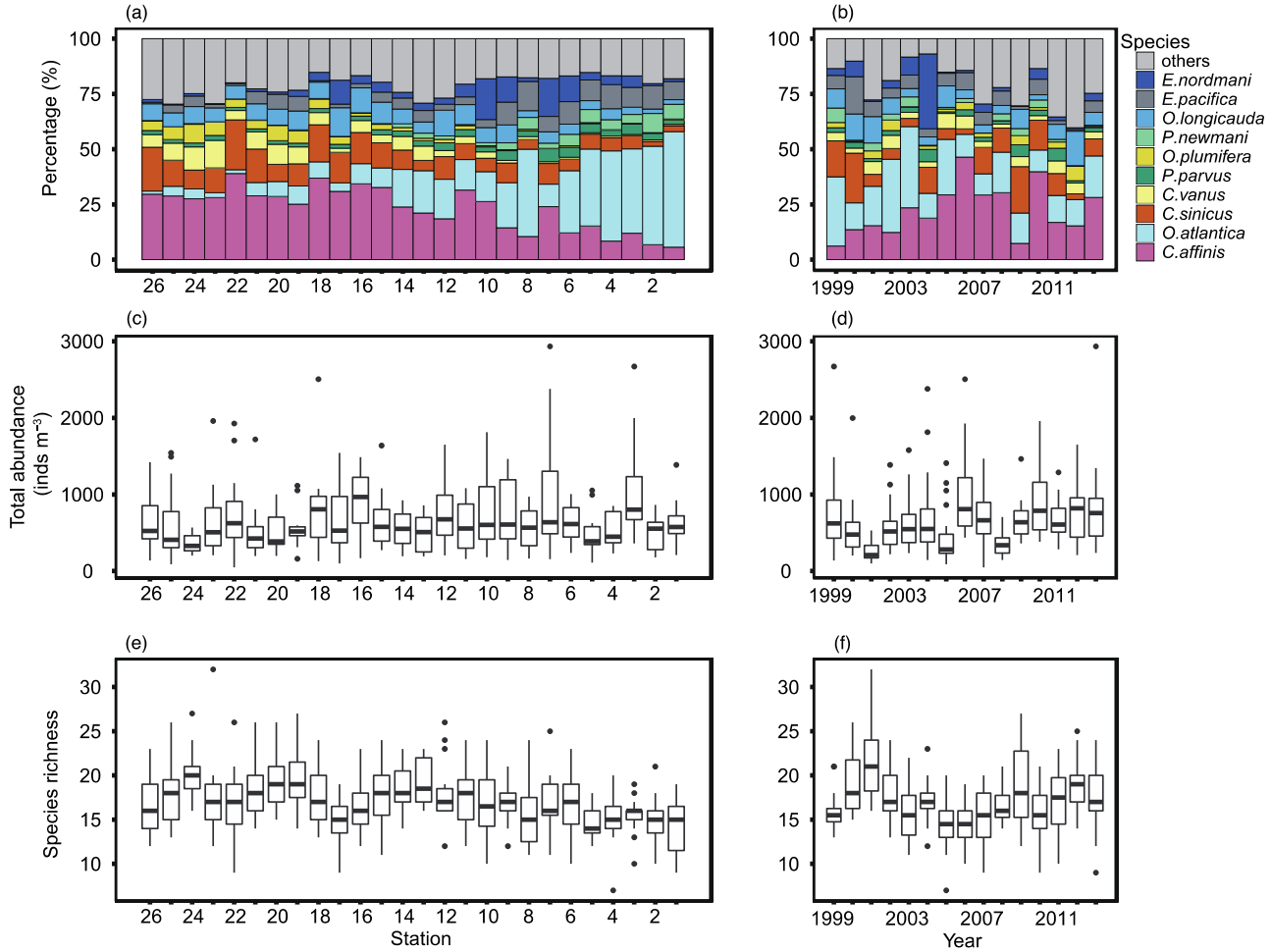

Figure R19-41. Spatial (left) and year-to-year (right) variations of the top 10 most abundant species percentage, (upper panel), total zooplankton abundance (middle panel), and species richness (lower panel). Total zooplankton abundance plots show the median (horizontal lines within boxes), upper and lower quartiles (boxes), quartile deviation (bars), and outliers (circles), (Kodama et al., 2018b).

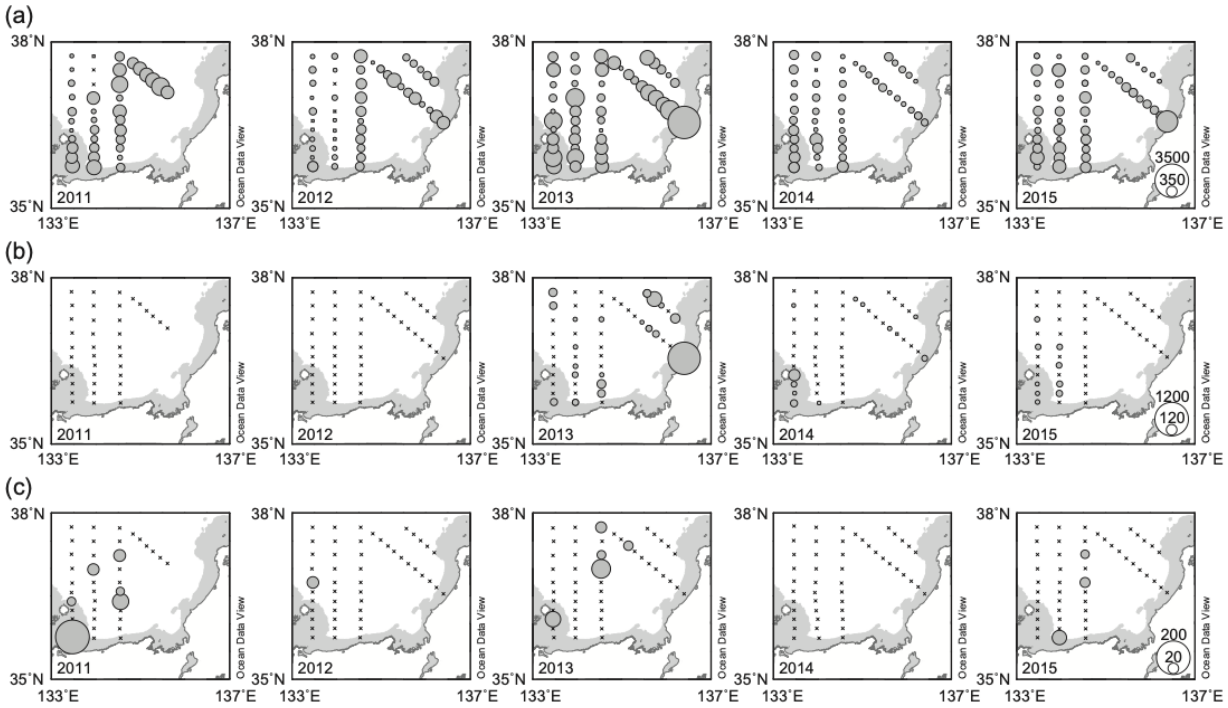

Figure R19-42. Spatial and yearly variations in the abundance of genus *Oikopleura* in Region 19 off Japan. (a) *O. longicauda*, (b) *O. fusiformis*, (c) *O. dioica*. The size of each circle denotes abundance and a reference scale for abundance is shown for each species in the panels for 2015. A cross indicated that abundance was 0 (modified from Kodama et al. 2018a).

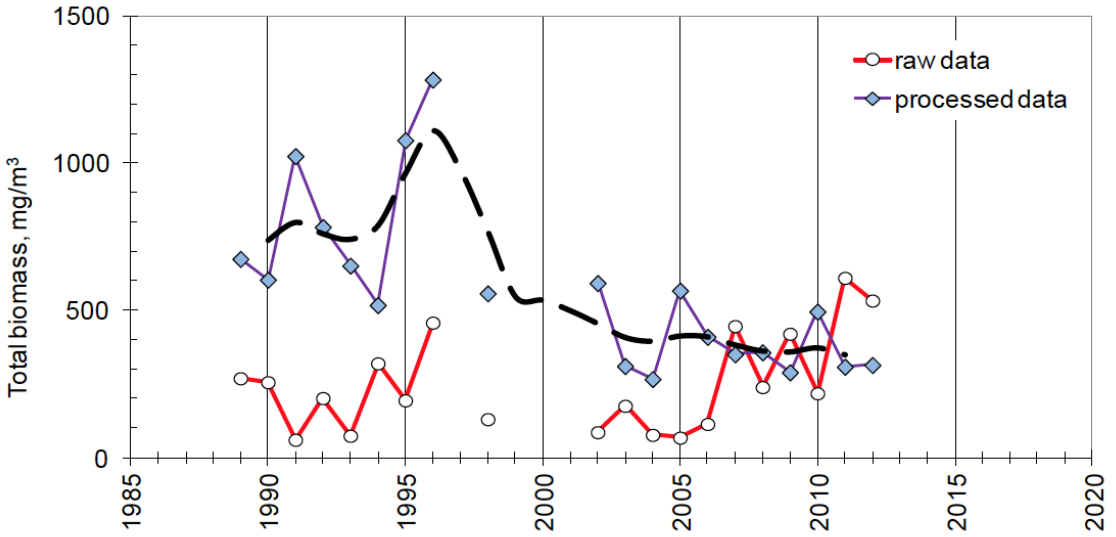

Figure R19-43. Year-to-year dynamics of total mesozooplankton biomass in the 0-200 m layer at Primorye coast in May, averaged for 41°30-42°30 N 131-134° E. Raw data – wet weight recalculated from number of animals in catches of Juday net; processed data – estimated wet weight *in situ* considering the Juday net catch efficiency by species. Results of 3-year running mean of the processed data are shown by a dotted line.

Monitoring of zooplankton in the northern part of Region 19 was conducted by Pacific Fisheries Research Center (TINRO, Russia), though it was stopped in 2013. Cold-water species prevail in these waters, with the highest biomass of copepods *Necalanus plumchrus*, *N. flemingeri*, *Calanus cristatus*, *Metridia pacifica*, *Oithona similis*, amphipod *Themisto japonica* and arrowworms, mainly *Parasagitta elegans* (Dolganova and Zuenko, 2004). Besides that, warm-water species are transported to the region from the subtropic zone in summer (*Calanus pacificus*, *Paracalanus parvus parvus*). Small-sized neritic copepods (*Pseudocalanus newmani*, *Acartia clausi*) and cladoceras (*Evadne nordmanni*, *Podon leuckartii*) are abundant in the coastal zone, and deep-water species penetrate there too. Recently the dominant cold-water species abundance had a tendency of decreasing (Fig. R19-43). This tendency coincided with and, supposedly, was caused by general warming of the sea and its productivity decreasing (Kang et al., 2012), whereas the abundance of southern migrants became larger (Nadtochy and Zuenko, 2016).

Among macrozooplankton species, jellyfish are the most important because of their great abundance and commercial value. The jellyfish *Nemopilema nomurai* is a large rhizostome medusa that primarily inhabits the Bohai Sea, the Yellow Sea, and the northern East China Sea, but since 2002 dense aggregations of *N. nomurai* appeared in Region 19, which had some negative economic consequences such as reduction of fish harvests owing to clogging of fishing nets. Mass occurrences of *N. nomurai* at the Japanese coast were observed in 2002–2003, 2005–2007, and 2009. In the last decade, no mass occurrence of this medusa was observed along the Japanese coast. However, some insignificant cases happened in the southwestern area, as it was observed in the coastal waters of Korea near Pohang city in August of 2018 (UPI, 2018).

Kitajima et al. (2015) investigated the spatial distribution of *N. nomurai* in the area off Japan in September-October of each year from 2006 to 2012 using a midwater trawl (Table R19-2). In the years of high abundance of this species, 2006, 2007, and 2009, the medusas were mainly distributed following the path of the second (offshore) branch of the Tsushima Warm Current >40 km off the coast of Japan in the western part of the area (Oki Island) and coming closer (>25 km) in the eastern part.

Table R19-2. *Nemopilema nomurai* abundance and size by the data of 7 surveys (Kitajima et al., 2015).

Sampling period	Mean abundance of *N. nomurai* [$(10^6\ m^3)^{-1}$]	Bell diameter [cm]		
		Range	Mean	*n*
Sept. 21 – Oct. 5, 2006	32.6	21–184	82	263
Sept. 24 – Oct. 7, 2007	9.9	45.4–147.0	89.0	92
Sept. 25 – Oct. 4, 2008	0			
Sept. 9–23, 2009	44.3	33.3–159.0	82.6	315
Sept. 5–21, 2010	0			
Sept. 17 – Oct. 2, 2011	0			
Sept. 8–22, 2012	0.7	42.8–98.5	70.2	7

8. Fishes and Invertebrates

Y. Zuenko, H. Kubota, K. Fujiwara, S. Kang, C. I. Lee

8.1 Northern area, off Russia

For the northwestern part of Region 19, walleye pollock *Theragra chalcogramma* (the species name is now being revised to *Gadus chalcogrammus*, but the appropriate procedure of revision is not completed yet) is the main commercial object of the Russian fishery nowadays. Japanese common squid *Todarodes pacificus* migrate to this area in the summer-fall season even in higher abundance but is poorly exploited. Japanese sardine *Sardinops sagax melanosticta* feeds here in mass in periods of the high stock years which is expected in the near future.

The pollock dwell in all parts of Region 19, excluding the southernmost area to the west of Noto Peninsula, mainly at depths of 50-450 m. The largest pollock stock is located traditionally in the East-Korean Bay. Other populations have their own spawning grounds located at Hokkaido and Northern Honshu, at Southern Primorye including Peter the Great Bay, and at Sakhalin. Different populations of pollock are distinguished by different seasons of spawning: fall-winter (December-March) in the East-Korea Bay and at Hokkaido but spring at Southern Primorye and Sakhalin. The life spans of these populations of pollock are shorter than in the Okhotsk and Bering seas and do not exceed 10-12 years, with high mortality after 5-6 years (Vdovin et al., 2017). Therefore the 2 to 6-year-old fishes dominate in the biomass.

Walleye pollock are caught mainly by trawls, Danish seine and gill nets in Korea, by trawls, longlines and gill nets in Japan, and by trawls and Danish seine in Russia. The main season of the pollock fishery is January-March. In the 1970s-1980s, pollock dominated in the northwestern part of Region 19, but later its biomass and catch dynamics had a strong negative trend. Annual landings of pollock in Rep. of Korea waters exceeded 100,000 t in the 1980s, but the stock was completely exhausted in the 2000s. Pollock fishery has almost ceased in Honshu and Sakhalin, though it still continues with low landings in Hokkaido and Primorye (Fig. R19-44, R19-45).

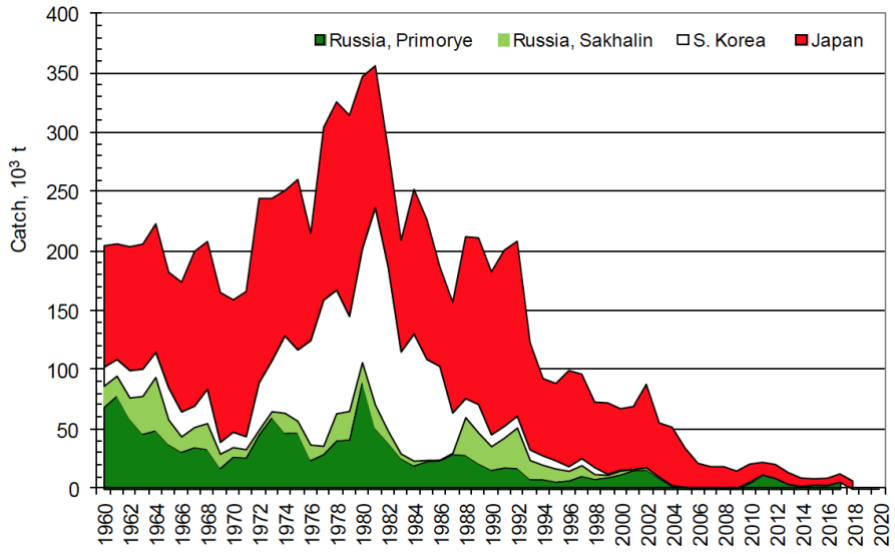

Figure R19-44. Walleye pollock annual landings in Region 19, by country.

Climate change is considered the main reason for the simultaneous declining of the pollock stocks, though interannual dynamics of reproduction for both populations corresponds to the stock-recruitment dependence described by Ricker curve that determines the maximum recruitment with an optimal value of stock equal to the carrying capacity of the biotope for the species and the lower recruitment if the stock is either lower or higher than this optimal value (Ricker, 1954). Under the environmental impacts, in particular weakening of winter monsoon, parameters of Ricker curve change, and their recent changes are unfavorable for the reproduction of the pollock populations which caused a decrease of pollock stocks with a sharp decline in the early 1990s. Reproduction of the Primorye population decreased because of unfavorable pollock reconstructions in the local ecosystem located in the southern periphery of the subarctic zone in conditions of increasing water temperature that is explained in terms of Ricker curve as a shrinkage of the biotope carrying capacity for pollock from approximately $150 \cdot 10^3$ t to almost zero level (Zuenko and Nuzhdin, 2018; 2019). Reproduction of the Hokkaido population decreased, too, as Ricker curve indicates a decrease in its population fecundity (Funamoto, 2011). This was caused by the increase in the transfer of its eggs and larvae out of the area favorable for spawning and larvae growth due to the strengthening of the Tsushima Warm Current. For the Korean population, besides the climate impact, excessive fishery of immature fish by use of non-selective fishing gears is considered as a possible reason of the stock exhaustion.

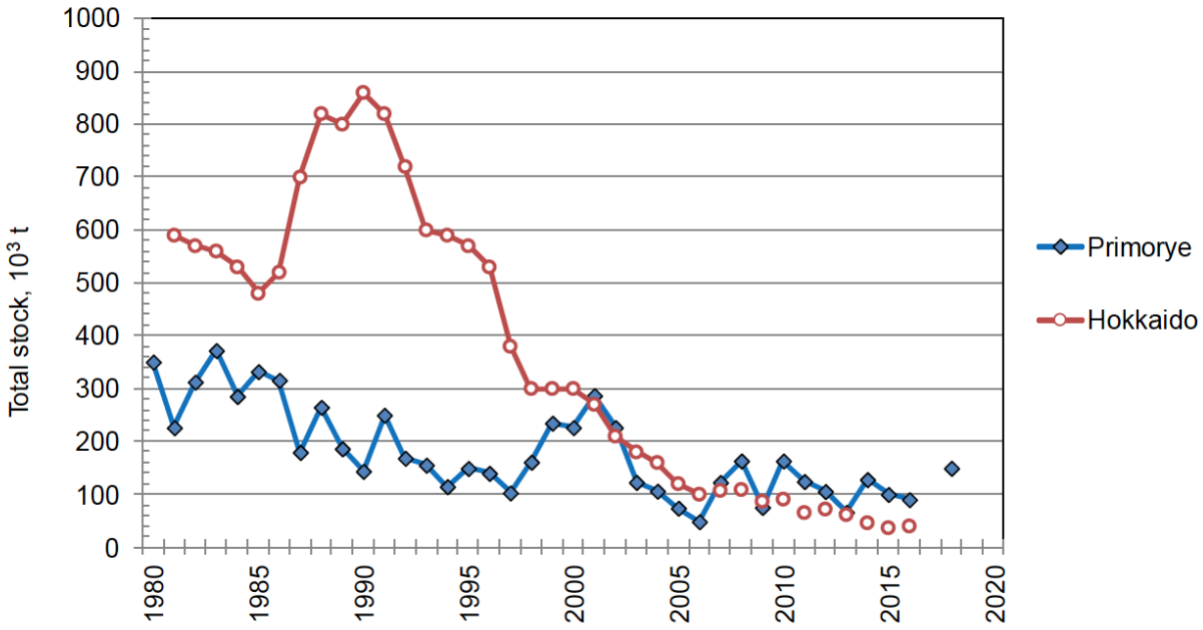

Figure R19-45. Dynamics of total stock for the Hokkaido and Primorye populations of walleye pollock (Funamoto, 2011, with the addition of restored data by Zuenko and Nuzhdin, 2019). The data for the Hokkaido population in 2007-2016 are restored following the annual catch dynamics.

8.2 Southern area, off Japan

Japanese sardine (*Sardinops melanostictus*) is distinguished by extremely high fluctuations in its stock. Annual catch in Region 19 and adjacent areas of the East China Sea by Japan has changed significantly in over 1500-fold magnitude, with the highest amount of 1.6 million metric ton in 1988 and the lowest amount of 1 thousand mt in 2001 (Fig. R19-46). The stock increased from low levels in the early 1970s to the highest biomass of 10 million mt in 1988, declined drastically to the lowest biomass of 4 thousand mt in 2003, and then has recovered in the recent years.

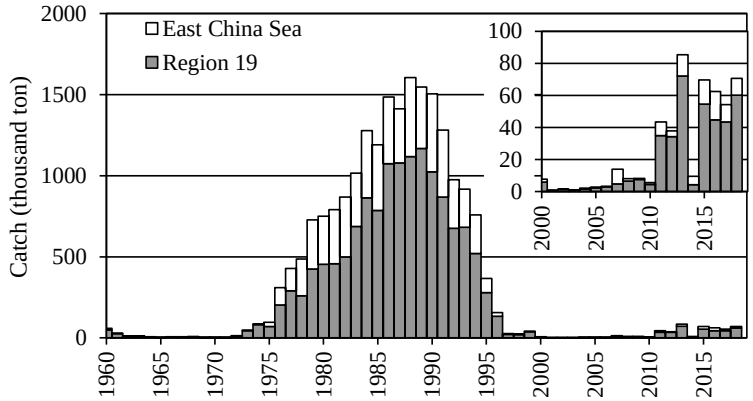

Figure R19-46. Annual catch of Japanese sardine in Region 19 and the East China Sea in Japan.

Jack mackerel (*Trachurus japonicus*) distributes mainly on the continental shelf of the East China Sea, from the waters off Kyushu, Japan, to the northern waters of Taiwan and the western part of Region 19. It is one of the most important target species for Japanese purse seiners (Yoda et al., 2014). Annual catch of jack mackerel in Region 19 and adjacent areas of the East China Sea by Japan and the Republic of Korea was the highest amount of 277 thousand metric ton, has been flat to down slightly in recent 20 years (Fig. R19-47). Fishing effort to the stock has been decreased since 1990's, and stock of jack mackerel was assessed in middle state in recent years.

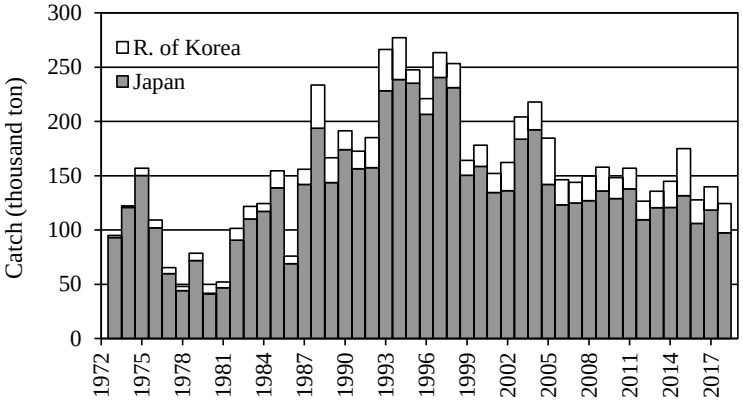

Figure R19-47. Annual catch of Jack mackerel a in Region 19 and the East China Sea in Japan and Republic of Korea.

Japanese flying squid (*Todarodes pacificus*), is the most economically important cephalopod species in the Northwest Pacific, mostly caught by jigging and trawling. The stock of the squid comprises 3 to 4 seasonal spawning stocks, of which the autumn and winter stocks are the largest. The autumn spawning stock prevails in Region 19 from the late spring to autumn seasons, and then the winter spawning stock becomes dominant in the winter season.

The annual catch of squid in the North Pacific (including the Pacific Ocean, Okhotsk Sea, Region 19, East China Sea and Yellow Sea) by Japan and the Republic of Korea was high with over 300 thousand metric tons before the mid-1970s and from the 1990s to the mid-2010s (Fig. R19-48). The annual catch was lower during the 1980's and after 2016. The stock level has also synchronously fluctuated with the catch. Both natural and artificial functions were suspected to affect the stock fluctuations: the climatic regime shifts which affected its life history traits (Sakurai et al., 2002, Kidokoro et al., 2010) and high fishing mortality including the other countries' fisheries activities (Park et al., 2020, Takasaki et al., 2020).

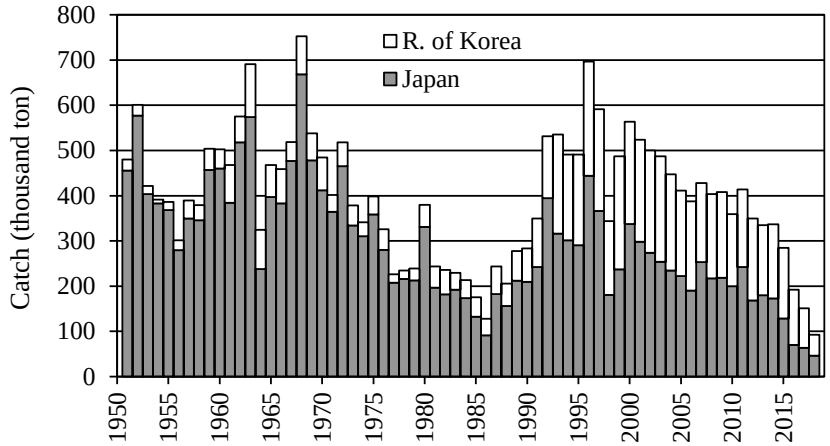

Figure R19-48. Annual catch of Japanese flying squid in the North Pacific by Japan and the Republic of Korea.

Yellowtail (*Seriola quinqueradiata*) is one of the most important fisheries resources as well as aquaculture species in this region. Spawning grounds of yellowtail are located mainly at the edge of the continental shelf of the East China Sea and extend to the coastal areas of western Japan. Yellowtail grows quickly to attain a weight of over 6 kg and a length of about 70 cm in 2 years. From late spring to summer, young and adult yellowtail migrate northward and expand their habitat to the northern Japan coast including Hokkaido, especially after the 2000s. The geographical center of the catch in Japan shifted corresponding to the climatic regime shifts and sea surface temperature fluctuations (Shishido et al., 2016).

Yellowtail is caught in the juvenile stage for aquaculture's sake, and young to adult are caught mainly by set nets and purse seines. The catch of yellowtail generally increased since 1990 (Fig. R19-49), and reached the highest levels of above 100 thousand metric tons in the 2010s. However, the catch has decreased in the recent years, that was due to the high fishing pressure on young immature fish, and the degradation of the recruitment ratio.

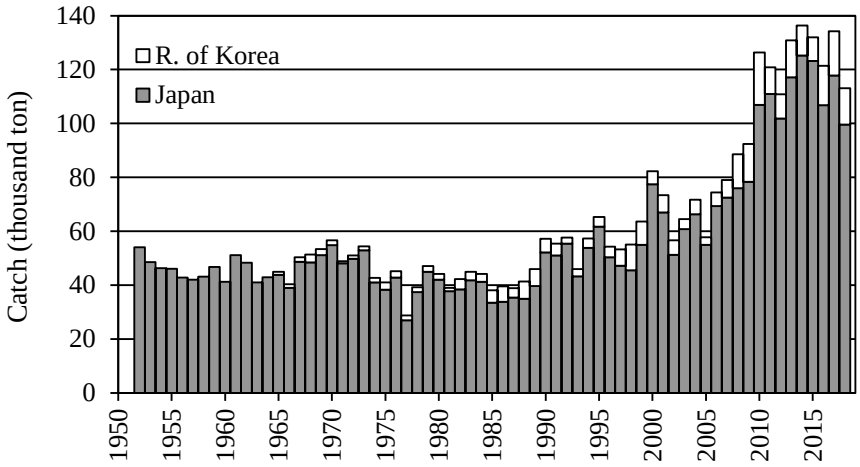

Figure R19-49. Annual catch of yellowtail in the North Pacific by Japan and Republic of Korea.

Sailfin sandfish, *Arctoscopus japonicus*, are widely distributed on the continental shelves of Korea, Honshu and Hokkaido, mainly on sandy and muddy bottom grounds with depths of 50–200 m. The sandfish have two populations, with centers at Korea and at northern Honshu (Fig. R19-50). The fish along the western Honshu were considered as the mixture of these populations (Okiyama 1970) and that hypothesis was later supported by genetic analysis (Shirai et al. 2006).

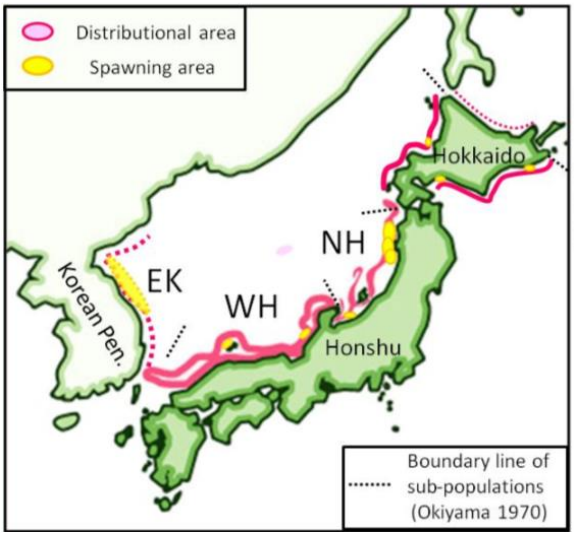

Figure R19-50. Schematic of distribution, spawning grounds, and population structure of sailfin sandfish. EK - East Korean population, NH - North Honshu population, WH - West Honshu area of mixed stock.

Sandfish are caught mainly in offshore waters in April–October by Danish seine and in coastal waters in October–December (in spawning grounds) by gill nets and set nets. Catches were very high in the 1960s (>30,000 t in Japanese waters, mostly at northern Honshu) but

dramatically decreased from 1975–1990. To stop the degradation, the sandfish fishery off Akita prefecture was prohibited in 1992–1995. After plummeting to a minimum in 1996, the catch in Japanese waters, as well as in Korean waters, began to increase. After 2000, the catch in Japanese waters and Korean waters had a peak in 2008 and maintained 10,000 t from 2009 to 2017 (Fig. R19-51). Nonetheless, new limits for the sandfish catch were introduced in Japan in 2008.

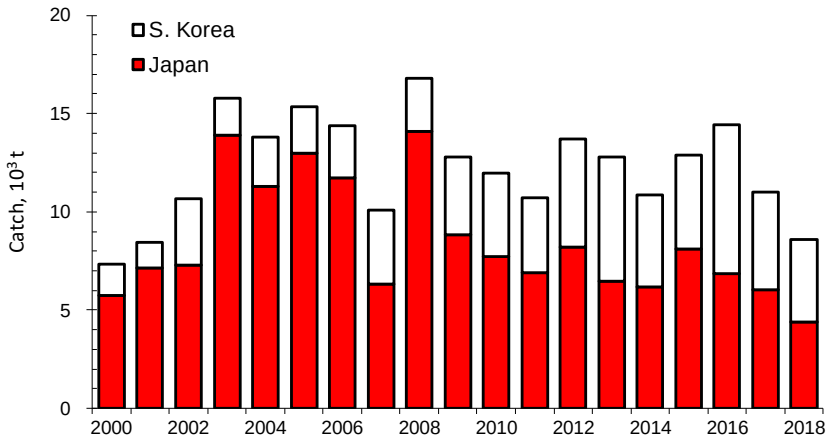

Figure R19-51. Sailfin sandfish annual landings by Japan and Korea.

8.3 Southwestern area, off Korea

Walleye pollock *Gadus chalcogrammus* (pollock hereafter) is a semi-demersal species residing in cold and deep water over the continental shelf and slope areas (> 200 m) along the Asian and North American coasts. In the northwestern Pacific, the Korean Peninsula is regarded as the southern boundary of their distribution (Kim and Kang, 1998). Pollock is one of the important fish species culturally and economically in Korean history. Pollock has been an important seafood for Koreans since the early 19th century and became a major commercial fishery from the early 20th century in Korean waters occupying two-thirds of monetary value in total fishery production during the 1930s. After the peak of pollock yield in the late 1930s, fishing activity was much depressed during the 1940s~1960s. Annual catches of pollock increased again in the 1970s, and peaked in 1981 showing about 166 thousand metric tons (MT) of pollock production (Fig. R19-52). The mean pollock catch was 107 thousand MT during 1976~1985, which was equivalent to 44% of the total fishery yield of the eastern coastal areas (Kang et. al, 2013). The catch of pollock had shown a tremendous decline from the late 1980s through the 1990s, and the pollock stocks have completely collapsed in Korean waters since the 2000s.

Walleye pollock which is a cold-water species had a positive shift in 1973 might be related to lower temperatures north of Region 19 (1962-1975). Also, the negative shift of seawater temperature in 1975 south of Region 19 had a positive influence on the higher abundance of this species. A regime shift within the Eastern Bering Sea in 1977 also favored the survival of walleye pollock juveniles (Duffy-Anderson et al., 2016). The collapse of this fishery around the mid-1980s might have influenced positive shifts in seawater temperature in the north of Region 19 (100m) and south of Region 19 (50m, 100m). Sea water temperature might have influenced the early life cycle of this species. When walleye pollock spawns in the upper layer of the water

column, the eggs float on the surface due to buoyancy. The increased sea water temperature in the upper layer seems unsuitable for the hatching and survival of young walleye pollock because eggs and early life stages are sensitive to oceanic conditions. After 2000, walleye pollock almost disappeared in the eastern coastal waters of Korea. In this regard, the reason for the reduction in the walleye pollock catch has not been clear. According to recent research, the cumulative impact of fishing in the early 1980s and climate change in the late 1980s has an influence on the change of the stock off Korea.

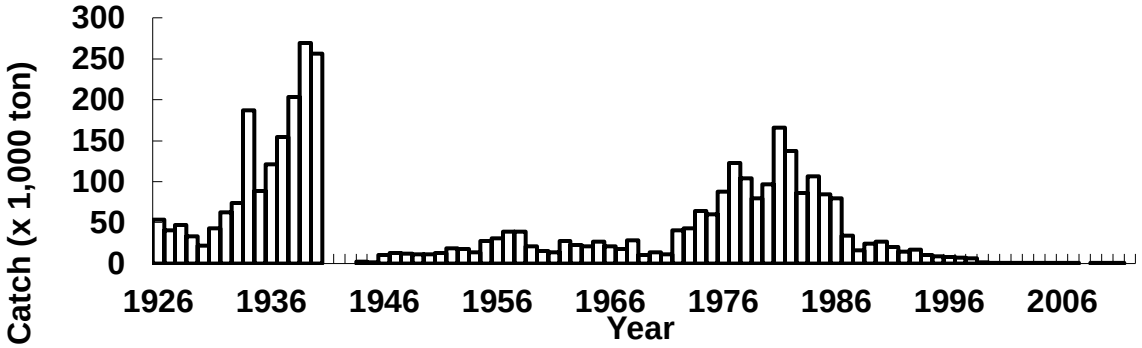

Figure R19-52. Catch of walleye pollock (1926-2014). Notice that pollock catches in the early 20th century were mostly from North Korean waters, while those since 1946 were only from South Korean waters.

Common squid (*Todarodes pacificus)* is an important commercial species in Korean and Japanese fisheries. Most of the catch is taken by jigging and trawl fisheries. In Korea, catches were less than 50 thousand metric tons during the 1950s–1980s but began to increase dramatically in the early 1990s (Fig. R19-53). During the 1990s–2000s, the catch reached 200 thousand metric tons. However, common squid catch in Region 19 by Korean fishery has decreased since the late 1990s. The catch has highly fluctuated between seasons and the catch in autumn accounts for the largest part of the total catch. Catch in autumn has been continuously decreasing so far after the late 1990s. On the other hand, catch in winter increased until 2015 and since then, it has decreased rapidly. The recent trend is that catches are increasing in the northern part of the subpolar front and decreasing in the south. It is consistent with the trend of changes in primary production.

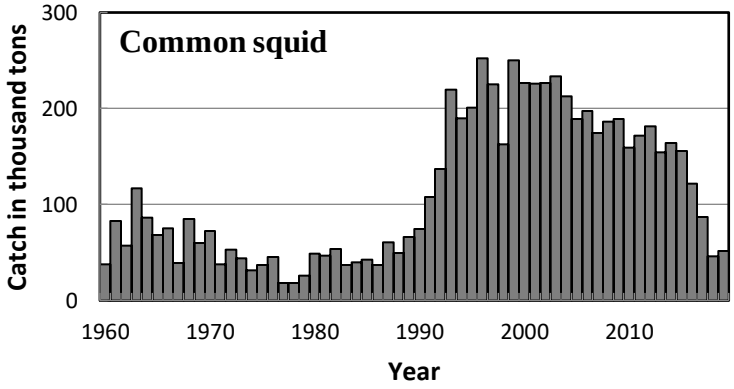

Figure R19-53. Catch of common squid in Korean waters (1960-2019).

Chub mackerel (*Scomber japonicus*) is widely distributed in the Pacific Ocean and is one of the major representative pelagic species in Korean waters. This species migrates to wintering grounds in the northern East China Sea during December–March, and to spawning ground areas between Jeju Island and Tsushima Island, and the northern East China Sea during April–June. This species is mostly caught by large purse seine in Korea. Annual catches were around 100,000 metric tons from the 1970s to the mid-1980s and then gradually increased (Fig. R19-54). The annual catches of chub mackerel reached their highest level of 415,003 mt in 1996 and then declined below 100,000 mt in 2010. In the 2010s, annual catches fluctuated from 100,000 mt to 215,000 mt.

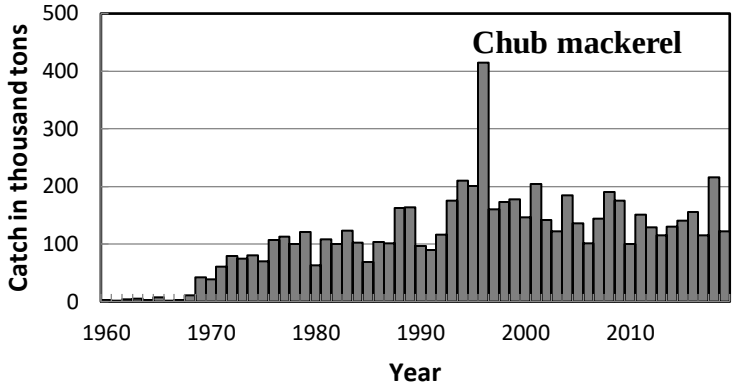

Figure R19-54. Catch of chub mackerel in Korean waters (1960-2019). Notice that Korea has distinguished the catches of chub mackerel and spotted mackerel since 2008, and the data used in the figure is the sum of the catch of chub mackerel and spotted mackerel for data continuity.

The regime shifts in the catch of the major 10 species in Korean waters from the 1950s to 2010s are shown in Fig. R19-55. Because of the changes in the fishing environment and technology, it is difficult to fully explain the impact of climate change. Around the 1976 climatic regime shift, a positive shift was detected in cold-water demersal walleye pollock and a negative shift in warm-water common squid. Two small pelagic species (Japanese sardine and Pacific saury) changed most abruptly and inversely in 1977. Also, abrupt positive changes were detected in Japanese anchovy (1973), hairtail (1973) and yellow croaker (1972). Around the 1988 climatic regime shift, Japanese sardine and walleye pollock collapsed quite early in 1983 and 1985, respectively. The positive shifts were detected in yellow croaker (1987), Pacific herring (1988), common squid (1989), chub mackerel (1989) and Japanese anchovy (1991); and negative shifts were detected in hairtail (1988) and Pacific cod (1989). Around the1998 climatic regime shift, positive changes were detected in Japanese anchovy (1998), Pacific herring (1996), Pacific saury (1996) and Pacific cod (2001); negative shifts were detected in Pacific sardine (1998) and chub mackerel (2001). The catches of hairtail (1997) and yellow croaker (1998) declined; common squid was shifted positively in 1995. In the 2000s, positive shifts were detected in Pacific herring (2006) and Pacific cod (2007); negative shifts were detected in common squid (2006) and yellow croaker (2005). Also, negative shifts were detected in Pacific saury (2004) and hairtail (2010).

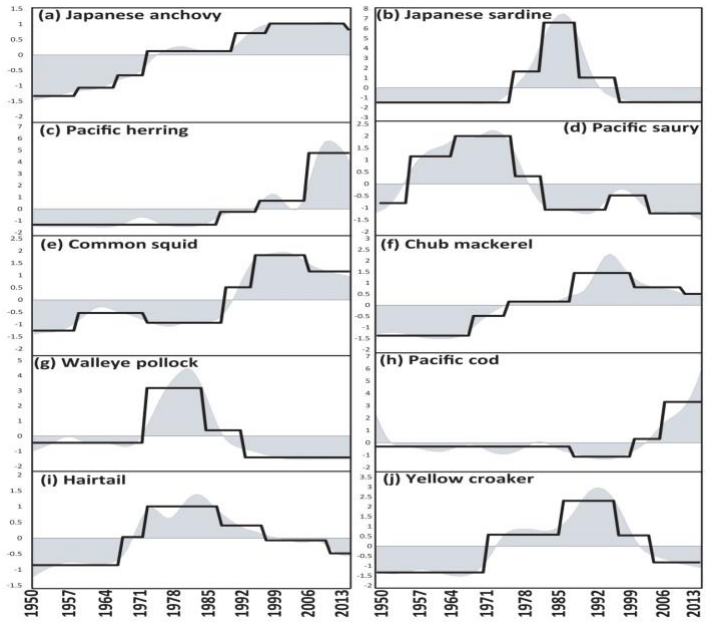

Figure R19-55. Decadal variations (grey shaded, low pass Butterworth filtered with the 10-yr cut-off period) and step changes in anomalies (solid black line) detected by sequential t-test analysis of regime shift (STARS) of the major ten species in Korean commercial catch (modified from Rahman et al., 2019).

In Korean waters, after the 1970s, total fisheries catch increased while mean trophic level and diversity decreased (Fig. R19-56). The hierarchical clustering and nMDS ordination plot based on total fish assemblage data allowed three distinct groups (Group A: 1965 to 1974, Group B: 1993 to 2015, and Group C: 1975 to 1992), all of which were divided into two subgroups (Fig. R19-57) (Rahman et al, 2019). The fish community structure in the East Asian Marginal Seas waters differed significantly among the three periods (ANOSIM test, $p < 0.001$). Group A mostly consisted of warm water species (dominant species: squid, anchovy, and saury) indicating the influence of the warm climatic regime before the mid-1970s. Group B mainly included warm species (dominant species: anchovy, squid, and hairtail) revealing that the environmental conditions changed from a cold regime to a warm regime after the early 1990s. In contrast, Group C represented cold water fish community structure (dominant species; walleye pollock and sardine) indicating the influence of the cold climatic regime after the mid-1970s (Fig. R19-58).

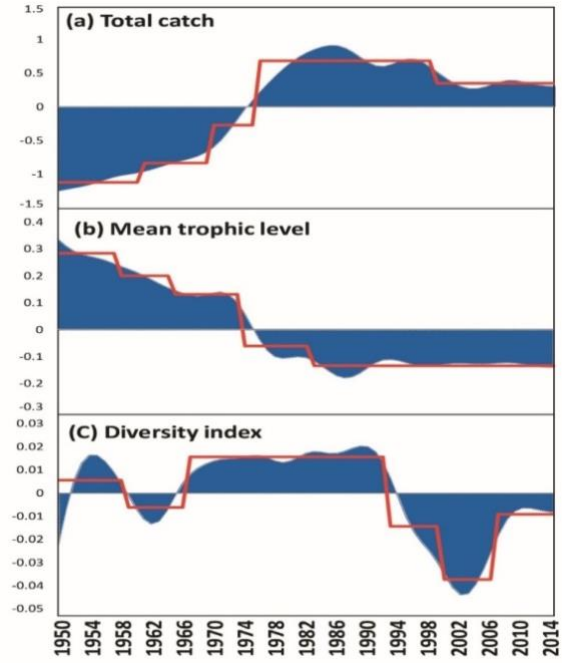

Figure R19-56 (right). Decadal variations (grey shaded, low pass Butterworth filtered with the 10-yr cut-off period) and step changes in anomalies (solid black line) detected by sequential t-test analysis of regime shift (STARS) of the major ten species in Korean commercial catch (Rahman et al., 2019).

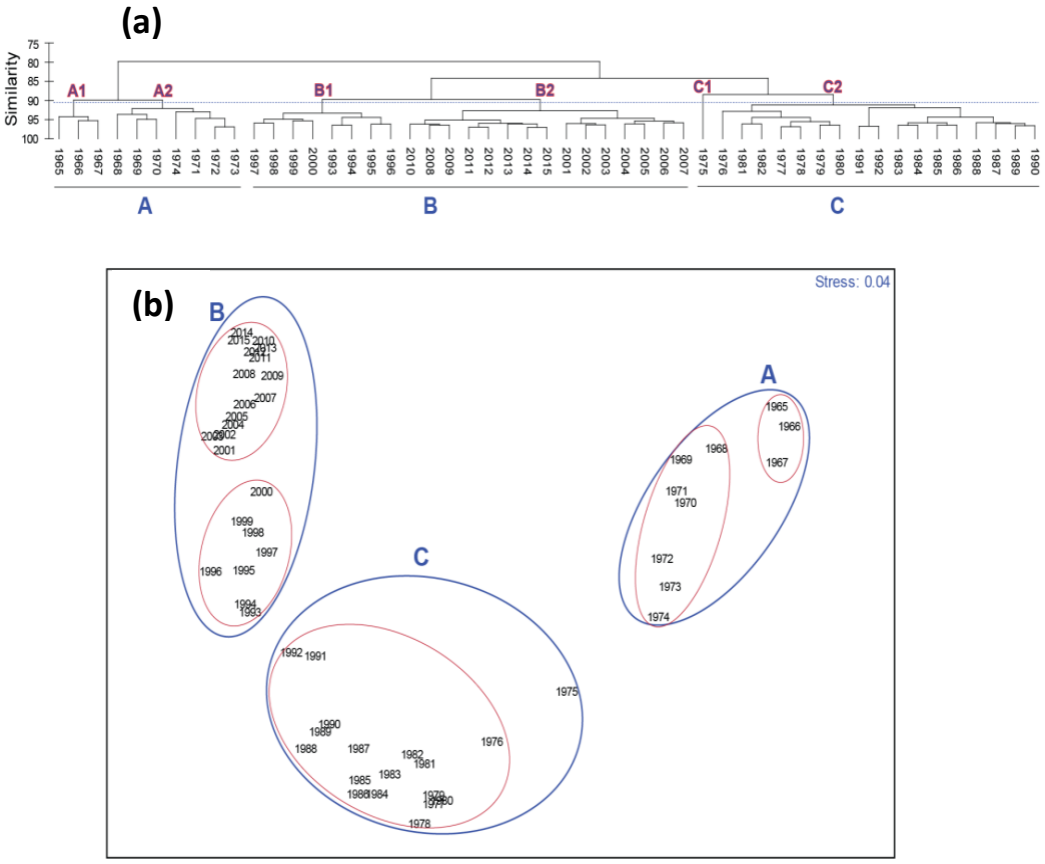

Figure R19-57. Comparison of fish assemblages from 1975 to 2015 using (a) hierarchical cluster and (b) non–metric multidimensional scaling ordination (nMDS) analyses based on Bray-Curtis similarity (modifired from Rahman et al., 2019).

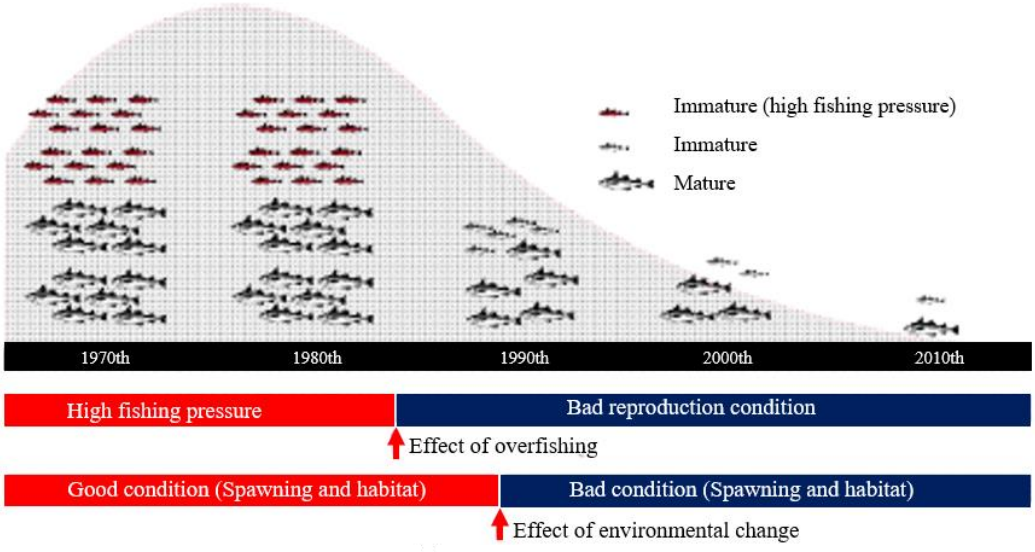

Figure R19-58. Schematic diagram for the long-term change in walleye Pollock resources in the eastern coastal water of Korea (Jung et al., 2020).

9. Marine Birds

M. Kim, D. Ochi

8.1 Marine birds off Korea

The wintering population of seabirds has been monitored in the east coast of Korea in January between 2009 and 2020 by the National Institute of Biological Resources, Rep. of Korea (NIBR 2009, 2010, 2011, 2012, 2013, 2014, 2015, 2016, 2017, 2018, 2019, 2020). Seabirds were observed at 15 sites on the same day of January every year to avoid double counts (Fig. R19-59). In total 42 species of seabirds including cormorants, loons, scoters, mergansers, murres, murrelets, guillemots and gulls were recorded over 12 years.

Population size and number of species of wintering seabirds were annually varied. The wintering population was large a total 113,043 individuals in 2014 and small as total 61,761 individuals in 2010. Seabird population seemed to be related to the amount of prey although other factors still need to be tested (Fig. R19-60). Pelagic cormorants (*Phalacrocorax pelagicus*) increased whilst Red-throated loons (*Gavia stellata*) and White-winged scoters (*Melanitta deglandi*) tended to decline after 2010 (Fig. R19-61). The number of gulls and auklets showed no apparent trend.

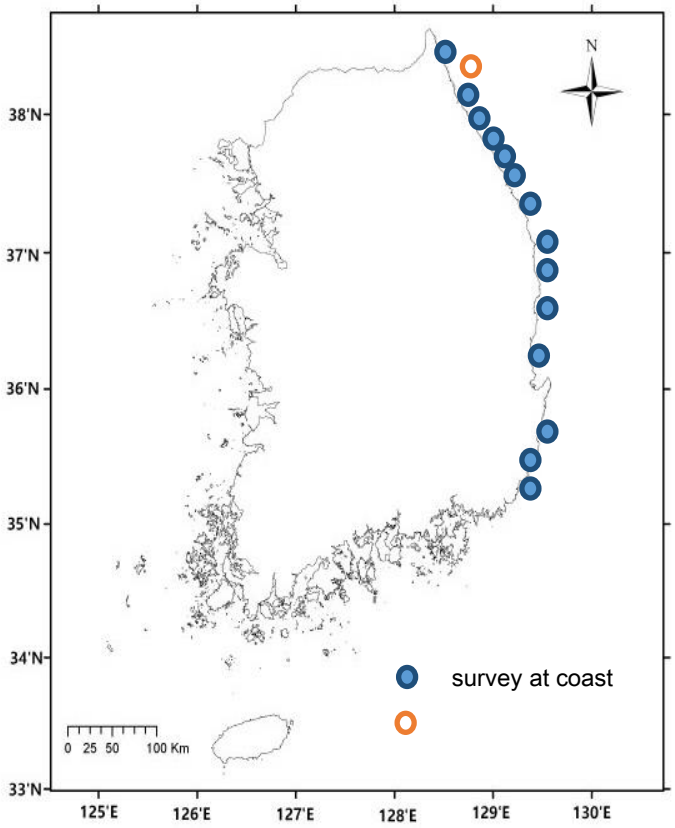

Figure R19-59. Survey sites of marine birds at the east coast of Korea.

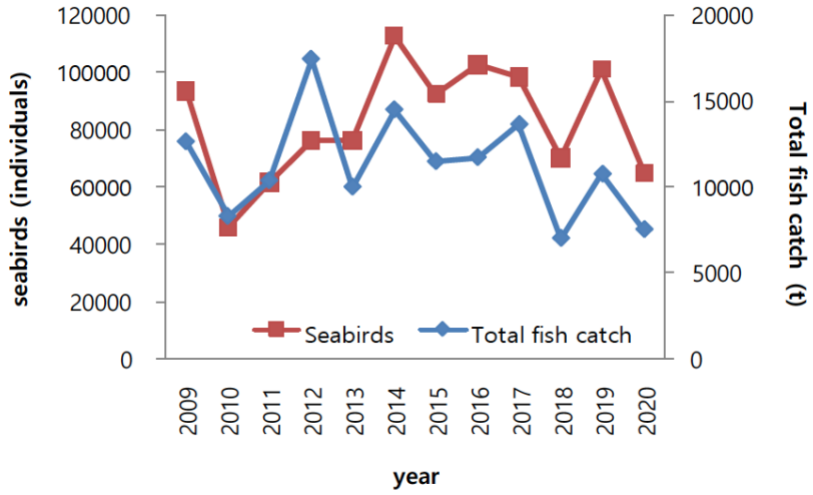

Figure R19-60. Annual variations of wintering seabird population and total fish catch (t) in the east coast of Korea. Total fish catch was the amount of fish caught in January at the survey area (Gangwon-do and Gyeongsangbuk-do).

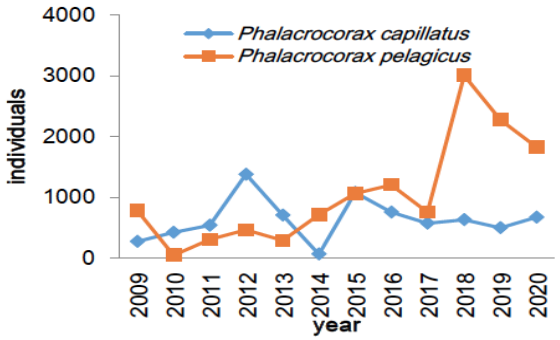

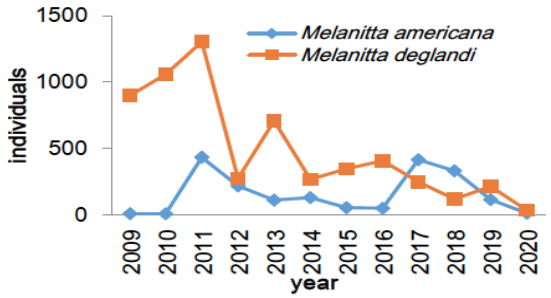

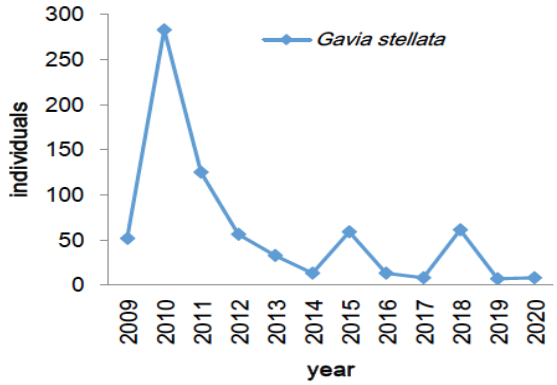

Figure R19-61. Wintering population of Pelagic cormorants (*Phalacrocorax pelagicus*), Red-throated loons (*Gavia stellata*), Black scoters (*Melanitta americana*) and White-winged scoters (*M. deglandi*) in the east coast of Korea.

9.2 Marine birds off Japan

Seabird breeding populations in Japan are regularly monitored at several breeding colonies and reported by the Biodiversity Center of Japan, the Ministry of the Environment (Biodiversity Center of Japan 2020, 2021a,b). There are six monitoring sites along the Japanese coast of Region 19 (Figure 19-62), which record the number of breeding nests of Black-tailed Gull (*Larus crassirostris)*, Common Murre (*Uria aalge*), Crested Murrelet (*Synthliboramphus wumizusume)*, Japanese Cormorant (*Phalacrocorax capillatus)*, Pelagic Cormorant (*Phalacrocorax pelagicus)*, Rhinoceros Auklet (*Cerorhinca monocerata)*, Slaty-backed gull (*Larus schistisagus),* Spectacled Guillemot (*Cepphus carbo)*, Streaked Shearwater (*Calonectris leucomelas)* and Swinhoe's Storm-petrel (*Oceanodroma monorhis)*.

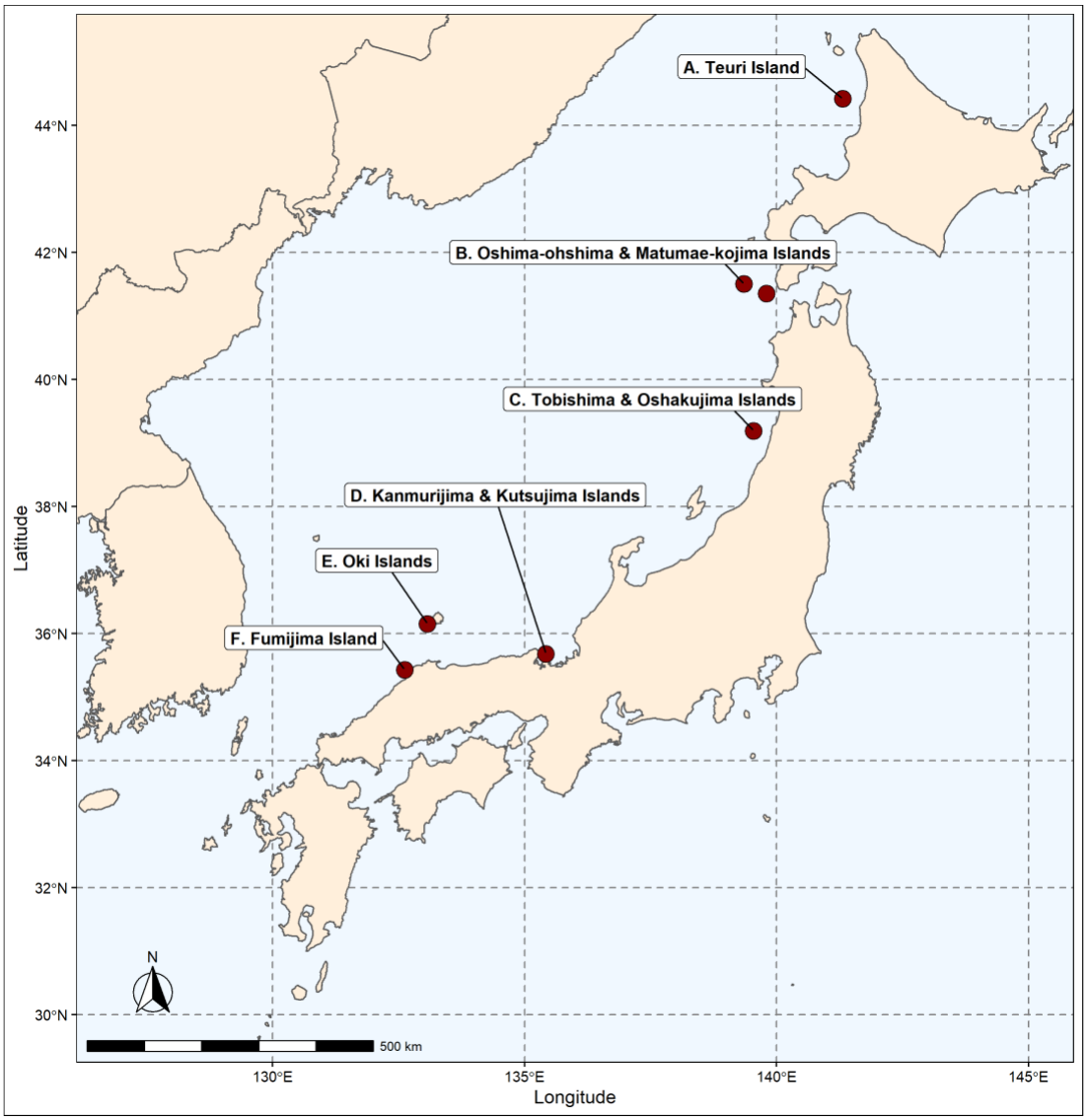

Figure R19-62. Monitoring sites for seabird breeding population in Region 19 (based on Biodiversity Center of Japan 2020, 2021a, b).

The survey was started in 2004, and the results have been publicly released. The total number of breeding nests was estimated by total nest counts, nest density using the quadrat method, and estimated total nest number from the nest density and an area of breeding sites (Figure R19-63, R19-64).

Except for a few sites, the total number of breeding nests at each monitoring site was relatively stable, but the decline was observed in Black-tailed Gull at Site A (Teuri Island) and Swinhoe's Storm-petrel at Site D (Kanmurijima & Kutsujima Islands). The decline of Black-tailed Gull was thought to be due to predation of chicks and adult birds by feral cats but the reason for the decline of Swinhoe's Storm-petrel was uncertain. The population of Streaked Shearwaters at Site B (Oshima-ohshima & Matumae-kojima Islands) remained extremely low level, probably due to the disturbance by humans in the past and introduced species (rats and hares). On the other hand, the breeding nests of Common Murre at Site A increased by the implementation of the recovery project.

The main factor affecting the breeding population is the non-native predators such as rats and feral cats (Biodiversity Center of Japan 2021b), but it has also been pointed out that the breeding population of Rhinoceros Auklet at Site A may be affected by the fluctuation in local abundance of its prey species, Japanese Anchovy (*Engraulis japonicus)*, due to rise of spring water temperature in Region 19 (Takahashi et al., 2001; Deguchi et al., 2004). In addition, the interaction with fisheries such as bycatch at some sites may also have had an impact on this species (Biodiversity Center of Japan 2021a).

Additional breeding monitoring survey of Black-tailed Gull, Japanese Cormorant and Slaty-backed Gull on Rishiri Island (45° 10’N, 141° 15’E) was conducted by Waseda University.

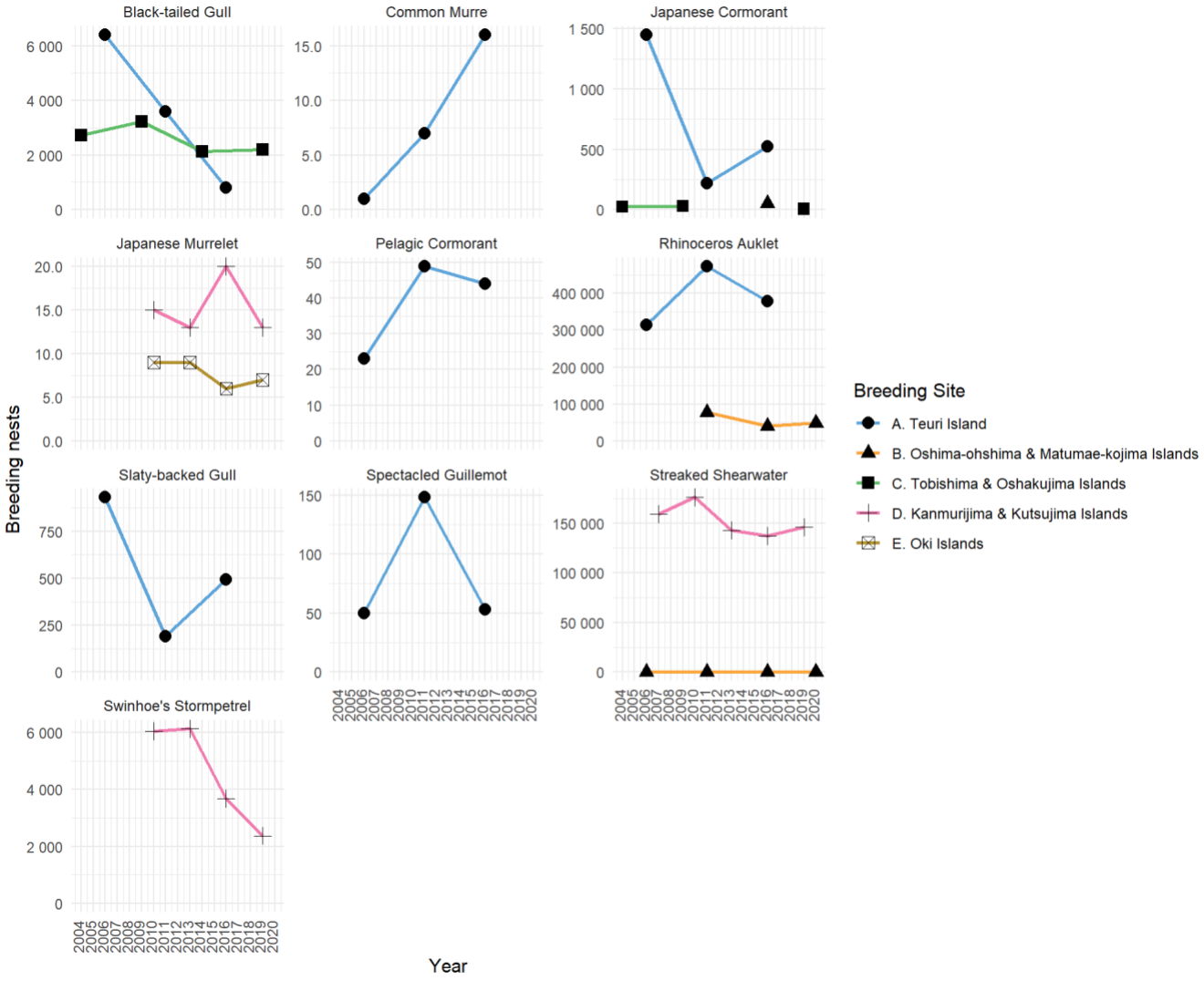

Figure R19-63. Number of breeding nests of 10 bird species at five monitoring sites along the coast of Japan (prepared by D. Ochi based on Biodiversity Center of Japan 2012, 2020, 2021a,b).

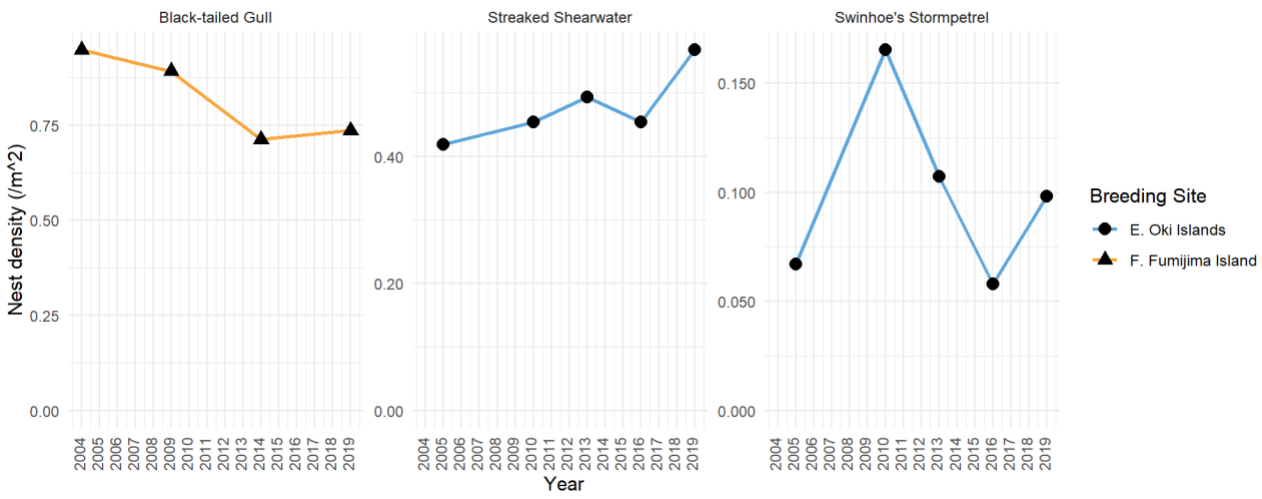

Figure R19-64. The density of breeding nests (/m^2) of three bird species at two monitoring sites along the coast of Japan (based on Biodiversity Center of Japan 2020, 2021a,b).

10. Marine Mammals

A. Trukhin, H. W. Kim, *Y.-R. An, K. Hattori, S. Minamikawa*

10.1 Pinnipeds

Marine mammals in Region 19 are less diverse and much less studied in comparison with the Okhotsk or Bering seas, where their commercial importance has a long history. There are 6 species of pinnipeds in the region: Largha seal (also known as spotted seal) (*Phoca largha)*, Steller sea lion (*Eumetopias jubatus)*, northern fur seal (*Callorhinus ursinus)*, bearded seal (*Erighnatus barbatus)*, ringed seal (*Pusa hispida)*, and ribbon seal (*Histriophoca fasciata)*. This region is the southern distribution boundary of the half of the species above. The detailed surveys have been conducted for only Steller sea lion and Largha seal. Information on the other species is too fragmented to trace any trends. The observations in the Okhotsk Sea and the North Pacific, where most of the seals have rookeries, show that their numbers have been steadily growing over recent years. As these species use Region 19 during post-reproduction or wintering migrations, an increase in their occurrences is expected. In the southern part of Region 19 off the Korean and Japanese coast, there are only three pinniped species have been observed: Spotted seal, northern fur seal, and Steller sea lion.

In the waters off Japan, the conflict between these three species and coastal commercial fisheries is an issue faced by local communities. Spotted seals and Steller sea lion have been culled for population control as one of the mitigation measures for damage to the fisheries. Bycatch of these three pinnipeds by coastal set nets and gill nets has been reported (Kiyota and Baba, 1999; Horimoto et al., 2012; Hokkaido Government, 2017; Isono and Hattori, 2021).

These species are transient in Korean waters, but only bycatch numbers are available through the Cetacean Research Institute (CRI) of Korea, and it is difficult to estimate their interannual variability. Most of them were caught incidentally by coastal fishing gears such as set nets, pound nets or gill nets; some carcasses were found along the coast of Korea.

Spotted seal:
Spotted seal *(Phoca largha*) is the only ice-living seal species that resides in Region 19 whole year round and is comparatively abundant. There are two major populations of spotted seals: one inhabits the Tatar Strait and the other in Peter the Great Bay. Although there are no recent survey data available for the Tatar Strait spotted seals, it is expected that their abundance is similar to that observed in the 1960s, 8,000–11,000 individuals (Fedoseev, 1970) as no commercial catches have been taking place, and the prey availability has been quite stable. In Peter the Great Bay and along the eastern coast of Primorye, over 50 spotted seal haul-outs have been found (Trukhin and Mizuno, 2002; Trukhin, 2005; Nesterenko and Katin, 2014). But seals breed only in Peter the Great Bay at Rimsky-Korsakov archipelago. At least 800 pups were counted here in 2017, while the total population of seals was around 3,200–3,600 individuals (Trukhin, 2019) and it is steadily growing (Table R19-3). 996 pups were counted in 2022 (Trukhin, 2023). Taking into account the proportion of newborns not included in the count, the recruitment of spotted seal pups in Peter the Great Bay in 2022 amounted to at least 1100 individuals, and the size of the total population (excluding offspring) was estimated at around 4 thousand individuals (Trukhin, 2023).

Table R19-3. Numbers of spotted seal pups counted in Peter the Great Bay based on one-off surveys in 2002–2022

Date of count	Number of spotted seal pups	Reference
February 24–25, 2002	167	Trukhin, 2005
February 27, 2003	189	Trukhin, 2005
February 19, 2004	193	Nesterenko and Katin, 2014
February 24, 2005	240	Nesterenko and Katin, 2014
February 18, 2008	273	Nesterenko and Katin, 2014
March 5-6, 2015	667	Trukhin, 2015
March 4, 6, 2016	692	Trukhin, 2019
March 1, 2017	739	Trukhin, 2019
March 1-2, 2022	996	Trukhin, 2023

Even if the number of spotted seals in Peter the Great Bay has increased in recent years, industrial development and increasing recreational activities in this area are becoming a serious threat to the spotted seal population (Katin and Nesterenko, 2010; Trukhin 2015 and 2019). In particular, shipping, commercial fishery, illegal catches of sea cucumber close to the haul-out sites, as well as intense net fishing in winter contribute to seal mortality.

In the waters off Japan in Region 19, spotted seals were rarely observed until the late 1970s, but since the 1990s their winter migration has been confirmed, and several winter haul-out sites have been established along the coast of Hokkaido in this region (Mizuno et al., 2001). The range of distribution is expanding, the number of seals observed at haul-out sites has increased, and some seals reside throughout the year at some sites currently (Shibuya and Kobayashi, 2014). About 2,000 seals were counted in winter and 685 in summer at haul-out sites along the coast of Hokkaido in 2015 (Hokkaido Government, 2017).

Although spotted seals are transient visitors in the water off Korea in Region 19, there is a big haul-out site in the Yellow Sea where half of the Yellow Sea population stays from early spring to late autumn. More than 350 individuals have been identified at the haul-out site by the CRI research team using photo ID, and Chinese scientists have estimated about 600 seals when the population congregates at rookery sites in the Bohai Sea during the winter breeding season.

There is no haul-out site for spotted seals in the waters off Korea, although several animals have been found alive or dead along the coast. Most of them were regarded as transient visitors from Russian populations although a genetic study revealed that some might have come from the Yellow Sea population (Y.-R. An, pers. comm.).

Northern fur seal:
Northern fur seal (*Callorhinus ursinusis)* is distributed in open sea areas and was never observed in the coastal waters of Primorye. It usually migrates southward and overwinters in the Yamato Rise area, in the southern part of the Ulleung Basin, and the East Korea Bay. Northern fur seals are the most abundant pinniped species in the waters off Korea. Two hundred and seventy-nine seals were caught as bycatch in this area between 2001 and 2015, most caught incidentally by pound nets in the winter season (Kim et al., 2021). During sighting surveys of cetaceans conducted by the CRI in 2000-2020, 44 seals were found in this area (Kim et al., 2021).

In the coastal waters off the northern part of Japan, the northern fur seals are migratory species in winter. Mature males are more dominant in Region 19 compared to Region 22 where juveniles and adult females are dominant (Horimoto et al., 2017). They are generally pelagic species, but they can be found within a few kilometers of the shore in this region, and fisheries damage by northern fur seals is also a problem for coastal commercial fishery (Horimoto et al., 2012).

Steller sea lion:
Steller sea lion (*Eumetopias jubatus)* is a migrant species in Region 19. One of the breeding ground is Moneron Island, off Sakhalin (Burkanov and Loughlin 2005). Its total abundance was dramatically reduced in the second half of the 20th century all over in this region. It has nearly disappeared in the southern part of Region 19 while it is still common along Sakhalin and Hokkaido. In the 1930s there was a large hall-out in Peter the Great Bay when around 400 individuals congregated along the coast of Askold Island while there were only occasional occurrences of single juvenile animals occupying the area in recent years. Only some individuals or small groups of seals have been reported every year off the eastern and southern coasts of Primorye (Trukhin, 2001).

The coastal waters off Hokkaido Island in Region 19 are the wintering ground of Steller sea lions bred at rookeries in the Okhotsk seas. There are some haul-out sites for a few to hundreds of sea lions, and the number of sea lions and haul-out sites had been decreasing in the 1980s but has been increasing in recent years (Isono and Hattori, 2021). Massive landings (over 1,000 animals) have been observed at Benten-jima Rock located at the northern tip of Hokkaido Island since 2016 (Hattori et al. 2021; Goto et al., 2022). Abundance in spring is estimated to be up to about 6,000 animals based on aerial line transect sampling (Hattori et al., 2021). Conflict between commercial fisheries and sea lions is most severe among the three pinnipeds, and fisheries damage includes not only the loss of fishing yield but also damage to fishing gear.

In the waters off Korea, Steller sea lions are transient visitors. Four stranded or bycaught animals and six sighting records have been reported in the coastal area between 2000 and 2020 (Kim et al., 2021). Most of the reported animals were immature.

Other species:
A recent analysis of the bearded seal (*Erignathus barbatus*) distribution in Region 19 showed that contrary to previous belief, the southern boundary of their range is not in Peter the Great Bay, but is farther north around 48°N (Trukhin, 2002). However, there is a possibility that they

occur in more southern areas. Bearded seal abundance is low in the Tatar Strait in spring. The existence of any coastal haul-outs of this seal in Region 19 has never been reported and there appears to be no coastline with geomorphological properties suitable for their haul-outs.

The ringed seal (*Pusa hispida)* is observed only in the northernmost area of Region 19. In spring it hauls out on the ice in the Tatar Strait where some reproduction takes place. The number of ringed seals compared to other ice-living seals in this region during the reproductive season remains low with about 2% of whole pinnipeds. It is not clear if the Tatar Strait is an area where the ringed seal resides during summer and fall. There is no evidence of the seals being found south of the Tatar Strait.

A small number of ribbon seals (*Histriophoca fasciata*) is known to haul out on ice in the Tatar Strait to reproduce in spring. Single animals are occasionally observed on ice in Peter the Great Bay but they do not reproduce in the bay (Trukhin, 1997). During the summer and fall, they probably move to other areas in open water, but it is difficult to observe this pelagic species in the open sea.

10.2 Cetaceans

At least 23 species of cetaceans have been found in Region 19, among which 16 species belong to the toothed whale group and 7 species to baleen whales (Kim et al., 2009). Among the baleen whales, the common minke whale (*Balaenoptera acutorostrata)* is the most common in the area. Fin whale (*B. physalus)* and humpback whale (*Megaptera novaeangliae)* are rarely found by caught incidentally. In this area, the last sightings of North Pacific right whale (*Eubalaena japonica)* and gray whale (*Eschrichtius robustus)* were in 1974 and 1977 respectively. In 2003, a new baleen whale species, Omura's whale (*B. omurai)*, was discovered in Tsunoshima, Japan, in the southwestern part of Region 19 (Wada et al., 2003). There are two bycatch records of Omura's whale in Korean waters (Kim et al., 2018).

In the toothed whale group, the following are found: common dolphin (*Delphinus delphis)*, Pacific white-sided dolphin (*Lagenorhynchus obliquidens)*, Risso's dolphin (*Grampus griseus)*, false killer whale (*Pseudorca crassidens)*, common bottlenose dolphin (*Tursiops truncates)*, Killer whale (*Orcinus orca)*, Dall's porpoise (*Phocoenoides dalli)*, harbor porpoise (*Phocoena phocoena)*, finless porpoise (*Neophocaena asiaeorientalis)*, Stejneger's beaked whale (*Mesoplodon stejnegeri)*, Baird's beaked whale (*Berardius bairdii)* and Cuvier's beaked whale (*Ziphius cavirostris)*. Several vagrant species have been rarely found, such as melon headed whale (*Peponocephala electra)*, Indo-Pacific bottlenose dolphin (*Tursiops aduncus)* and Pantrophical spotted dolphin (*Stenella attenuate)*.

Because of the intense commercial whaling practices up to about the second half of the 20th century, large species such as the North Pacific right whale, gray whale and humpback whale were severely depleted to the limit of disappearance. These critically endangered species were listed in the Red Book of the IUCN (International Union for the Conservation of Nature) and their catches were banned in Russia from 1964 to 1981 and in Korea in 1986. Commercial whaling in the North Pacific has been prohibited by the International Whaling Commission (IWC) for North Pacific right whales since 1937, and humpback whales since 1966. These positive actions for animal surveillance, on the other hand, have resulted in reduced scientific surveys and the absence of reliable data on their status for a while. It may be that the population of the whales is steadily growing, but at a slower pace for the species with low reproduction rates, and it may require a few decades before any significant rebounding in populations can be seen.

Japanese survey:
In Japan, commercial whaling in the Region 19 was conducted until 1975 for fin whales and until 1985 for minke whales (Allison, 2013). Commercial whaling for Baird's beaked whales was conducted from 1999 until 2016 (Maeda and Kishiro, 2021). Dall's porpoises were also caught off Hokkaido. However, due to the decrease in the number of vessels operating after the Great East Japan Earthquake in 2011, the number of animals caught has decreased significantly (Kanaji, 2021).

In Japanese sighting surveys, minke whales (*Balaenoptera acutorostrata*), fin whales (B*alenoptera physalus)*, right whales (*Eubalaena glacialis)*, Baird's beaked whales (*Berardius* bairdii), Cuvier's beaked whale (*Ziphius cavirost*ris), Stejneger's beaked whale (*Mesoplodon stejnegeri*), killer whales, (*Orcinus orca*), false killer whales (*Pseudorca crassidens*), common dolphins (*Delphinus delphis*), Pacific White-sided dolphins (*Lagenorhynchus obliquidens*), Risso's Dolphin (*Grampus griseus*), bottlenose dolphins (*Tursiops truncates*), finless porpoise (*Neophocaena phocaenoides*） and Dall's Porpoise (*Phocoenoides dalli*) have been sighted in the Region 19 (Fisheries agency of Japan, 2017 a-h; Kasuya and Miyashita, 1997; Miyashita and Kasuya, 1988; Miyashita et al., 1995; Ogawa, 2017).

In addition to the species listed above, stranding and bycatch of the following species have been documented: Bryde's whale (*Balaenoptera edeni),* humpback whale (*Megaptrera novaeangliae),* gray whale (E*schrichtius robustus),* sperm whale (*Physetermacrocephalus),* pygmy sperm whale *(Kogia breviceps),* dwarf sperm whale (*Kogia simus),* beluga whale (*Delphinapterus leucas),* Hubb's beaked whale (*Mesoplodon carlhubbsi),* short-finned pilot whale (*Globicephala macrorhynchus),* pygmy killer whale (*Feresa attenuate),* rough-toothed dolphin (*Steno bredanensis),* striped dolphin (*Stenella coeruleoalba),* harbour porpoise (*Phocoena phocoena).*

The top five species of these, with the largest number of stranding and incidental catch are, in order from top to bottom: Pacific white-sided dolphin, mesoplodont whale, minke whale, finless porpoise, Dall's porpoise. Gray whale, right whale, humpback whale, beluga whale, sperm, whale, Hubb's beaked whale, pygmy killer whale and rough-toothed dolphin were only recorded in one case during this period, and are considered rare species in this region (Ishikawa, 2003). Recently, several Indian Ocean bottlenose dolphins (*Tursiops* aduncus) are known to have settled on Noto Island in Ishikawa Prefecture, Japan (Kasuya, 2011).

The main distribution area of finless porpoise in the Region 19 is limited to the sea area north of Kyushu centered on the Hibikinada Sea, although there are records of stranding or mortality incidental to fishing operations in the Noto Peninsula and Wakasa Bay (Kasuya et al., 2002). There are two major color morphs in Dall's porpoises, dalli type with a flank patch that extends forward to about the level of the dorsal fin and truei type with a flank patch extending to about the level of the flippers. Only dalli type animals are distributed in the region 19 (Miyashita and Kasuya, 1988).

Korean survey:
The southern area adjacent to the east coast of Korea is a seasonal migratory corridor and feeding ground for cetaceans. Many cetaceans in this area inhabit near coastline where the bottom topography characterized with very narrow continental shelves and steep slopes. Systematic sighting surveys have been conducted in this area by the National Institute of Fisheries Science in Korea from 2000 in order to estimate the abundance of minke whales and other cetacean species. However, though some cetacean species were occasionally caught

incidentally, there were no sightings of baleen whales except minke whale. Unlike baleen whales, various species of toothed whales are found in Region 19. The most abundant species is the common dolphin followed by the Pacific white-sided dolphin (Sohn et al., 2012). Distribution of the cetaceans based on these surveys is shown in Fig. R19-65.

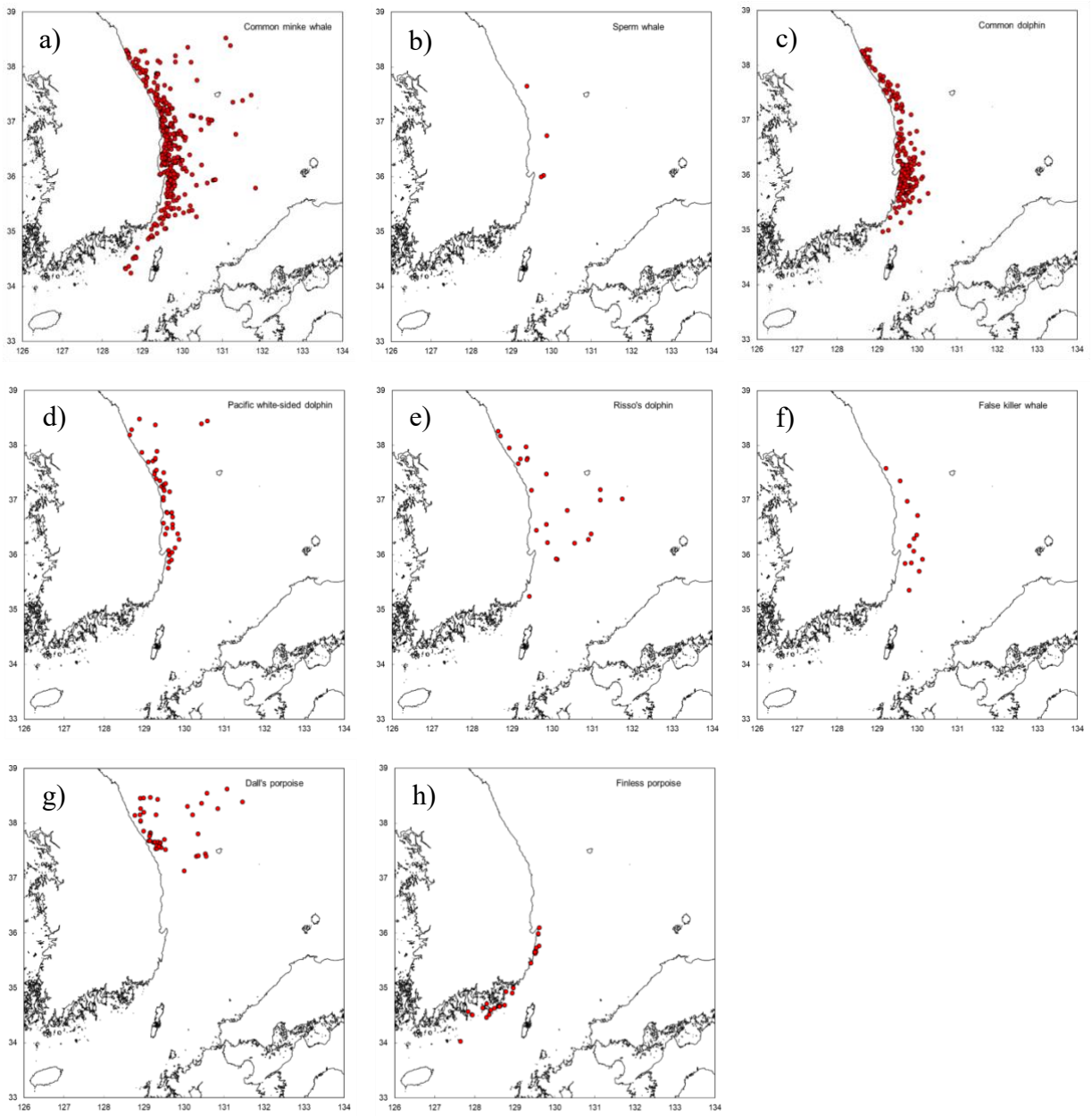

Figure R19-65. Sighting locations of (a) common minke whales, (b) sperm whales, (c) long-beaked common dolphins, (d) Pacific white-sided dolphins, (e) Risso's dolphins, (f) false killer whales, (g) Dall's porpoises and (h) finless porpoises from 2000–2019.

Common minke whales (*Balaenoptera acutorostrata)* are cosmopolitan animals which are distributed throughout the world oceans. They migrate seasonally between their winter breeding grounds in subtropical regions and summer feeding areas in subarctic regions. Region 19 is the

migratory corridor for minke whales, so they are found in this region all year round (Fig. R19-65a). Most minke whales are solitary animals although mother and calf stay together in spring.

Sperm whales (*Physeter macrocephalus)* are well known as deep open sea dwellers, so this species is only a transient visitor to Region 19 (Fig. R19-65b). A pod of sperm whales composed of mothers and juveniles was observed in the southern part of Region 19 in 2004, 2015, 2017 and 2019.

Common dolphins (*Delphinus delphis)* are the most abundant marine mammal in this region. They usually travel in a big school composed of hundreds to thousands of animals in the coastal waters (Fig. R19-65c) They are found in all seasons, but closer to the coast in winter than summer.

Pacific white-sided dolphins (*Lagenorhynchus obliquidens)* are the second most abundant animals in the area (Fig. R19-65d). They form small groups of several tens to hundreds of individuals, but groups of up to 1,200 have been sighted. They prefer the cold waters of higher latitudes.

Risso's dolphins (*Grampus griseus)* are found in most areas of Region 19. They are most frequently seen dolphins outer continental shelf in the area (Fig. R19-65e). In most cases, the group size was less than 50 individuals.

False killer whales (*Pseudorca crassidens)* are tropical or subtropical species that prefers open waters. The northern limit of their distribution is at 38°N (Fig. R19-65f) where they can be found from early summer to late autumn. Their pod sizes ranges from tens to hundreds of animals. Sometimes they congregate together with a school of common bottlenose dolphins in Region 19.

Dall's porpoises (*Phocoenoides dalli)* are boreal animals and they are observed in the northeastern waters off the Korean Peninsula (Fig. R19-65g) from winter to late spring. They form small pods of several animals.

Finless porpoises (*Neophocaena asiaeorientalis)* are neritic and the most abundant porpoise species in Korean waters. Several animals have been observed in the coastal waters in the East coast of Korea (Fig. R19-65h) although numerous individuals also inhabit in the coastal waters of the Yellow Sea and the Korea Strait.

11. Marine Pollution

based on submitted ETSOs by S. Hong, W. J. Shim, M. Choi, B.- S. Yoon, D.-W. Hwang, Y.-W. Lee, H. Maki, A. V. Sevastianov, T. S. Lishavskaya, T. A. Belan, K. Aksentov

11.1 Korean waters

Marine pollution in Region 19 calls for no serious warning. There are no drastic changes over the last decade. It seems some protective actions taken by the countries to save the environment have provided positive results. In particular, the volume of marine debris off Korea is decreasing (Fig. R19-66) and the concentration of antifouling biocides has decreased, too (Fig. R19-67). The concentration of led (Pb) and mercury (Hg) in coastal sediments off the

southern part of Korea has been decreasing; while in the northern part of South Korea it has been steadily growing (Fig. R19-68, R19-69, R19-70, R19-71).

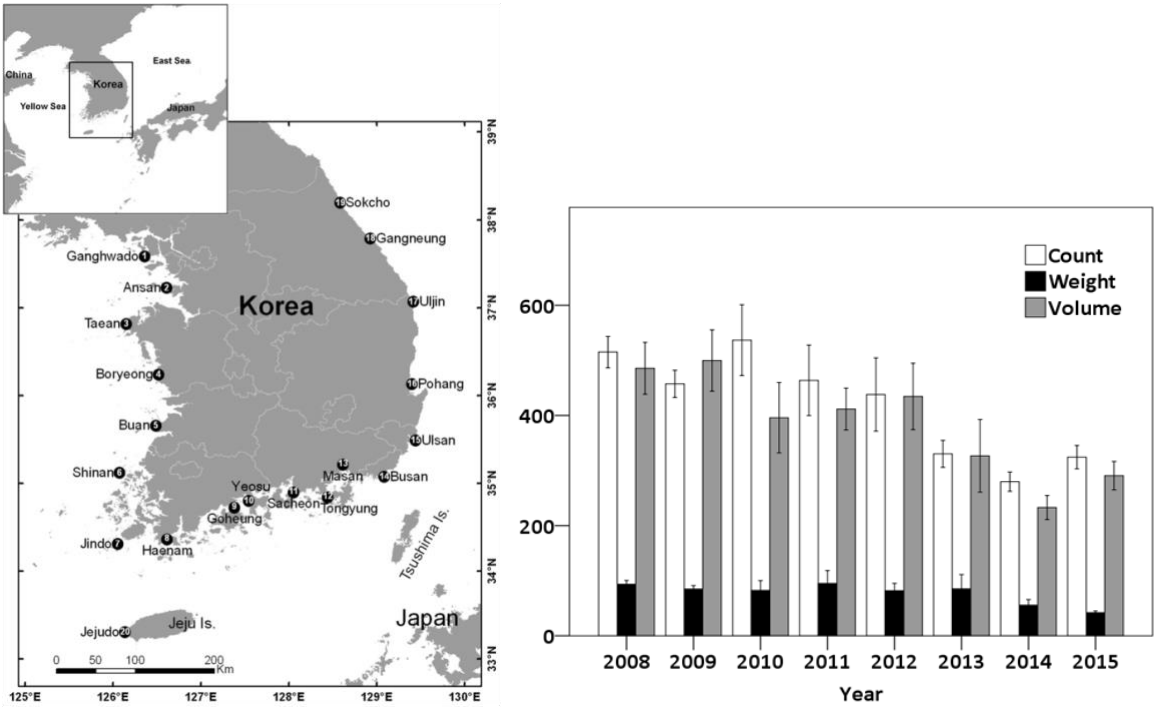

Figure R19-66. Location of marine debris monitoring sites in Korea (left) and temporal trend of marine debris quantities in Korea over 2008-2015 (right) (mean ± SE) (Unite: counts/100 m; weight: kg/100 m; volume: 10^{-3} m^3/100 m*).* (Hong S. W., and Shim W. J., ETSO).

11.1.1 Marine debris

Marine debris pollution is a global concerning issue. A total of 20 beaches have been monitored along the coasts of the Republic of Korea since 2008 with governmental support (Figure R19-66a, Hong et al., 2014). A 100-m-long transect located by GPS at each beach has been surveyed by the trained NGO researchers every two months (i.e. at the end of odd-numbered months ± 5 days) using the fully standardized protocol. All debris larger than 2.5 cm in diameter between the low tide mark and the vegetation boundary or artificial barriers were collected. The debris was classified into twelve categories such as plastics other than Styrofoam, metal, wood, cloth, etc. and measured in terms of number, weight and volume. Individual debris collected was further classified into 94 items to identify abundant debris and contributing sources. Before the survey (i.e. January 2008), all existing marine debris on the selected beaches was removed in order to remove possible effects accumulated during the past years.

Hong et al. (2014) reported the level of marine debris pollution and identified its main sources based on the analysis of the first two-year surveys (i.e. total of 220 surveys from March 2008 to November 2009). The mean quantities of marine debris were estimated as 481.9 (±267.7 SD) count/100 m, 86.5 (±78.6 SD) kg/100 m, and 0.48 (±0.38 SD) m^3/100 m. Plastics and Styrofoam occupied the majority of debris composition in terms of number (66.7%) and volume (62.3%). Wood (timber) was the major material in weight. Main sources of debris were suggested from fishing activities (51.3%). Styrofoam buoy debris was the most frequent item, which potentially

originated from aquaculture. Fisheries operations as the sources of these debris have been also reported by other studies (Jang et al., 2014a, b).

According to the preliminary analysis, the number, weight, and volume of marine debris have significantly decreased over 8 years, from 2008 to 2015 (MOF & KOEM, 2015) as shown in Figure R19-66. A decrease of inputs from land-based and/or sea-based sources, active cleaning by local authorities and/or residents, less intensity of storm rainfalls and wind, and effective policies could be the factors affecting the overall decrease in the amount of beach debris. Seasonality in marine debris abundance was observed; debris was more abundant from summer to early fall (late July to late September) and less abundant in winter. Typhoons, wind direction changes, and beachgoers in summer holiday season may affect the result. Further analysis should be accomplished to identify which factors have significantly contributed to the observed long-term decrease and seasonality.

Marine debris has negatively affected wildlife through entanglements or ingestion (Hong et al., 2013). Forty-five cases collected in this research showed that at least 21 species, including 18 bird species, two mammal species, and one crustacean species, have ingested or been entangled by marine debris, especially of recreational fishing gears (e.g., fishing hooks, monofilament lines, sinker) and commercial fishing gears (e.g., nets, ropes, traps). Five threatened or protected species were included among them: Black-faced spoonbill (*Platalea minor)*, Whooper swan (*Cygnus cygnus)*, Greater painted snipe (*Rostratula benghalensis)*, Finless porpoise (*Neophocaena phocaenoides)*, and Water deer (*Hydropotes inermis)*.

The studies on quantities of marine debris and its impacts on wildlife show that management and legislation on fishing gear (both commercial and recreational) should be prioritized in Korea.

11.1.2 Biocidal additives

Biocidal additives have been used in antifouling paints for ship hulls and marine structures to prevent the immersed solid surfaces from fouling of colonizing marine organisms. Antifouling biocides can be directly introduced from ship hulls to marine environments and cause adverse biological effects on non-target marine organisms (U.S. Environmental Protection Agency, 2004).

Tributyltin (TBT), an antifouling agent found in seawater, bivalves and sediments, has annually been monitored at twenty five site along the coast of Republic of Korea by the Korean Ministry of Ocean and Fisheries (MOF) since 2001 (Figure R19-67). As a consequence of the total ban on TBT use in Korea from 2003, the mean concentrations of TBT in seawater and bivalves has significantly decreased. However, TBT levels in sediments were not significantly reduced due to its persistence in the benthic environments. In Korea, restrictions addressing the use of TBT-based antifouling paints were partially introduced in 2000 for small boats, but their use was totally banned in 2003, and their residues on ships were banned in 2008 (Korean Ministry of Ocean and Fisheries, 2008), following the action of the International Maritime Organization. The total ban on TBT usage in Korea was quite effective to reduce its level in seawater and biota, but longer periods will be required for reduction of sedimentary TBT level.

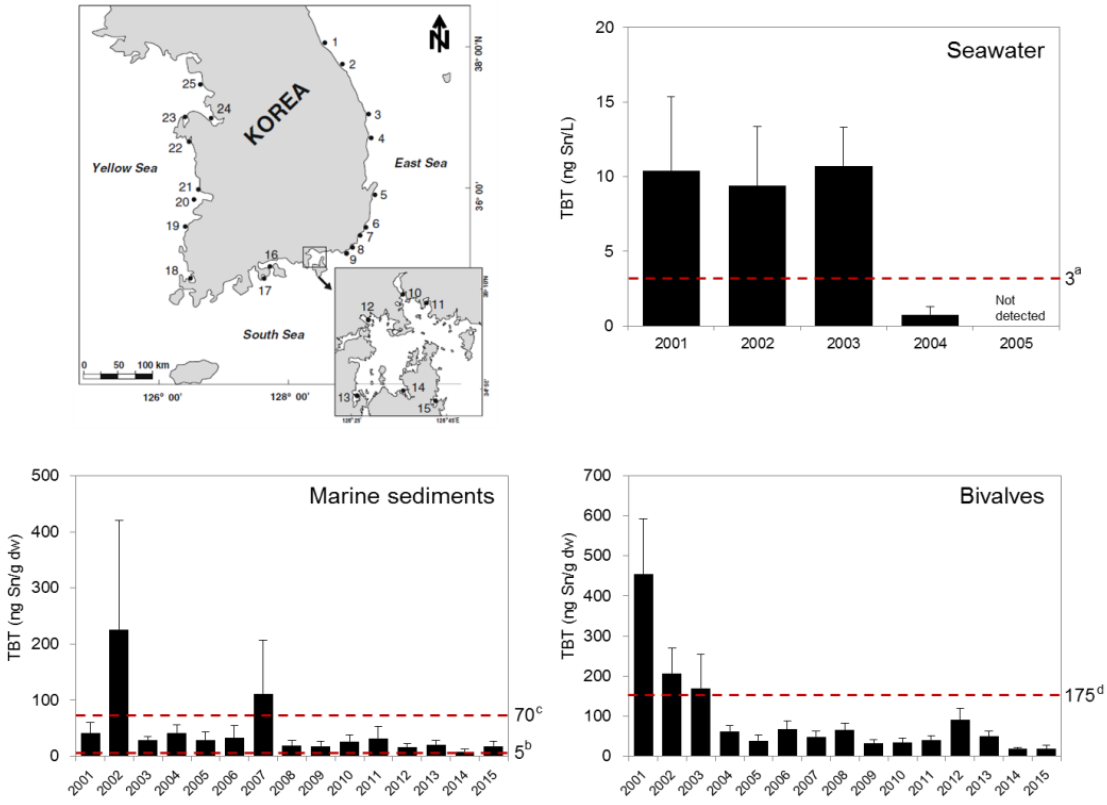

Figure R19-67. Temporal trends of the mean tributyltin (TBT) concentrations in seawater, marine sediments, and bivalves at twenty-five sites along the coast of Republic of Korea in 2001-2015, with a comparison of screening values reported elsewhere: Chronic criterion of USEPA (2004); AMWQG-LT (Australian Marine Water Quality Guideline-low trigger value); AMWQG-HT (high trigger value; Burton et al. 2004); Upper lower ecotoxicological assessment criteria of OSPAR (2004). *(Choi M., Yoon B. S., Shim W. J., ETSO)*.

Following the ban of TBT based antifouling agents, alternative biocides were introduced into the market. Only limited data are currently available regarding the occurrence of alternative antifouling agents (i.e. Organotin (OT)-free antifouling biocides) in marine environments in Korea. In the 2009-2010 survey (Kim et al., 2014), Diuron and Irgarol in seawater were widely distributed along the coastal areas of Korea, while the levels of pyrithiones and dichlofluanid were below the detection limits at all sites, and Sea-Nine 211 was detected occasionally at some sites. In 2015, seawater contamination levels by Diuron and Irgarol were monitored at 71 stations from five major industrialized harbors in Korea (NIFS, 2015). Diuron and Irgarol were commonly detected in seawater of Korea, with concentrations ranged from 33 to 640 ng/L for Diuron and from 0.1 to 15 ng/L for Irgarol. The current Diuron concentrations in Korean coastal water occasionally exceeded the EU-predicted no-effect-concentration (PNEC, 200 ng/L) and UK Environmental quality standard (EQS, 100 ng/L), while Irgarol levels were not high enough to cause the adverse health effects on marine organisms (EU PNEC 43.9 ng/L and UK EQS 24 ng/L). These monitoring results indicate that Diuron is an antifouling agent of concern in the Korean coastal waters since the ban of TBT use.

11.1.3 Trace metals

The Ministry of Oceans and Fisheries of the Republic of Korea (MOF) has investigated the concentrations of trace metals in Korean coastal sediments collected at 71 stations from 2004 to 2015 (*n* = 828 and 833, for mercury (Hg) and lead (Pb), respectively).

Mercury (Hg) is a highly toxic and bio-accumulative trace metal. Mercury occurs naturally at low levels in rock, soil, and natural water including seawater. However, about half of all Hg in the natural environment originates from anthropogenic sources, including the burning of fossil fuels, waste incineration, mining and other industrial activities.

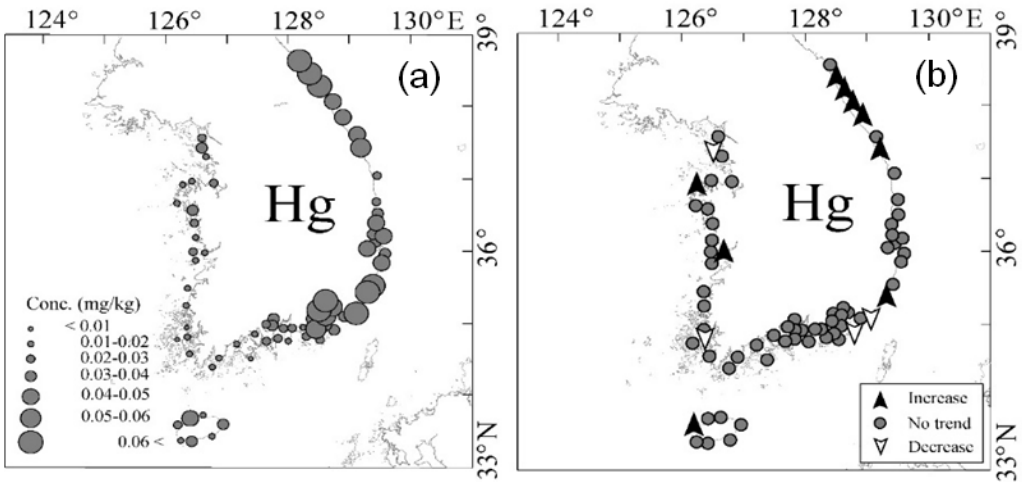

Figure R19-68. Horizontal distributions (a) and temporal trends (b) of mean Mercury (Hg) concentration in coastal sediment collected at 71 stations along the Korean coast from 2004 to 2015. (Hwang D. W. and Lee Y. W., ETSO).

The Hg concentrations in Korean coastal sediments showed large spatial differences. The mean Hg concentrations at each sampling site during the monitoring periods ranged from 0.009 to 0.466 mg/kg-dry weight (dw) (mean 0.038 mg/kg-dw) and the highest mean concentration was found at the Onsan coast located in the southeastern part of Korea (Fig. R19-68a). Compared to the threshold effect level by the sediment quality guidelines for Hg (MOF, 2013) (i.e. TEL, 0.11 mg/kg-dw) used in Korea, the mean Hg concentrations were below the TEL value at all sampling sites, except for one site (Onsan coast). Most of the mean Hg concentrations in sediments were much higher in the southeastern and northeastern coasts of Korea.

The mean Hg concentrations in Korean coastal sediments gradually increased every year during the monitoring periods. Though the Hg concentration did not show a temporal change at most of the sampling sites, it increased and decreased significantly at nine and four sites, respectively, as shown in Fig. R19-68b. Although there are no special anthropogenic sources such as large metropolitan areas, industrial complexes, and large-scale fish and shellfish farms along the northeastern coast of Korea, the increasing trends of Hg were mainly found in the northeastern coast. The trend could have been caused by the increase in releases of the metals into the atmosphere from inland-based sources in Korea and China. It is reported that the events of yellow sand and micro-dust storms, which contain many toxic metals originating from inland China and Korea, frequently occur in the northeastern coast of Korea (Hwang et al., 2016).

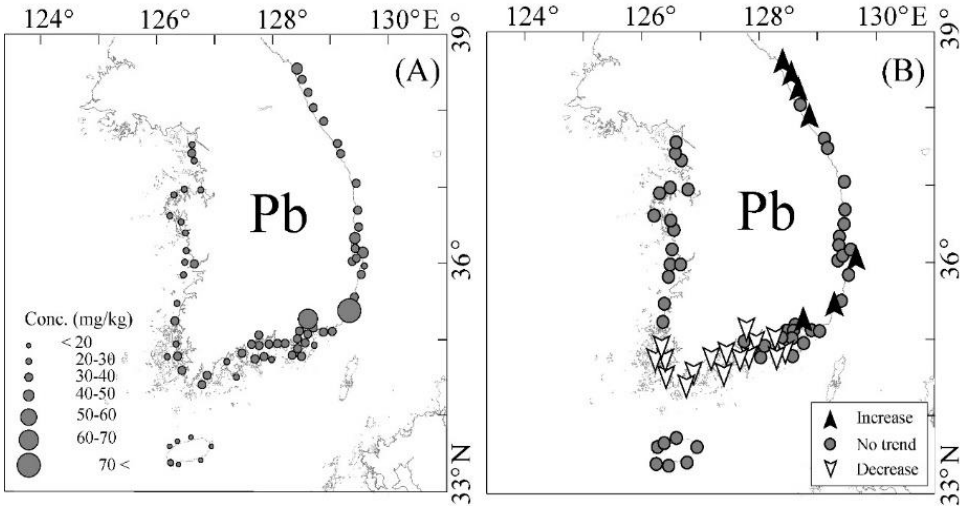

Figure R19-69. Horizontal distributions (A) and temporal trends (B) of the mean Pb concentration in coastal sediment collected at 71 stations along the Korean coast from 2004 to 2015. (Hwang D. W. and Lee Y. W., ETSO).

Lead (Pb) is one of the trace metals that occur naturally in the earth's crust. The Pb concentrations in the natural environment have significantly increased worldwide over the past century because of anthropogenic activities such as manufacturing processes, paint and pigment applications, and fossil fuel burning (Kimbrough et al., 2008). Lead (Pb) in coastal environments mainly originates from anthropogenic sources by human activities rather than natural processes such as the weathering and erosion of soils and rocks.

The Pb concentrations in Korean coastal sediments showed large spatial differences during the monitoring periods. The Pb concentrations in the sediment of each sampling site ranged from 17.1 to 92.2 mg/kg-dry weight (dw) (mean 32.3 mg/kg-dw) and the highest mean Pb concentration was found at the Onsan coast located in the southeastern part of Korea (Fig. R19-69A). Compared to the threshold effect level by the sediment quality guidelines (MOF, 2013) for Pb applied in Korea (i.e. TEL, 44.0 mg/kg-dw) the mean concentrations were below the TEL value at all except two sampling sites (Onsan coast and Masan Bay). In addition, the mean Pb concentrations were significantly higher in the southeastern coast of Korea, where large metropolitan areas, industrial complexes, and fish and shellfish farms are heavily concentrated. Thus, these results indicate that human activities in the Korean coastal zone likely influenced the distribution of Pb concentrations in the coastal sediment (Hwang et al., 2016).

The mean Pb concentrations in Korean coastal sediments did not show any marked overall trend during the monitoring periods. However, the concentrations increased and decreased at seven and sixteen sites, respectively, as shown in Fig. R19-69B. Especially, the decreasing trends of Pb were mainly found in the southern coast where the influence of human activities is conspicuous. This could result from the sustainable coastal management fostered by the Korean Government because most parts of the southern coast of Korea have been designated as special management areas, marine environment conservation areas, and marine protected areas (Hwang et al., 2016).

The monitoring of trace metals provides policymakers with the scientific evidence to devise effective management plans for improving coastal environments. The findings of Hg and Pb

pollution have been used to manage the sediment quality of the Korean coast to implement the marine environmental policy (e.g., regulation of contaminant loadings in the special management areas, dredging of contaminated sediment in the harbors, and designation of marine protected areas). Thus, continuous monitoring of the trends of trace metals including Hg and Pb is necessary to manage the environmental quality in the Korean coastal waters.

Marine bivalves have been extensively used as bioindicators to assess the pollution of the coastal environment because of their sedentary behavior, broad distribution, abundance, and high ability to accumulate metals (Weng and Wang, 2014). The concentrations of trace metals in soft tissues of mussels (*Mytilus edulis*, *n* = 270) and oysters (*Crassostrea gigas*, *n* = 107) collected at 25 stations along the coast of the Republic of Korea were investigated by the Ministry of Oceans and Fisheries of Republic of Korea (MOF) from 2000 to 2015. The Pb concentrations in two shellfish species showed large spatial differences during the monitoring periods. The mean Pb concentrations in mussels and oysters of each sampling site ranged from 0.10 to 0.83 mg/kg-wet weight (ww) (overall mean 0.27 mg/kg-ww) and from 0.14 to 0.28 mg/kg-ww (overall mean 0.19 mg/kg-ww), respectively (Fig. R19-70). Relative to mussels, oysters have lower Pb concentrations. Compared to the safety threshold (2.0 mg/kg-ww) of Pb for shellfish applied in Korea (MFDS, 2015), the Pb concentrations in mussels and oysters were below the threshold in all samples except mussels of the Onsan coast in 2014. The highest mean Pb concentrations were found in mussels and oysters near urban and industrial areas (Onsan coast for mussels and Asan coast for oysters). However, mussels and oysters at some sampling sites near the large urban and industrial complexes showed low Pb concentrations. This finding implies that Pb concentration in two shellfish species of Korea is not necessarily dependent on anthropogenic activities in the coastal zone.

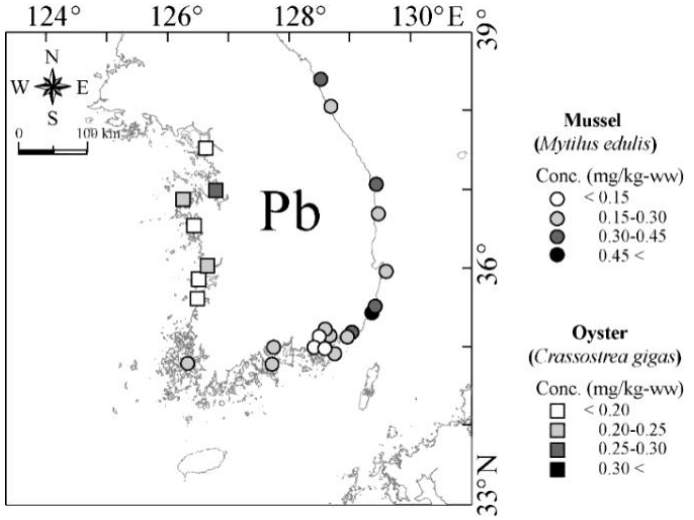

Figure R19-70. Horizontal distributions of mean Pb concentration in the tissues of mussels and oysters collected at 25 stations along the Korean coast from 2000 to 2015 (Hwang D. W. and Lee Y. W., ETSO).

The mean Pb concentrations in mussels were below 0.5 mg/kg-ww except 2000 and exhibited little temporal variation during the monitoring periods (Fig. R19-71A), while the mean Pb concentrations in oysters showed larger annual variaiton (Fig. R19-71B). In present, It is difficult to find the main cause for these variations because there are distinct differences in potential of

bioaccumulation of trace metals between mussels and oysters (Kimbrough et al., 2008). It is known that the metal accumulation in tissues of bivalves depends on various biological (i.e. size, age, clearance rate, and reproductive cycle etc) and environmental (i.e. temperature, salinity, pH, and dissolved organic matter) factors (Langston and Spence, 1995). Thus, more extensive studies are necessary to understand the mechanism of temporal variations of Pb concentration in tissues of mussels and oysters of the Korean coast.

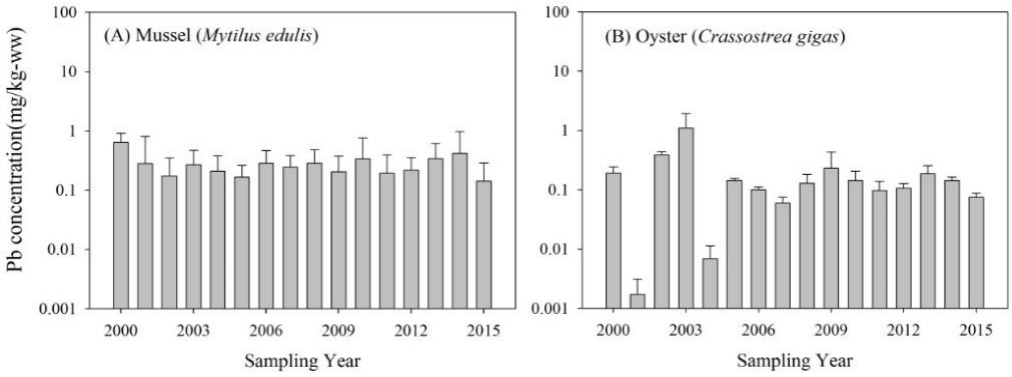

Figure R19-71. Annual variations of mean Pb concentration in the tissues of mussels (A) and oysters (B) collected at 25 stations along the Korean coast from 2000 to 2015 (Hwang D. W. and Lee Y. W., ETSO).

11.2 Waters around Japan

As mercury (Hg) is ubiquitously distributed in marine environments because of its multilateral sources, including atmospheric deposition originating from the combustion of coal, gold mining, geological conditions (volcanoes) and anthropogenic releases into water systems, many monitoring efforts targeting various marine environmental media such as seawater, sediment and biota have been conducted to protect human health from Hg poisoning via dietary intakes of fisheries products. Significant attention has so far been paid to Hg pollution in Japan since the Minamata disease tragedy was recognized as a consequence of anthropogenic Hg pollution in the coastal sea of Minamata Bay in Kumamoto, Kyushu. As a regulatory measure to protect human health, commercial deliveries of some marine fishes caught in the coastal seas of Japan have been occasionally banned because of accidental Hg contamination in them. To protect human health from the effect of anthropogenic emissions and releases of Hg, and to reduce Hg contamination in marine environments, the Minamata Convention on Mercury (UNEP, 2016) was adopted as an international environment treaty and has already been signed by 128 countries. In Japan, industrial demand for Hg has been drastically reduced because of the regulation and source controls (Fig. R19-72). For instance, enforcement for curtailment of use has been implemented.

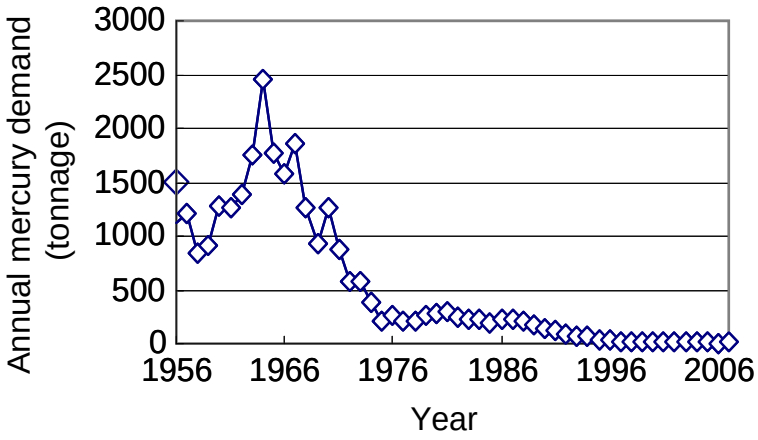

Figure R19-72. Fifty-year variations of mercury (Hg) demand in Japan (METI, 2009).

The Ministry of the Environment (MoE, formerly, Environmental Agency, the Government of Japan), has set the provisional removal standards for Hg to prevent the discharging of elution to the water column in marine environments (MoE, 2009). MoE has been conducting rigorous monitoring works of marine sediments by setting eight transects in the coastal seas around Japan since 1975 (Fig. R19-73; MoE, 2009). This monitoring was initially aimed to evaluate the influence of terrestrial human activities on the coastal sea environments but recently the purpose was shifted to the evaluation of the influence of ocean dumping of various sludges and waste soils. Sampling depths for the monitoring stations varied from 20 to 6,500 m.

Figure R19-73 shows the horizontal distribution of total mercury (T-Hg) concentrations (µg/g dry) in sediments in the coastal seas around Japan from 2004 to 2014. Data for each transect are summarized in Table R19-4. The concentrations in the Pacific Ocean (transects A, B and C) are higher than those in the marginal seas (transects E, F, G and H). Average T-Hg concentrations in transects B and C are 0.13 and 0.16 µg/g-dry, respectively, which are higher than in other transects and seem to reflect influences of anthropogenic pollution from the huge urbanized and heavily industrialized areas around Tokyo Bay (transect B) and Osaka Bay (transect C). All detected T-Hg concentration values are lower than the provisional removal standards set by MoE.

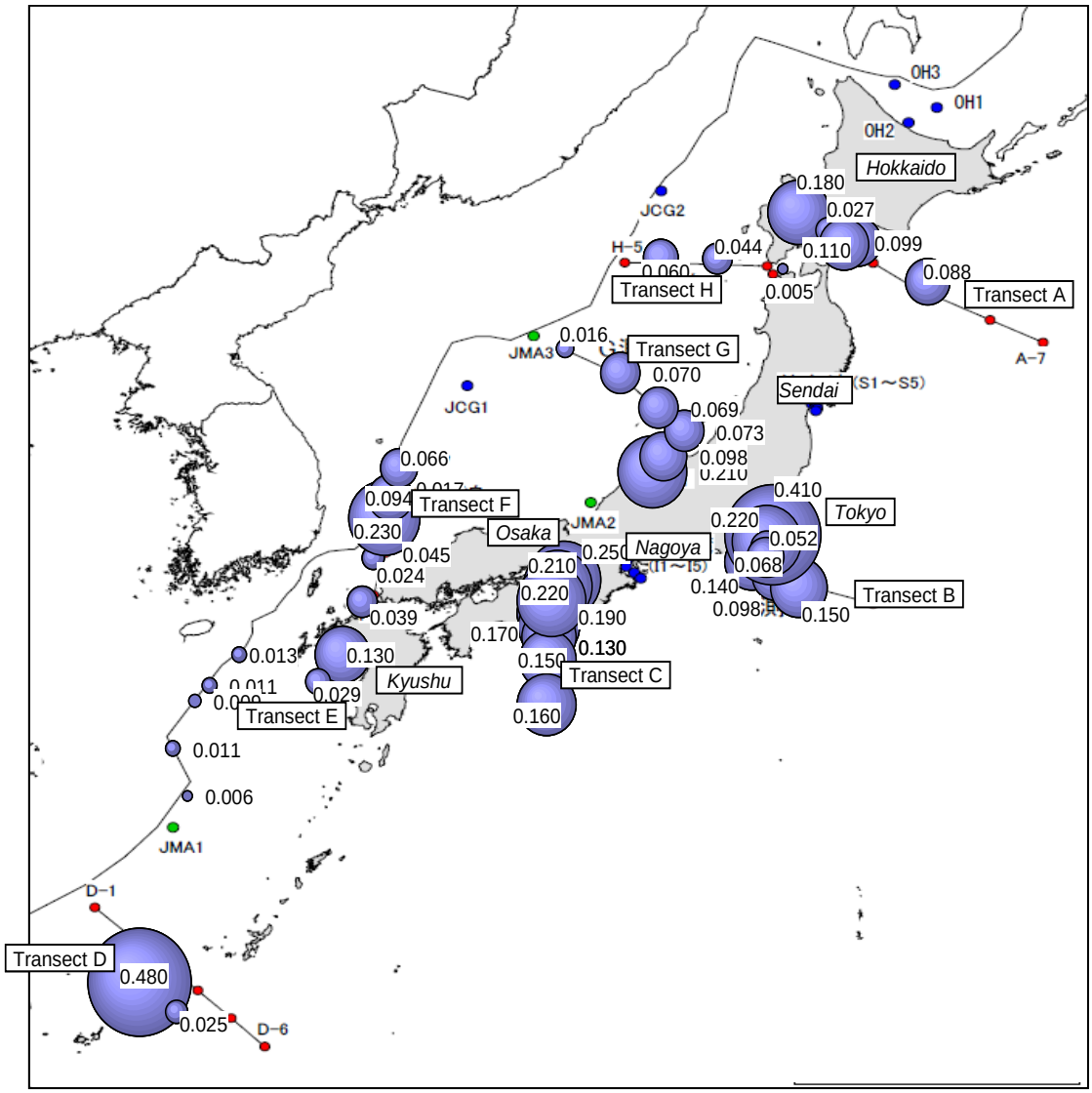

Figure R19-73. Horizontal distribution of sedimentary mercury (Hg) in the coastal seas around Japan from 2004 to 2014 (NIES, 2016). Each value on bubbles shows T-Hg concentration (μg/g-dry).

Table R19-4. Summary of total mercury (T-Hg) concentrations in sediments in eight transects in the coastal seas around Japan (2004 to 2014, NIES, 2016).

Transect	T-Hg concentration (µg/g-dry)			Data acquisition	
	Lowest	Highest	Average	Year	The number of stations
A	0.027	0.180	0.101	2005	5
B	0.098	0.150	0.129	2008	3
C	0.130	0.190	0.160	2010	5
D	0.025	0.480	0.253	2013	2
E	0.016	0.130	0.030	2012	8
F	0.017	0.230	0.074	2004	7
G	0.016	0.210	0.089	2009	6
H	0.005	0.060	0.036	2005	3

11.3 Russian waters

Vladivostok city situated along the Peter the Great Bay coastline is one of the main seaports of Russian Far East with high anthropogenic pressure derived by large human populations (about 620, 000 individuals) industrial development, and transportation. The main sources of pollution near Vladivostok are municipal and industrial waste waters, urban runoff, marine transportation, and dredged materials. As the result of chemical loads and run-off inputs (i.e. including nutrients and dissolved organic matter) the marine-coastal zone near Vladivostok is exposed to permanent anthropogenic impacts.

For this report, three areas in Peter the Great Bay (Amurskiy Bay, Ussuriyskiy Bay and Golden the Horn Bay) with different level of pollution are analyzed using the Principal Components Analysis. Concentrations of petroleum hydrocarbons, trace metals (i.e. lead: Pb) and chlorinated hydrocarbons in bottom sediments were used to assess the degree of pollution. Inter-annual variation of Pb concentrations (mg/kg dw) in bottom sediments in three sampling locations of Peter the Great Bay is shown in Fig. R19-74.

Golden the Horn Bay (Vladivostok inner harbor) was considered to be an extremely polluted area by Pb, while Amurskiy Bay exhibited high to moderate levels of sediment contamination by Pb. These are semi-closed coastal areas with comparatively weak water dynamics and containing silt sediments with a high concentration of total organic carbon (up to 127.4 mg/kg dw), petroleum hydrocarbons (up to 2.83 mg/kg dw) and trace metals. Moderate pollution levels were observed in bottom sediments from Ussuriyskiy Bay. In general, no discernable trends of sediment Pb concentrations over time are observed at all locations.

The Pb content in Amurskiy and Ussuriyskiy Bays does not exceed the maximum permissible concentration (MPC)45-85 ppm, whereas in the Golden the Horn Bay the maximum Pb content in bottom sediments (131.68 ppm) was higher than MPC.

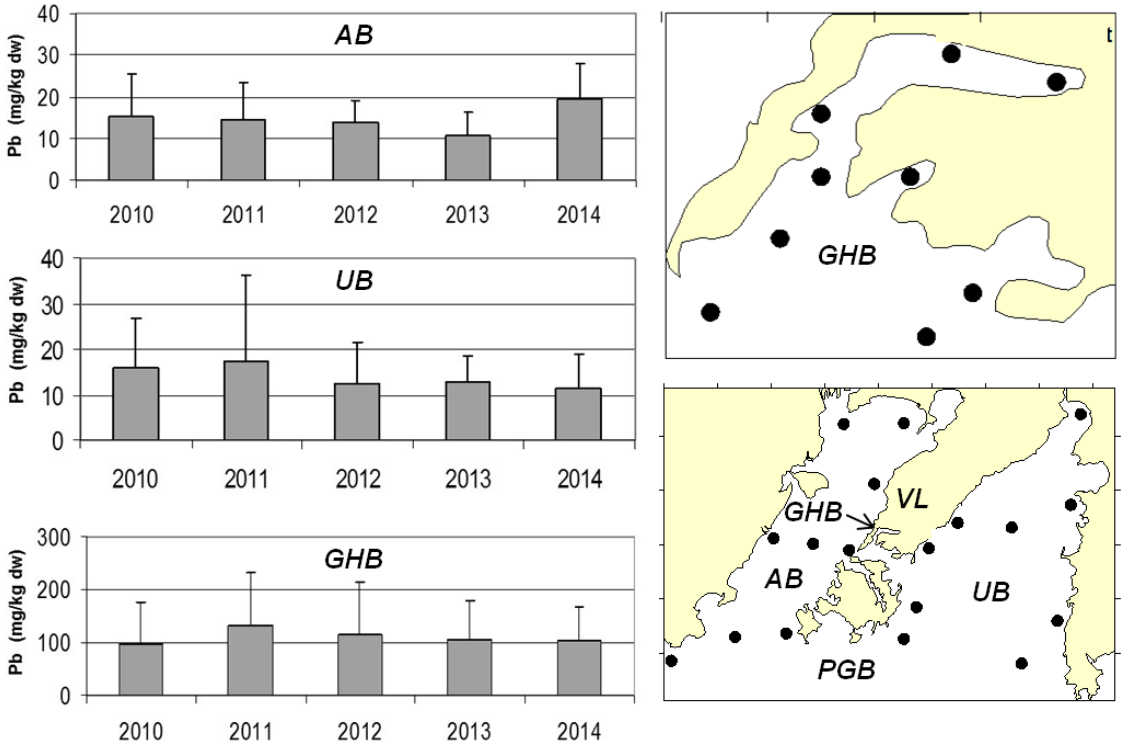

Figure R19-74. Inter-annual variation of Pb concentrations (mg/kg dw) in bottom sediments of Amurskiy Bay (top, AB), Ussuriyskiy Bay (middle, UB) and Golden the Horn Bay (bottom, GHB) and scheme of sampling station's location. PGB - Peter the Great Bay, VL – Vladivostok city (Sevastianov, Lishavskaya and Belan, personal).

Studying the processes influencing the distribution and transportation of mercury (Hg) in the environment is of paramount importance because of its high toxicity. Since the onset of the industrial period, anthropogenic emissions of Hg have increased and its global cycling have been significantly altered (Fitzgerald et al., 2007; Schuster et al., 2002). The Amurskiy Bay has been being exposed to the intense anthropogenic impacts since the middle of the 20th century. The sources of pollutants are the industrial discharges of the enterprises located in the Razdol'naya River basin and Vladivostok city.

The sediment samples were collected by the small gravity core GOIN-1.5 in the northern part of Amurskiy Bay and the Golden the Horn Bay (Vladivostok). Total Hg concentration in samples (dried weight) was determined at 50 °C by atomic absorption spectroscopy on an RA-915+ analyzer equipped with pyrolysis system. The accuracy of the method was tested using a Certified Reference Material Marine Sediments (MESS-3 and PACS-2) (Aksentov, 2013).

Mercury content in bottom sediments of the northern Amurskiy Bay ranged from 50 to 760 ppb with an average value of 120 ppb (Polyakov et al., 2008). The higher concentrations were found in Golden the Horn Bay (2500 ppb) (Aksentov, 2013). The sedimentation rate of 4.1 mm/year

was determined for the past 200 years in the core I08-3 based on unsupported ^{210}Pb (Kalugin et al. 2015). Vertical Hg distribution shows the stages of its accumulation in sediments associated with the increase of human activities (Fig. R19-75).

Cleaning of the Golden Horn Bay and dumping of contaminated sediments in the Amurskiy Bay are demonstrated by the gradients of Hg concentrations in cores M06-34 (GHB) and I07-8 (AB) (Fig. R19-75).

The baseline levels of Hg, estimated from core horizons and deposited before the impacts of human activities, are in the order of 30 ppb. There are also bottom sediments with high Hg content located near natural source, for example, sand in the wave-cut terrace along the abrasion bench in Cape Nizkiy of Popov Island contain Hg concentrations ranging 1000-2500 ppb (Aksentov, 2015). The level of bottom sediment pollution in the Amurskiy Bay varied in time. Industrial development of the Southern Primorye region in the 1900s and especially in modern time (since 1960) has increased an accumulation of Hg in the bottom sediments of the bay.

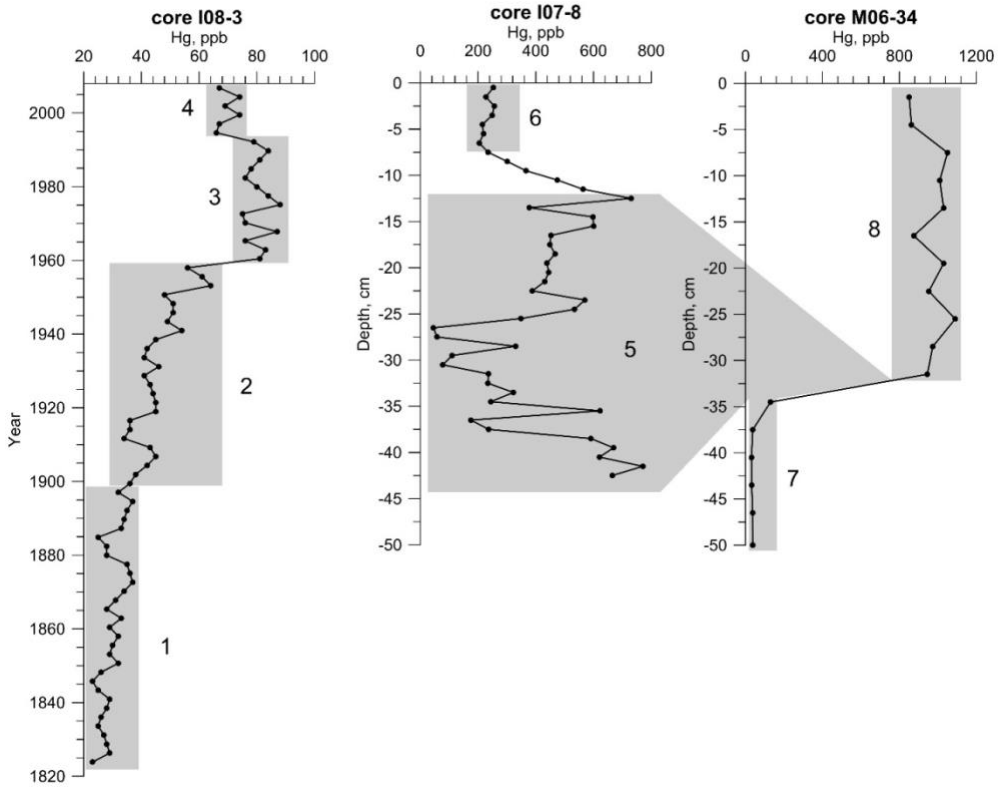

Figure R19-75. Vertical profiles of total mercury (Hg) concentrations in the sediment cores from the Amurskiy Bay (I08-3, I07-8) and the Golden the Horn Bay (M06-34). 1, 7 – background concentration; 2 – moderate impact, 3, 5 – intensive contamination; 4, 6, 8, - recent level. I08-3: 131° 48,192′ 43° 10,743′; I07-8: 131° 50,335′ 43° 05,373′; M06-34: 131° 52,850′ 43° 06,105′.

12. Marine Trophic Level

V. Kulik

Trophic levels of fisheries landings declined in recent decades (Pauly, 1988). Our preliminary research of the trophic level changes in the catch in the Pacific Large Marine Ecosystems (LMEs) also shows a negative trend, but only in the waters around Russia of Region 19 (Kulik, 2017).

The data were selected from the database of daily catches maintained by the Regional Data Center of TINRO-Center from 1995. The data before 1995 were excluded because of significant changes in the rules and data protocols applied in 1994. We didn't include data on catches by small vessels which were operated only in the near shore waters because we didn't have the data before 2004.

First, we selected species or taxonomic groups (e.g. flatfish) that accounted for at least 90% of total monthly catch or were in the top 3 of the monthly catch list. Then we identified their Trophic level – TL, based on the data from stable isotope analysis (Gorbatenko at al., 2008, 2011, 2012, 2013). A mass of catch in thousands of metric tons (Kton) was used for the calculation of the weighted average TL. Trends were extracted using Seasonal Decomposition of Time Series by Loess (STL) with span (in lags = 9) of the loess window for seasonal extraction, which should be odd and at least 7 (Cleveland et al., 1990).

Totally 33 target fish taxa were identified in the top 3 catch or summed to at least 90% of monthly catch (Table 19-5). We abbreviated names of fisheries objects to eight characters using Cornell Ecology Programs standard names (CEP), which have four first letters of the generic name and four first letters of the specific epithet of a Latin name.

Table 19-5. TLs of dominant fisheries objects

	Species	TL	CEP
1	*Ahnfeltia sp.*	1.00	Ahnfsp
2	*Anadara broughtoni*	2.00	Anadbrou
3	*Berrytheuthis magister*	4.10	Berrmagi
4	*Chionoecetes japonicus*	3.80	Chiojapo
5	*Chionoecetes opilio*	3.90	Chioopil
6	*Clupea pallasii*	4.00	Cluppall
7	*Cololabis saira*	2.50	Colosair
8	*Cottidae*	5.00	Cottidae
9	*Eleginus gracilis*	4.60	Eleggrac
10	*Erimacrus isenbeckii*	4.20	Erimisen
11	*Gadus macrocephalus*	5.10	Gadumacr
12	*Gastropoda*	4.80	Gastropd
13	*Hexagrammidae*	4.90	Hexgrmmd
14	*Laminaria sp.*	1.00	Lamisp
15	*Mercenaria stimpsoni*	2.00	Mercstim
16	*Mollusc*	2.00	Mollusc
17	*Octopus dofleini*	4.30	Octodofl

18	*Oncorhynchus gorbuscha*	3.70	Oncogorb
19	*Oncorhynchus keta*	3.40	Oncoketa
20	*Pandalus borealis*	4.00	Pandbore
21	*Pandalus goniurus*	3.90	Pandgoni
22	*Pandalus hypsinotus*	4.30	Pandhyps
23	*Pandalus sp.*	4.00	Pandsp
24	*Paralithodes brevipes*	3.80	Parabrev
25	*Paralithodes camtschatica*	3.80	Paracamt
26	*Paralithodes platypus*	3.80	Paraplat
27	*Pleuronectidae*	4.40	Plernctd
28	*Sebastidae*	4.50	Sebastid
29	*Spisula sp.*	2.00	Spissp
30	*Strongylocentrotus intermedius*	3.20	Strointe
31	*Strongylocentrotus nudus*	2.20	Stronudu
32	*Theragra chalcogramma*	4.50	Therchal
33	*Todarodes pacificus*	3.50	Todapaci

Since 2010 a negative trend in the dynamics of the TLs over 1995-2017 has been observed except for the last two years (2016-2017). As we expected the stabilization of the TL dynamics occurred when the low level was achieved (Fig. R19-76) using the forecast with exponential smoothing (Hyndman et al., 2008).

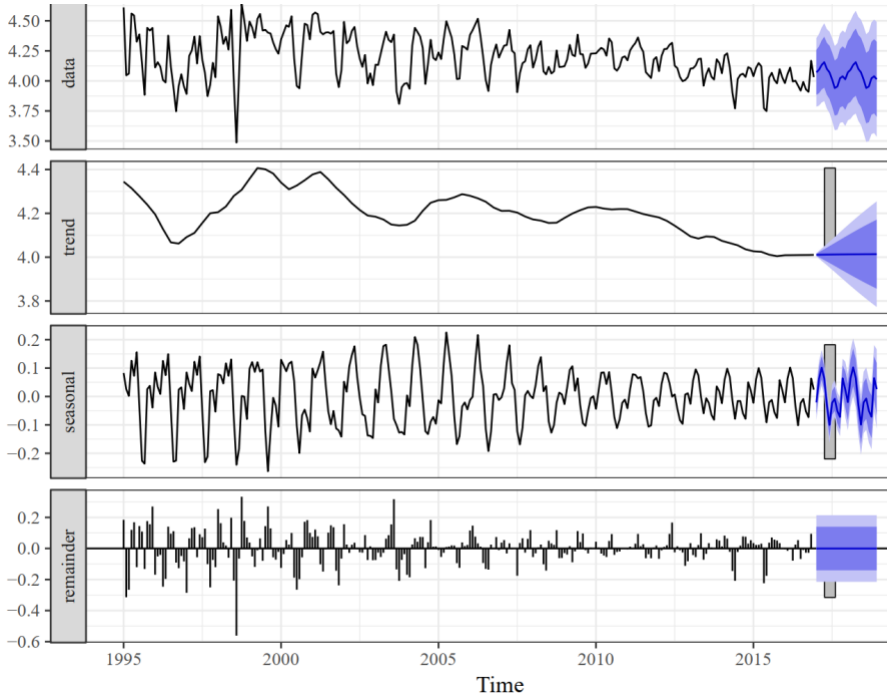

Figure R19-76. Trophic level interannual variability over 1995-2017 based on observations and forecast on 2018-2019 using STL + ETSO of TL.

Over the recent decade mean TL has been gradually decreasing since 2012 (Figure R19-77). This decrease appeared after the highest catch of dominant species in 2012 (Figure R19-78). Pearson's product-moment correlation between the catches and mean TLs is not significant ($p > 0.3$). Supposing that an effect after high catches of dominant species could be lagged in time, we checked cross-correlation. We found out that the highest correlations were lagged by 2-4 years. We made a simple linear model when $TL = 3.93 - 0.00116\ C$, where C is the catch in thousands of metric tons of 3 years before. Globally in recent decades, the rate of TL decrease was about 0.1 per decade without substantial increase in the landings (Pauly, 1988). In our data, the catches are negatively related to TL with 3-year lag. However, the relation between TL and catch will always break down as catches increase because TL of aquatic organisms are inversely related to size (Pauly, 1988).

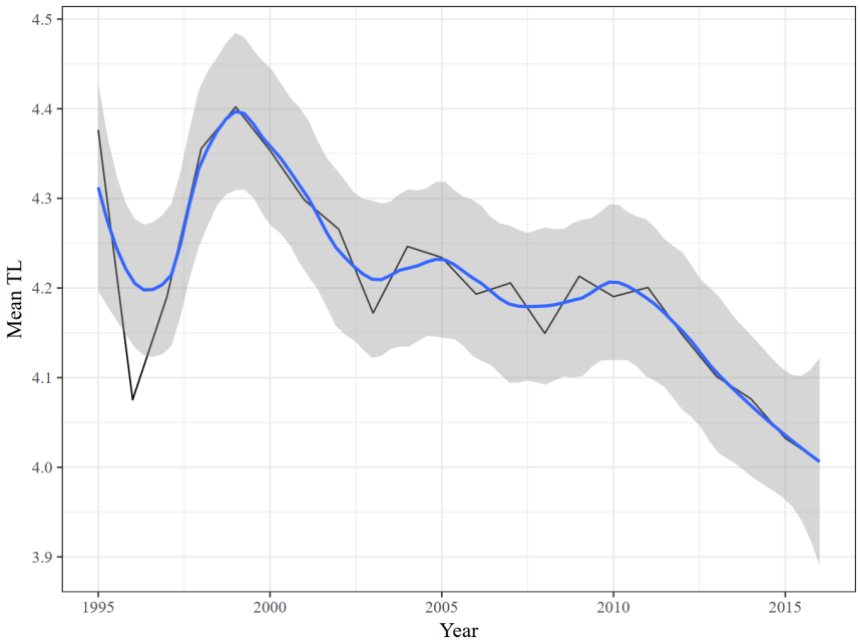

Figure R19-77. Mean annual TL weighted by sum of catches (black line) with Loess smoother (blue line) with its confidence Interval (grey shadow region).

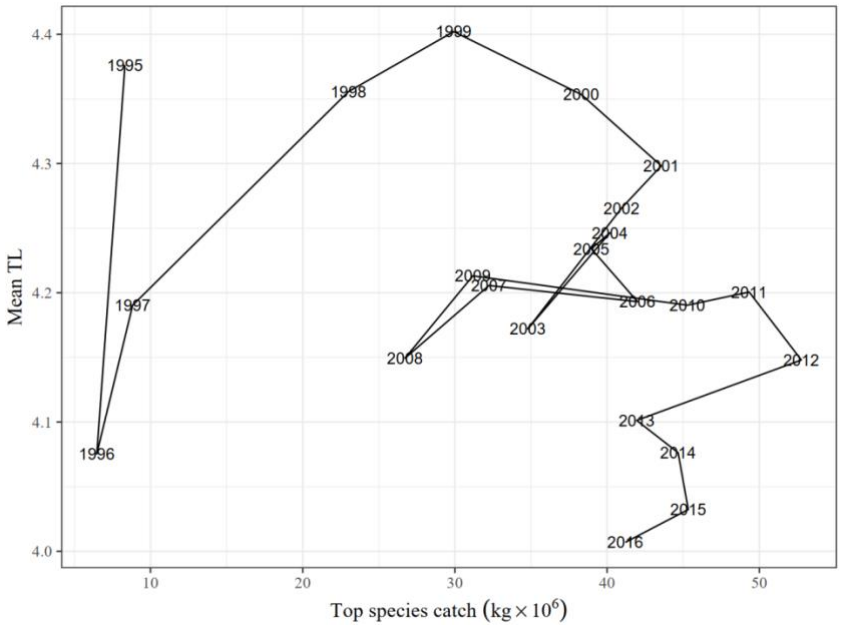

Figure R19-78. Mean TLs in catches versus the catches.

Principal Component Analysis (PCA) helped us highlight species contributing to TL changes. PC1 and PC2 explain 68.6% of the variance. Catches of taxa with significant contributions to PC1 and PC2 are shown by years in Figures R19-79 and R19-80, respectively.

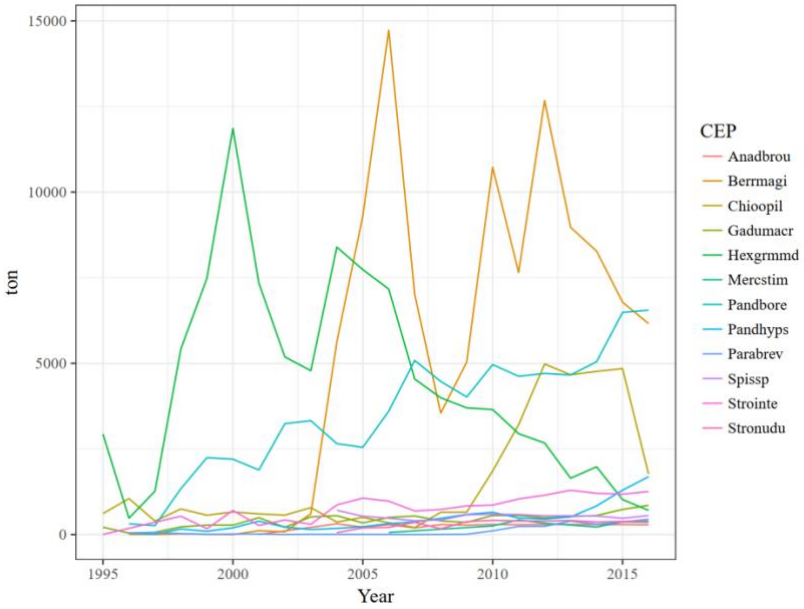

Figure R19-79. Catches of taxa significantly contribute to PC 1.

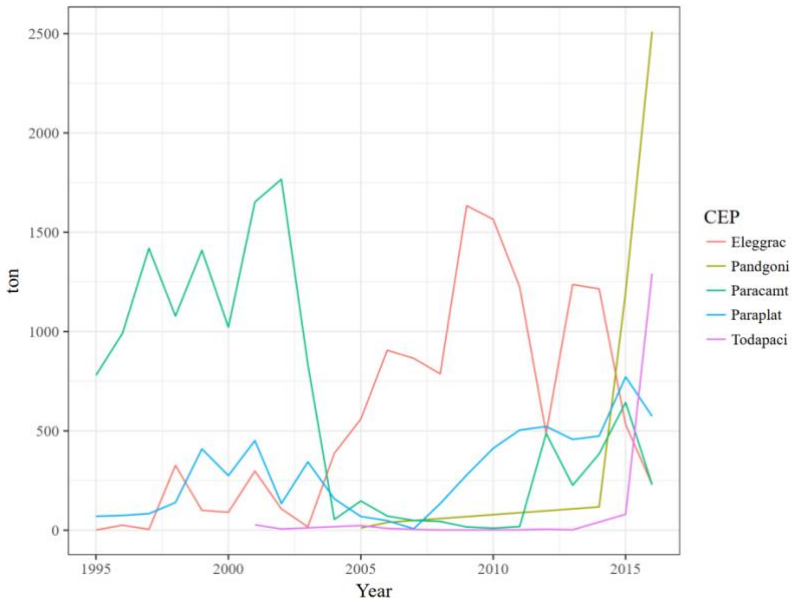

Figure R19-80. Catches of taxa significantly contribute to PC 2.

Okhotsk atka mackerel (*Pleurogrammus azonus,* Jordan and Metz, 1913) had a high trophic level (4.9) as a main fishing target in Hexagrammidae family. The fall in the average annual values of TL is directly related to the fall in catches of this fish, and associated with an increase in the catches of objects with lower trophic levels, for example, shrimps and squids. In our study, it is extremely important to note that the catches of Okhotsk atka mackerel fell because of the decrease in fishing intensity due to the loss of fisheries interest in this fish over the past 10 years. This object is not a target (today), but a bycatch with flounder fishery.

Acknowledgement

Apologies for the preparation of this section took such a long time because so many authors were involved. Many thanks to all the contributers. Special thanks to AP-CREAMS members who organized and edited whole sections: Drs. SungHyun Nam (4. Physical ocean), Guebuem Kim (5. Chemical ocean), Joji Ishizaka (6. Phytoplankton) and Yury Zuenko (7. Zooplankton and 8. Fishes). Many thanks to Drs. Tetsuo Fujii, Hidetada Kiyofuji, Toru Nagasawa and Osamu Katoh for encouraging Japanese contributions as well to Drs. Jae Hak Lee and Se-Jong Ju for support with contributions from Korea. Special thanks to Dr. Sanae Chiba of PICES for her hard work in editing the manuscript.

References

Ahn, J.H., Park, Y.J., Kim, W., Lee, B. and Oh, I.S. 2015 Vicarious calibration of the geostationary ocean color imager. Optics Express, 23: 23236–23258.

Ahn, J.H, Park, Y.J., Kim, W. and Lee B. 2016. Simple aerosol correction technique based on the spectral relationships of the aerosol multiple-scattering reflectances for atmospheric correction over the oceans. Optics Express, 24(26): b29659. doi:10.1364/oe.24.029659.

Aksentov, K.I., 2013. Mercury in bottom sediments of the Peter the Great Bay. Ph.D. Thesis, POI FEB RAS: 140.

Aksentov, K.I., 2015. Mercury in the sea water of the Amur Bay (the Sea of Japan): Recent content and geochemical processes. Russ. Meteorol. Hydrol., 40: 606–611.

Allison, C. 2013. IWC individual catch database version 6.1 (18 July 2016). International Whaling Commission, Cambridge.

Antonov, J.I., Seidov, D., Boyer, T.P., Locarnini, R.A., Mishonov, A.V., Garcia, H.E., Baranova, O.K., Zweng, M.M., Johnson, D.R. 2010. World Ocean Atlas 2009. 2: Salinity, In Levitus S. (ed.), NOAA Atlas NESDIS 68, U.S. Government Printing Office, Washington D.C., 184.

Bauer, J. E., Williams, P. M., Druffel, E. R. M., 1992. 14C activity of dissolved organic carbon fractions in the north central Pacific and Sargasso Sea. Nature, 357: 667–670.

Biodiversity Center of Japan. 2012. Monitoring Site 1000 Seabird Investigation Report Fiscal year Heisei 23. Nature Conservation Bureau, Ministry of the Environment, Fujiyoshida, Japan. (http://www.biodic.go.jp/moni1000/findings/reports/pdf/h23_seabirds.pdf)

Biodiversity Center of Japan. 2020. Monitoring Site 1000 Seabird Investigation Report Fiscal year 2019. Nature Conservation Bureau, Ministry of the Environment, Fujiyoshida, Japan. (http://www.biodic.go.jp/moni1000/findings/reports/pdf/2019_seabirds.pdf)

Biodiversity Center of Japan. 2021a. Monitoring Site 1000 Seabird Investigation Report Fiscal year 2020. Nature Conservation Bureau, Ministry of the Environment, Fujiyoshida, Japan. (http://www.biodic.go.jp/moni1000/findings/reports/pdf/2020_seabirds.pdf)

Biodiversity Center of Japan. 2021b. Monitoring Site 1000 Summary Report for Islets (Seabird) Survey during Fiscal Year 2004-2018. Nature Conservation Bureau, Ministry of the Environment, Fujiyoshida, Japan. (http://www.biodic.go.jp/moni1000/findings/reports/pdf/third_term_seabirds.pdf)

Burkanov, V.N., Loughlin, T.R. 2005. Distribution and abundance of Steller sea lions, Eumetopias jubatus, on the Asian coast, 1720's–2005. Marine Fisheries Review, 67(2): 1–62.

Burton, E.D., Phillips, I.R., Hawker, D.W., 2004. Sorption and desorption behavior of tributyltin with natural sediments. Environmental Science and Technology, 38: 6694-6700.

Carlson, C.A. and Ducklow, H.W. 1995. Dissolved organic carbon in the upper ocean of the central equatorial Pacific Ocean, 1992: daily and finescale vertical variations. Deep-Sea Research II, 42: 639–656.

Chen, C.T.A., Lui, H.K., Hsieh, C.H., Yanagi, T., Kosugi, N., Ishii, M. and Gong, G.C., 2017. Deep oceans may acidify faster than anticipated due to global warming. Nat. Clim. Change, 7: 890–894.

Chen, C.T.A., Wang, S.L., 1995. Carbonate chemistry of the Sea of Japan. J. Geophys. Res.-Oceans, 100: 13737-13745.

Cleveland, R.B., Cleveland, W.S., McRae, J. and Terpenning 1990. I. STL: A Seasonal Trend Decomposition Procedure Based on Loess. Journal of Official Statistics, 6(1): 3–73.

Duffy-Anderson, J.T., Barbeaux, S.J., Farley, E., Heintz, R., Horne, J.K., Parker-Stetter, S.L., Petrik, C., Siddon, E.C. and Smart, T.I. 2016. The critical first year of life of walleye

pollock (*Gadus chalcogrammus*) in the eastern Bering Sea: Implications for recruitment and future research. Deep Sea Research Part II: Topical Studies in Oceanography, 134, pp.283-301.

Danchenkov M.A., Lobanov V.B., Riser S.C., Kim K., Takematsu M. and Yoon J.H. 2006. A history of physical oceanographic research in the Japan/East Sea. J. Oceanography, 19: 18–31.

Deguchi, T., Watanuki, Y., Niizuma, Y., and Nakata, A. 2004. Interannual variations of the occurrence of epipelagic fish in the diets of the seabirds breeding on Teuri Island, northern Hokkaido, Japan. Progress in Oceanography, 61(2–4): 267–275.

Dolganova, N.T. and Zuenko, Y.I. 2004. Seasonal and inter-annual dynamics of mesoplankton in the northwestern Japan Sea. Progress in Oceanography, 61 (2-4): 227-243.

Doval, M. and Hansell, D. A., 2000. Organic carbon and apparent oxygen utilization in the western South Pacific and central Indian Ocean. Marine Chemistry, 68: 249–264.

Fedoseev, G.A., Goltsov, V.N. and Kosygin, G.M. 1970. Air-visual registration of seal pups haul-outs in the Okhotsk Sea. (Aerovizualniy uchet tyuleney na shchennih zalezhkah v Okhotskom more). Izvestiya TINRO, 70: 107–113.

Fisheries agency of Japan. 2017a. Cuvier's beaked whale, *Ziphius cavirostris.* Assessment of the rarity of marine organisms. Reference No.67. Available at: https://www.jfa.maff.go.jp/j/sigen/attach/pdf/20170321redlist-37.pdf (Accessed 2 November 2021, in Japanese).

Fisheries agency of Japan. 2017b. Stejneger's beaked whale, *Mesoplodon stejnegeri*. Assessment of the rarity of marine organisms. 70. Available at: https://www.jfa.maff.go.jp/j/sigen/attach/pdf/20170321redlist-63.pdf (Accessed 2 November 2021, in Japanese).

Fisheries agency of Japan. 2017c. Hubb's beaked whale. *Mesoplodon carlhubbsi*. Assessment of the rarity of marine organisms. 71. Available at: https://www.jfa.maff.go.jp/j/sigen/attach/pdf/20170321redlist-63.pdf (Accessed 2 November 2021, in Japanese).

Fisheries agency of Japan. 2017d. False killer whale, *Pseudorca crassidens.* Assessment of the rarity of marine organisms. 76. Available at: https://www.jfa.maff.go.jp/j/sigen/attach/pdf/20170321redlist-54.pdf (Accessed 2 November 2021, in Japanese).

Fisheries agency of Japan. 2017e. Common dolphin, *Delphinus delphis.* Assessment of the rarity of marine organisms. 80. Available at: https://www.jfa.maff.go.jp/j/sigen/attach/pdf/20170321redlist-48.pdf (Accessed 2 November 2021, in Japanese).

Fisheries agency of Japan. 2017f. Pacific white-sided dolphin, *Lagenorhynchus obliquidens*. Assessment of the rarity of marine organisms. 86. Available at: https://www.jfa.maff.go.jp/j/sigen/attach/pdf/20170321redlist-44.pdf (Accessed 2 November 2021, in Japanese).

Fisheries agency of Japan. 2017g. Risso's dolphin, *Grampus griseus*. Assessment of the rarity of marine organisms. 89. Available at: https://www.jfa.maff.go.jp/j/sigen/attach/pdf/20170321redlist-45.pdf (Accessed 2 November 2021, in Japanese).

Fisheries agency of Japan. 2017h Bottlenose dolphin, *Tursiops truncatus.* Assessment of the rarity of marine organisms. 90. Available at: https://www.jfa.maff.go.jp/j/sigen/attach/pdf/20170321redlist-45.pdf (Accessed 2 November 2021, in Japanese).

Fitzgerald W.F., Lamborg, C.H. and Hammerschmidt, C.R., 2007. Marine biogeochemical cycling of mercury. Chem. Rev, 107: 641–62.

Funamoto, T. 2011. Causes of walleye pollock (*Theragra chalcogramma*) recruitment decline in the northern Sea of Japan: implications for stock management // Fish. Oceanogr., 20(2): 95-103.

Gamo, T. et al. 2014. The Sea of Japan and its unique chemistry revealed by time-series observations over the last 30 years. Monogr. Environ. Earth Planets, 2: 1–22.

Gamo, T., Nozaki, Y., Sakai, H., Nakai, T., Tsubota, H. 1986. Spacial and temporal variations of water characteristics in the Japan Sea bottom layer. Journal of Marine Research, 44: 781–793.

Garcia, H.E., Locarnini, R.A., Boyer, T.P., Antonov, J.I., Baranova, O.K., Zweng, M.M. and Johnson, D.R. 2010. World Ocean Atlas 2009, Volume 3: Dissolved Oxygen, Apparent Oxygen Utilization, and Oxygen Saturation, In Levitus S. (ed.) NOAA Atlas NESDIS 68, U.S. Government Printing Office, Washington D.C., 344.

Glebova, S.Y., Ustinova, E.I. and Sorokin, Y.D. 2009.Long-term tendencies of atmospheric processes over the the Far Eastern Seas and thermal regime over recent 30 years. Isvestiya TINRO, 159: 285–298 (in Russian with English abstract).

Gorbatenko, K.M., Kiyashko, S.I., Lazhentsev, A.Y., Nadtochii, V.A. and Savin, A.B. 2008. Benthic-pelagic trophic interactions within the fish assemblage in the western Bering Sea shelf area according to stomach content analysis and ratios of C and N stable isotopes. Russian Journal of Marine Biology, 34: 497–506.

Gorbatenko, K.M., Kiyashko, S.I., Lazshentsev, A.E. and Figurkin, A. 2011. “Isotopic composition and food webs in pelagic communities in the North-Western part of the Pacific Ocean in Feb.-Apr. of 2010,” Bulletin of the Research of Pacific Salmon on the Far East of Russia, 6: 259–270.

Gorbatenko, K.M., Kiyashko, S.I., Lazshentsev, A.E., Nadtochy, V. and Savin, A. 2013. “Trophic relationships and bento-pelagic relations on the western Kamchatka shelf by the data of stomach contents and stable isotopes 13C and 15N,” Izvestiya TINRO, 175: 3–25.

Gorbatenko, K.M., Nadtochy, V. and Kiyashko, S. 2012. Trophic status of macrobenthos on West Kamchatka shelf from analysis of stable isotopes of nitrogen (d15N) and carbon (d13C). Izvestiya TINRO, 171: 168–174.

Goto, Y., Isono, T., Ikuta, S., and Burkanov V. 2022. Origin and abundance of Steller sea lions (Eumetopias jubatus) in winter haulout at Benten-Jima Rock off Cape Soya, Hokkaido, Japan between 2012–2017. Mammal Study 47: 87–101

Hansell, D. A. and Carlson, C. A., 1998a. Net community production of dissolved organic carbon. Global Biogeochemical Cycles, 12: 443–453.

Hansell, D. A. and Carlson, C. A., 1998b. Deep-ocean gradients in the concentration of dissolved organic carbon. Nature, 395: 263–266.

Hattori, K., Kitakado, T., Isono, T. and Yamamura, O. 2021. Abundance estimates of Steller sea lions (Eumetopias jubatus) off the western coast of Hokkaido, Japan. Mammal Study, 46: 3-16.

Hirose, N., and Ostrovskii, A.G. 2000. Quasi-biennial variability in the Japan Sea. J. Geophys. Res. 105(6): 14011-14027.

Hokkaido Government. 2017. Management Plan of Seals in Japan (Second period). https://www.pref.hokkaido.lg.jp/fs/2/4/8/8/2/3/0/_/azarasi2ki2.pdf (Accessed 4 November 2021, in Japanese).

Hong, S. W., Lee, J. M., Jang, Y. C., Kim, Y. J., Kim, H. J., Han, D. G., Hong, S. H., Kang, D. S., Shim, W. J. 2013. Impacts of marine debris on wild animals in the coastal area of Korea, Marine Pollution Bulletin, 66: 117-124.

Hong, S. W., Lee, J. M., Kang, D. S., Choi, H.-W., Ko, S.-H. 2014. Quantities, composition, and sources of beach debris in Korea from the results of nationwide monitoring. Marine Pollution Bulletin, 84: 27–34

Horimoto, T., Mitani, Y., Kobayashi, Y., Hattori, K. and Sakurai, Y. 2012. Distribution and stranding records of the northern fur seal Callorhinus ursinus near Tsugaru Strait during winter and spring 2009. Nippon Suisan Gakkaishi, 78: 256-258 (in Japanese).

Horimoto, T., Mitani, Y., Kobayashi, M., Hattori, K. and Sakurai, Y. 2017. Seasonal and spatial occurrence of northern fur seals Callorhinus ursinus around northern Japan. Mammal Study, 42: 51-56.

Hwang, D. W., Kim, S. G., Choi, M., Lee, I. S., Kim, S. S. and Choi, H. G. 2016. Monitoring of trace metals in coastal sediments around Korean Peninsula. Marine Pollution Bulletin, 102:230-239.

Hyndman, R., Koehler, A. Ord, K. and Snyder, R. 2008. Forecasting with Exponential Smoothing. Springer Series in Statistics, Berlin, Heidelberg: Springer Berlin Heidelberg: DOI: 10.1007/978-3-540-71918-2

Ishikawa, H. 2003. Stranding and incidental catch records in the Sea of Japan coast of Japan. Mammalian Science (supplement 3): 87-91 (in Japanese).

Isono, T. and Hattori, K. 2021. Steller Sea Lion. Available at: http://kokushi.fra.go.jp/R02/R02_59_SSL.pdf (Accessed 4 November 2021, in Japanese).

JMA, Climate change monitoring report, updated March, 2020, https://www.data.jma.go.jp/gmd/kaiyou/english/long_term_sst_japan/sea_surface_temperature_around_japan.html

Joo, H.T., Park, J.W., Son, S.H., Noh, J.H., Jeong, J.Y., Kwak, J.H., Saux-Picart, S., Choi, J.H., Kang, C.K., and Lee, S.H., 2014. Long-term annual primary production in the Ulleung Basin as a biological hot spot in the East/Japan Sea. J. Geophys. Res., 119: 3002-3011.

Jang, Y.C., Lee, J., Hong, S., Mok, J.Y., Kim, K.S., Lee, Y.J., Choi, H.-W., Kang, H. and Lee, S. 2014a. Estimation of the annual flow and stock of marine debris in South Korea for management purposes. Marine Pollution Bulletin, 86: 505–511.

Jang, Y.C., Lee, J., Hong, S., Lee, J.S., Shim, W.J. and Song, Y.K. 2014b. Sources of plastic marine debris on beaches of Korea: More from the ocean than the land. Ocean Science Journal, 49(2): 151-162.

Jung, H.K., Lee, C.I., Park, H.J., Park, J.M. 2020. Influences of oceanographic features on spatial and temporal distributions of size spectrum of walleye pollock, *Gadus chalcogrammus* inhabiting middle eastern coast of Korea. Korean J. Ichthyol., 32: 148–159.

Kalugin, I., Astakhov, A., Darin, A. and Aksentov, K. 2015. Anomalies of bromine in the estuarine sediments as a signal of floods associated with typhoons. Chinese Journal of Oceanology and Limnology, 33(6):1489–1495.

Kanaji, Y. 2021. Dall's porpoise, Phocoenoides dalli. available at: http://kokushi.fra.go.jp/R02/R02_50_PDA.pdf (Accessed 2. November 2021, in Japanese).

Kang, S., Park, J.H. and Kim, S. 2013. Size-class estimation of the number of walleye pollock Theragra chalcogramma caught in the southwestern East Sea during 1970s-1990s. Korean Journal of Fisheries and Aquatic Science, 46(4):445-453. (in Korean with English abstract)

Kang, S.K., Cherniawsky, J.Y., Foreman, G.G., Min, H. S., Kim, C.-H., and Kang, H.-W. 2005. Patterns of recent sea level rise in the East/Japan Sea from satellite altimetry and in situ data. J. Geophys. Res. 110(C07): Doi:10/1029/2004JC002565.

Kang, Y.S., Jung, S., Zuenko, Y., Choi, I. and Dolganova, N. 2012. Regional differences in response of mesozooplankton to long-term oceanographic changes (regime shifts) in the northeastern Asian marginal seas. Progress in Oceanography, 97-100: 120-134.

Kasuya, T. 2011. Conservation Biology of Small Cetaceans around Japan. University of Tokyo press. Tokyo. 640 p. (in Japanesse).
Kasuya, T. & Miyashita, T. 1997. Distribution of Baird's beaked whales off Japan. Rep. int. Whal. Commn. 47.963-968.
Kasuya, T., Yamamoto, Y. & Iwatsuki, T. 2002. Abundance decline in the finless porpoise population in the inland sea of Japan. Raffles Bull. Zoology (Supplement 10): 57-65.
Katin, I.O. and Nesterenko, V.A. 2010. Oceanological conditions and reproduction of the Spotted Seal (Phoca largha) in Peter the Great Bay of the Sea of Japan. Oceanology, 50: 77–82.
Kidokoro, H., Goto, T., Nagasawa, T., Nishida, H., Akamine, T. and Sakurai, Y. 2010. Impact of a climate regime shift on the migration of Japanese common squid (Todarodes pacificus) in the Sea of Japan. ICES Journal of Marine Science, 67(7), pp.1314-1322.
Kim, H.W., An, Y.R., Kim, Z.G. and Choi, S.G. 2009. First record of the Pomarine Skua (Stercorarius pomarinus) in Korea. Korean Journal of Ornithology, 16: 77–80 (in Korean).
Kim, H.W., Lee, S., Sohn, H. 2021. A review on the status of pinnipeds in Korea. Korean Journal of Fisheries and Aquatic science, 54 (2): 231-239 (in Korean).
Kim, J.H., Kim, H.W., Kim, E.M. and Sohn, H. 2018. First record of the Omura's whale (*Balaenoptera omurai*) in Korean waters. Animal Systematics, Evolution and Diversity, 34 (3): 162-167.
Kim, J.Y., Kang, D.J., Lee, T. and Kim, K.R., 2014. Long-term trend of CO_2 and ocean acidification in the surface water of the Ulleung Bain, the East/Japan Sea inferred from the underway observational data. Biogeosciences, 11: 2443-2454.
Kim, J. and Kim, G., 2015. Importance of colored dissolved organic matter (CDOM) inputs from the deep sea to the euphotic zone: Results from the East (Japan) Sea. Marine Chemistry, 169: 33–40.
Kim, J. and Kim, G., 2016. Significant anaerobic production of fluorescent dissolved organic matter in the deep East Sea (Sea of Japan). Geophysical Research Letters, 43(14): 7609–7616.
Kim, K., Kim K.R., Min, D.H., Volkov, Y., Yoon, J.H. and Takematsu, M. 2001. Warming and structural changes in the East (Japan) Sea: A clue to future changes in global oceans? Geophysical Research Letters, 28: 3293-3296.
Kim, K. R., Kim, K., Kang, D. J. et al. 2002. The changes in the East/Japan Sea found by CREAMS. Oceanogr. Jpn., 11: 419–429.
Kim, K. R., Kim, K., Kim, Y. G. et al. 2004. Water masses and decadal variability in the East Sea (Sea of Japan). Prog. Oceanogr., 61: 157–174.
Kim, M., Hwang, J., Rho, T., Lee, T., Kang, D.-J., Chang, K.-I., Noh, S., Joo, H., Kwak, J. H., Kang, C.-K. and Kim, K.-R. 2017. Biogeochemical properties of sinking particles in the southwestern part of the East Sea (Japan Sea), J. Mar. Sys., 167: 33-42.
Kim, N.S., Shim, W.J., Yim, U.H., Hong, S.H., Ha, S.Y., Han, G.M. and Shin, K.H. 2014. Assessment of TBT and organic booster biocide contamination in seawater from coastal areas of South Korea. Marine Pollution Bulletin, 78: 201-208.
Kim, S., and Kang, S. 1998. The status and research direction for fishery resources in the East Sea/Sea of Japan. Journal of Korean Society of Fisheries Resources, 1:44-58. (in Korean with English abstract)
Kim, T.H. and Kim, G. 2010. Distribution of dissolved organic carbon (DOC) in the southwestern East Sea in summer. Ocean and Polar Research, 32(3): 291-297.
Kim, T.H., Kim, G., Lee S.A. and Dittmar T. 2015. Extraordinary slow degradation of Dissolved Organic Carbon (DOC) in a cold marginal sea. Scientific Reports, 5, doi:10.1038/srep13808

Kim, W., Moon, J.E., Park, Y. and Ishizaka J. 2016. Evaluation of chlorophyll retrievals from Geostationary Ocean Color Imager (GOCI) for the North-East Asian region. Remote Sensing of Environment, 184: 482-495. doi:10.1016/j.rse.2016.07.031.

Kim, Z.G., Choi, S.G., An, Y.R., Kim, H.W. and Park K.J. 2009. Whales and dolphins off Korean peninsula. Hangeul, Busan, Korea: 135.

Kimbrough, K.L., Johnson, W.E., Lauenstein, G.G., Christensen, J.D. and Apeti, D.A. 2008. An assessment of two decades of contaminant monitoring in the nation's coastal zone. Silver Spring, MD. NOAA technical memorandum NOS NCCOS, 74: 105.

Kitajima, S., Iguchi, N., Honda, N., Watanabe, T. and Katoh, O. 2015. Distribution of *Nemopilema nomurai* in the southwestern Sea of Japan related to meandering of the Tsushima Warm Current. Journal of Oceanography, 71: 287–296.

Kiyota, M. and Baba, N. 1999. Records of northern fur seals and other pinnipeds stranded or taken incidentally by coastal fisheries in Japan, 1977-1998. Bull. Nat. Res. Inst. Far Seas Fish., 36: 9-16 (in Japanese).

Kodama, T., Iguchi, N., Tomita, M., Morimoto, H., Ota, T. and Seiji Ohshimo, S. 2018a. Appendicularians in the southwestern Sea of Japan during the summer: abundance and role as secondary producers. Journal of Plankton Research, 40: 269–283.

Kodama T., Wagawa T., Iguchi N., Takada Y., Takahashi T., Fukudome K., Morimoto H. and Goto T. 2018b. Spatial variations in zooplankton community structure along the Japanese coastline in the Japan Sea: influence of the coastal current. Ocean Science, 14: 355–369.

Korean Ministry of Ocean and Fisheries, 2008. Marine Environmental Management Act 40.

Kulik, V.V. 2017. Dynamics of Marine Trophic Index in catches of the northwestern Pacific. Analysis of ecosystem indicators at PICES // Report of the Laboratory "Regional Data Center" for the work 5.2.6.01 in 2016 year. TINRO-Center, 28030: 91.

Kwak, J.H., Hwang, J., Choy, E.J., Park, H.J., Kang, D.J., Lee, T., Chang, K.I., Kim K.R., and Kang, C.K., 2013a. High primary productivity and f-ratio in summer in the Ulleung basin of the East/Japan Sea. Deep-Sea Res. I, 79: 74-85.

Kwak, J.H., Lee, S.H., Park, H.J., Choy, E.J., Jeong, H.D., Kim, K.R., and Kang, C.K., 2013b. Monthly measured primary and new productivities in the Ulleung Basin as a biological "hot spot" in the East/Japan Sea. Biogeosciences, 10: 4405-4417.

Langston, W.J. and Spence, S.K. 1995. Biological factors involved in metal concentrations observed in aquatic organisms. In: Metal speciation and bioavailability in aquatic systems. (ed. By Tessier, A and Turner, DR): 407-478. John Wiley & Sons, Chichester.

Lee, E.Y. and Park K.A.. 2019. Change in the recent warming trend of sea surface temperature in the East Sea (Sea of Japan) over decades (1982-2018). Rem. Sen., 11: 2613.

Locarnini, R.A., Mishonov, A.V., Antonov, J.I., Boyer, T.P., Garcia, H.E., Baranova, O.K., Zweng, M.M. and Johnson, D.R. 2010. World Ocean Atlas 2009. 1: Temperature, In Levitus S. (ed.) NOAA Atlas NESDIS 68, U.S. Government Printing Office, Washington D.C., 184 pp.

Lobanov, V. B., Danchenkov, M. A., Luchin, V. A., Mezentseva, L. I., Ponomarev, V. I. Sokolov, O.V., … Khen, G. V. (2014). Dalnevostochnie morya Rossii (Far Eastern Seas of Russia). In: Vtoroy otsenochniy doklad Rosgidrometa ob izmeneniyah klimata i ih possledsntiyah on territorii Rossiyskoy Federatsii (Roshydromet second assessment report on climate change and its consequences on the territory of Russian Federation. Moscow, Russia: Roshydromet, 684-743 (in Russian).

Maeda, H. and Kishiro, T. 2021. Baird's beaked whale, Berardius bairdii. Available at: http://kokushi.fra.go.jp/R02/R02_51_BEW.pdf (Accessed 2. November 2021, in Japanese).

Mezentseva, L. I., Evdokimova, L.I. and Vrazhkin, A.N. 2019. Trends in Hazardous Phenomena over the Far Eastern Seas Caused by Tropical Cyclones**.** Russian Meteorology and Hydrology, 44: 837−843.

Ministry of the Environment (MoE). 2009. Present Status of Marine Pollution in the Sea around Japan as based on data from Marine Environment Monitoring Survey results, Fiscal Years 1998–2007. the Government of Japan. https://www.env.go.jp/water/kaiyo/monitoring/status_report/en-1.pdf; https://www.env.go.jp/water/kaiyo/monitoring/status_report/en-2.pdf

Ministry of Ocean and Fisheries (MOF), 2013. Marine Environment Management Act – Articles 8: Marine Environmental Standards. MOF Notice No.2013-186.

Ministry of Ocean and Fisheries (MOF) and Korea Marine Environment Management Corporation (KOEM), 2015. 2015 National Marine Debris Monitoring in Korea, KOEM, pp.186. (in Korean)

Ministry of Food and Drug Safety (MFDS), 2015. Korean Food Code – Chapter 6 A standards for marine products. p.1505

Ministry of Oceans and Fisheries (MOF) (2011). Annual report on marine environment monitoring in Korea 2011.

Ministry of Oceans and Fisheries (MOF) (2012). Annual report on marine environment monitoring in Korea 2012.

Ministry of Oceans and Fisheries (MOF) (2013). Annual report on marine environment monitoring in Korea 2013.

Ministry of Oceans and Fisheries (MOF) (2014). Annual report on marine environment monitoring in Korea 2014.

Ministry of Oceans and Fisheries (MOF) (2015). Annual report on marine environment monitoring in Korea 2015.

Miyashita T. and Kasuya, T. 1988. Distribution and Abundance of Dall's porpoise off Japan. Sci. Rep. whales Res. Inst. 39: 121-150.

Miyashita, T., Kato, H. and Kasuya, T. (Eds) 1995. Worldwide Map of Cetacean Distribution based on Japanese Sighting Data (Volume 1). National Research Insititute of Far Seas Fisheries. 140 p.

Mizuno, A.W., Suzuki, M. and Ohtaishi, N. 2001. Distribution of the spotted seal Phoca largha along the coast of Hokkaido, Japan. Mammal Study, 26: 109-118.

Na, H., Kim, K.Y., Chang, K.I., Park, J. J., Kim, H. and Minobe, S. 2012. Decadal variability of the upper ocean heat content in the East/Japan Sea and its possible relationship to northwestern Pacific variability. J. Geophys. Res. Ocean, 117: C02017.

Na, T., Hwang, J., Kim, S., Jeong, S., Rho, T., Lee, T., in preparation. Acidification-vulnerable carbonate system of the East Sea (Japan Sea).

Nadtochy, V.V. and Zuenko, Y.I. 2016. Mechanisms of subtropical plankton transport into the coastal waters of southern Primorye, a case of *Paracalanus parvus*. Izvestia TINRO (Newsletters of Pacific Fish. Res. Inst), 184: C.241-252.

Nam, S.H., Yoon, S.T., Park, J.H., Kim, Y.H. and Chang K.I. 2016. Distinct characteristics of the intermediate water observed off the east coast of Korea during two contrasting years. J. Geophys. Res. Ocean, 121: 5050–5068.

NASA Goddard Space Flight Center, Ocean Ecology Laboratory, Ocean Biology Processing Group. Moderate-resolution Imaging Spectroradiometer (MODIS) Aqua Chlorophyll Data; 2018 Reprocessing. NASA OB.DAAC, Greenbelt, MD, USA. doi: 10.5067/AQUA/MODIS/L3M/CHL/2018.

National Institute for Environmental Studies (NIES). 2016. Environmental GIS (in Japanese). Japan. http://envgis.nies.go.jp/kaiyo/

National Institute of Fisheries Science (NIFS), 2015. Final Report-Occurrence and distribution of Diuron and Irgarol 1051 in seawater from five major harbors of Korea. NIFS, Busan, 25 p.
Nesterenko, V.A., Katin, I.O. 2014. Largha in the Peter the Great Bay. Dalnauka, Vladivostok, 219 (in Russian).
NIBR. 2009. 2009 Wintering Waterbirds Census of Korea. NIBR.
NIBR. 2010. 2010 Wintering Waterbirds Census of Korea. NIBR.
NIBR. 2011. 2011 Wintering Waterbirds Census of Korea. NIBR.
NIBR. 2012. 2012 Wintering Waterbirds Census of Korea. NIBR.
NIBR. 2013. 2013 Wintering Waterbirds Census of Korea. NIBR.
NIBR. 2014. 2014 Wintering Waterbirds Census of Korea. NIBR.
NIBR. 2015. 2014-2015 Wintering Waterbirds Census of Korea. NIBR.
NIBR. 2016. 2015-2016 Wintering Waterbirds Census of Korea. NIBR.
NIBR. 2017. 2016-2017 Wintering Waterbirds Census of Korea. NIBR.
NIBR. 2018. 2017-2018 Wintering Waterbirds Census of Korea. NIBR.
NIBR. 2019. 2018-2019 Wintering Waterbirds Census of Korea. NIBR.
NIBR. 2020. 2019-2020 Wintering Waterbirds Census of Korea. NIBR.
Ogawa, N. 2017. Distribution and abundance of finless porpoises, Neophocaena asiaeorientalis, in coastal waters of Japan. Thesis for doctoral degree, Tokyo University of Marine Science and Technology. http://id.nii.ac.jp/1342/00001416/ (in Japanese)
Okiyama, M. 1970. Studies on the population biology of the sandfish, Arctoscopus japonics (STEINDACHNER) II, Population analysis (preliminary report). Bull. Jpn. Sea Reg. Fish. Res. Lab, 22, 59-69. (in Japanese).
OSPAR, 2004. OSPAR/ICES workshop on the evaluation and update of background reference concentration (BRCs) and ectoxicological assessment criteria (EACs) and how these assessment tools should be used in assessing contaminants in water, sediment and biota (Final report), 9-13 Februry 2004, The Hague. OSPAR Commission and ICESCIEM
Otosaka, S., Tanaka, T., Togawa, O., Amano, H., Karasev, E.V., Minakawa, M., and Noriki S., 2008. Deep sea circulation of particulate organic carbon in the Japan Sea. J. Oceanogr., 64: 911-923.
Park, K.A., Park, J.E., Choi, B.J., Byun, D.D. and Lee, E.L. 2013. An oceanic current map of the East Sea for science textbooks based on scientific knowledge acquired from oceanic measurements. Journal of the Korean Society of Oceanography, The Sea, 18: 234–265.
Park, G.H., Lee, K. and Tishchenko, P. 2008. Sudden, considerable reduction in recent uptake of anthropogenic CO_2 by the East/ Japan Sea. Geophys. Res. Lett., 35: L23611.
Park, G.H., Lee, K., Tishchenko, P., Min, D.H., Warner, M.J., Talley, L.D., Kang, D.J. and Kim, K.R. 2006. Large accumulation of anthropogenic CO_2 in the East (Japan) Sea and its significant impact on carbonate chemistry. Global Biogeochem. Cycles, 20: GB4013.
Park, J.J. and Nam, S.H., 2017. Interannual variability of winter precipitation linked to upper ocean heat content off the east coast of Korea. Int. J. Clim., 38: DOI:10.1002/joc.5354.
Park, J.J. and Nam, S.H., 2018. Causes of interannual variation of summer mean alongshore current near the east coast of Korea derived from 16-year-long observational data. J. Geophys. Res. Ocean, 123: 7781–7794.
Park, J., Lee, J., Seto, K., Hochberg, T., Wong, B.B., Miller, N.A., Takasaki, K. and Kubota, H. 2020. Illuminating dark fishing fleets in North Korea. Sci. Adv., 6, eabb1197.
Pauly, D. 1988. Fishing Down Marine Food Webs. Science, 279: 860–863.
Pishchalnik, V.M., Dorofeeva, D.V., Minervin, I.G., Shumilov, I.V., and Nikulina, I.V. 2019. Year-to-year dynamics of the ice cover anomalies in the Tatar Strait for the period from 1882

to 2018. Izv. TINRO, 196: 114–122.
Polyakov, D.M., Aksentov, K.I. and Ivanov, M.V. 2008. Mercury in the bottom sediments of the marginal filter of the Razdol'naya River, Amur Bay. Geochemistry Int., 46: 614–621.
Rahman, S.M.M., Jung, H.K., Park, H.J., Park J.M. and Lee, C.I. 2019. Synchronicity of climate driven regime shifts among the East Asian marginal sea waters and major fish species. Journal of Environmental Biology, 40: 948-961.
Ricker, W.E. (1954) Stock and Recruitment. Journal of the Fisheries Research Board of Canada, 11, 559-623.
Rostov, I.D., Dmitrieva, E.V., Rudykh, N.I. and Vorontsov, A.A. 2020. Climatic changes in thermal conditions of marginal seas in the Western Pacific. Russ. Meteorol. Hydrol., 45 (3): 169–178.
Sakurai, Y., Kiyofuji, H., Saitoh, S.I., Yamamoto, J., Goto, T., Mori, K. and Kinoshita, T. 2002. Stock fluctuations of the Japanese common squid, *Todarodes pacificus*, related to recent climate changes. Fisheries science, 68(sup1), pp.226-229.
Santinelli, C., Nannicini, L. and Seritti, A., 2010. DOC dynamics in the meso and bathypelagic layers of the Mediterranean Sea. Deep-Sea Research II, 57: 1446–1459.
Schuster, P.F., Krabbenhoft, D.P., Naftz, D.L., Cecil, L.D., Olson, M.L., Dewild, J.F., Susong, D.D., Green, J.R. and Abbott, M.L., 2002. Atmospheric mercury deposition during the last 270 years: a glacial ice core record of natural and anthropogenic sources. Environ. Sci. Technol., 36: 2303–10.
Sharp, J.H., Benner, R., Bennett, L., Carlson, C.A., Fitzwater, S.E., Peltzer, E.T. and Tupas, L. M. 1995. Analyses of dissolved organic carbon in seawater: The JGOFS EqPac methods comparison. Marine Chemistry, 41: 91–108.
Shibuya, M. and Kobayashi, M. 2014. Use of haul-out sites by spotted seals (Phoca largha) on Rebun and Todojima Islands in the Japan Sea from 2008 to 2009. Mammal Study, 39: 173-179.
Shin, C.W. 2019. Change of coastal upwelling index along the southeastern coast of Korea. The Sea J. Kor. Soc. Oceanogr., 24: 79–91.
Shirai, S.M., Kuranaga, R., Sugiyama, H. and Higuchi, M., 2006. Population structure of the sailfin sandfish, *Arctoscopus japonicus* (Trichodontidae), in the Sea of Japan. Ichthyological Research, 53, pp.357-368.
Shishido, H., Sakaji, H., and Tian Y., 2016. Catch fluctuation of yellowtail species in relation to fluctuations in the geographical catch center. Bull. Jpn. Soc. Fish. Oceanogr. 80(1), 27-34. (in Japanese with English abstract).
Sohn, H., Park, K.J., An, Y.R., Choi, S.G., Kim, Z.G., Kim, H.W., An, D.H., Lee, Y.R. and Park, T.G. 2012. Distribution of whales and dolphins in Korean waters based on a sighting survey from 2000 to 2010. Korean Journal of Fisheries and Aquatic Sciences, 45 (5), 486-492.
Takahashi, A., Kuroki, M., Niizuma, Y., Kato, A., Saitoh, S., and Watanuki, Y. 2001. Importance of the Japanese anchovy (*Engraulis japonicus*) to breeding Rhinoceros Auklets, (*Cerorhinca monocerata*) on Teuri Island, Sea of Japan. Marine Biology, 139(2): 361–371.
Talley, L.D., Lobanov, V.B., Ponomarev, V.I., Salyuk A.N., Tishchenko, P.Y., Zhabin, I.A. and Riser S. 2003. Deep convection and brine rejection in the Japan Sea. Geophys. Res. Lett., 30: 1159 DOI:10.1029/2002GL016451.
Talley, L.D., Min, D.H., Lobanov, V.B., Luchin, V.A., Ponmarev, V.I., Salyuk, A.N., Shcherbina, A.Y., Tishchenko, P.Y. and Zhabin, I. 2006. Japan/East Sea water masses and their relation to the sea's circulation. Oceanogr., 19: 32–49.

Tanaka, K., Kuma, K., Hamasaki, K. and Yamashita, Y. 2014. Accumulation of humic-like fluorescent dissolved organic matter in the Japan Sea. Scientific Reports, 4: 5292.

Takasaki, K., Saito, T, Oozeki, Y., Inagake, D., Kubota, H., Ichikawa, T., Sugisaki, H. and Shimizu, S., 2020. Bull. Jpn. Soc. Fish. Oceanogr. 82(2), 89-99. (in Japanese with English abstract)

Terauchi, G., Maure, E. de R., Yu, Z. Wu, Z., Lee, C., Kachur, V. and Ishizaka J. 2018. Assessment of eutrophication using remotely sensed chlorophyll-a in the Northwest Pacific region. Proc. SPIE 10778, Remote Sensing of the Open and Coastal Ocean and Inland Waters: 107780H doi:10.1117/12.2324641.

Thomas, C., Cauwet, G. and Minster, J.F. 1995. Dissolved organic carbon in the equatorial Atlantic Ocean. Marine Chemistry, 49: 155–169.

Tomita, M., Ikeda, T. and Shiga, N. 1999. Production of *Oikopleura longicauda* (Tunicata: Appendicularia) in Toyama Bay, southern Japan Sea. Journal of Plankton Research, 21: 2421–2430.

UPI, 2018 (www.upi.com/Top_News/World-News/2019/08/06).

Trukhin, A.M. 1997. Status of true seals in the Far Eastern Marine Reserve. 3rd Far Eastern Conference on Preservation. 119–120.

Trukhin, A.M. 2001. On the occurrence of the Steller sea lions in the Sea of Japan along the Primorsky Region coast. Biological grounding of the sustainable development of the coastal marine ecosystems, 243–245.

Trukhin, A.M. 2002. The south limits of the Bearded Seal area in the Sea of Japan and their ecological causes. Vestnik FEB RAS, 3: 105–109 (In Russian).

Trukhin, A.M. 2005. Spotted Seal. 246.

Trukhin, A.M. 2015. Current abundance of spotted seal (*Phoca largha*) in Peter the Great Bay (Japan Sea): unstable equilibrium or sustainable growth? Izvestiya TINRO, 182: 48–54.

Trukhin, A.M. 2019. Spotted seal (*Phoca largha*) population increase in the Peter the Great Bay, Sea of Japan. Marine Mammal Science, 35(3): 1183-1191.

Trukhin, A.M. 2023. Population growth and redistribution of reproductive burden between spotted seal rookeries in Peter the Great Bay. Regional'nye problemy, 26 (1): 45–51 (In Russian).

Trukhin, A. M. and Mizuno, A.W. 2002. Distribution and abundance of the Largha Seal (Phoca largha Pall.) on the coast of Primorye Region (Russia): a literature review and survey report. Mammal Study, 27: 1–14.

Trusenkova, O. O. 2018. Long-Term Changes in the Level of the Sea of Japan Based on Satellite Altimetry Measurements. Izvestiya, Atmospheric and Oceanic Physics, 54(9): 1023–1030.

Trusenkova, O.O., and Kaplunenko, D.D. 2013. Variability modes of sea level in the Sea of Japan. Oceanology 53(3): 308–316.

Tsypysheva, I.L., Muktepavel, L.S., Tsitsiashvili, G.Sh., Shatilina, T.A. and Radchenkova, T.V. 2016. Features of the sea ice cover variability in the Tatar Strait (Japan Sea) in connection with the regional atmosphere circulation. Izv. TINRO, 185: 135–149.

U.S. Environmental Protection Agency for Natural Resources and Energy, Ministry of Economy, Trade and Industry (METI) 2009, Non-Ferrous Metal Supply and Demand Statistics survey

USEPA, 2004. Ambient aquatic life water quality criteria for tirbutyltin (TBT)-Final. USEPA, Washington D.C. EPA 822-R-03-031.

Ustinova, E.I. and Sorokin, Yu. D. 2013. Recent state and variability of climate and oceanographic conditions in the Far-Eastern Seas. Ecology of the marginal seas and their basins – 2013. Materials of the International Scientific conference: 343-352.

UNEP. 2016. Minamata Convention on Mercury, http://www.mercuryconvention.org/

Vdovin, A.N., Chetyrbotskij, A.N. and Nuzhdin V.A. 2017. Dynamics of abundance for Primorye pollock Theragra chalcogramma Pallas, 1811 (*Gadidae, Gadoformes*) in the Japan Sea // Biologiya morya (Marine Biology), 43(5): 321-328.

Wada, S., Oishi, M., and Yamada, T.K. 2003. A newly discovered species of living baleen whale. Nature, 426(6964), 278-281.

Weng, N. and Wang W.X., 2014. Variations of trace metals in two estuarine environments with contrasting pollution histories. Science of the Total Environment, 485-486: 604-614.

Woo, H.J. and Park, K.A. 2017. Long-term trend of satellite-observed significant wave height and impact on ecosystem in the East/Japan Sea. Deep-Sea Res.II., 43: 1–14.

Yamada, K., Ishizaka, J., Yoo, S., Kim, H. C., & Chiba, S. 2004. Seasonal and interannual variability of sea surface chlorophyll a concentration in the Japan/East Sea (JES). Progress in Oceanography, *61*(2-4), 193-211.

Yamashita, Y. and Tanoue, E. 2008. Production of bio-refractory fluorescent dissolved organic matter in the ocean interior. Nature Geoscience, 1(9): 579–582.Yamada, K., Ishizaka, J., Yoo, S., Kim, H.C. and Chiba, S. 2004. Seasonal and interannual variability of sea surface chlorophyll a concentration in the Japan/East Sea (JES). Progress in Oceanography, 61(2-4):193-211. doi:10.1016/j.pocean.2004.06.001.

Yoda, M., Shiraishi, T., Yukami, R. and Ohshimo, S. 2014. Age and maturation of jack mackerel Trachurus japonicus in the East China Sea. Fisheries science, 80, pp.61-68.

Yoon, S.T., Chang, K.I., Na, H. and Minobe, S. 2016. A east-west contrast of upper ocean heat content variation south of the subpolar front in the East/Japan Sea. J. Geophys. Res. Ocean, 121: 6418–6443.

Yoon, S.T., Chang, K.I., Nam, S.H., Rho, T.K., Kang, D.J., Lee, T., Park, K.A., Lobanov, V.B., Kaplunenko, D.D., Tishchenko, P.Ya. and Kim, K.R. 2018. Re-initiation of bottom water formation in the East Sea (Japan Sea) in a warming world. Scientific Reports, 8:1576 |DOI:10.1038/s41598-018-19952-4.

Zuenko, Y.I. and Nuzhdin, V.A. 2018. Impact of modern changes of oceanographic conditions in the Japan Sea on state of the Primorye pollock population. Voprosy Rybolovstva (Problems of Fishery), 19(3): 377-386.

Zuenko, Y.I. and Nuzhdin, V.A. 2019. Ricker analysis of dynamics for two populations of walleye pollock in the Japan Sea. Trudy VNIRO (Bull. Russian Res. Inst. Fish. and Oceanogr.), 179: 156-173.